University of Zurich[UZH]

Percolation Transformation due to Vegetation Alteration: Does land-use change affect the chemical and physical properties of Eastern Malagasy soil and can Ksat be predicted by Pedotransfer Functions

GEO 511 Master's Thesis

Author
Florencio Zanitti
14-706-576

Supervised by
Dr. Ilja van Meerveld
Dr. Samuel Abiven

Faculty representative
Prof. Dr. Jan Seibert

27.06.2019
Department of Geography, University of Zurich

University of Zurich[UZH]

Percolation Transformation due to Vegetation Alteration

Does land-use change affect the chemical and physical properties of Eastern Malagasy soil and can K_{sat} be predicted by pedotransfer functions?

GEO 511 Master's Thesis

Author

Florencio Zanitti

florencio.zanitti@geo.uzh.ch

14-706-576

Supervised by
Dr. Ilja van Meerveld
ilja.vanmeerveld@geo.uzh.ch

and

Dr. Samuel Abiven
samuel.abiven@geo.uzh.ch

Faculty Representative
Prof. Dr. Jan Seibert
jan.seibert@geo.uzh.ch

27th June, 2019

Department of Geography, University of Zurich

Acknowledgement

First and foremost, I would like give gratitude to my supervisors, **Dr. Ilja van Meerveld** and **Dr. Samuel Abiven** without whom the I could not have completed this master thesis. Thanks for the constructive and encouraging feedbacks during our many meetings, for always supporting me during my thesis, for always taking your time, whenever I was in need of advice and for providing me (even at ungodly late hours) with helpful literature recommendations.

Also, I would like to thank the following researchers, employees, fellow students and family members their support:

- **Marc Vis**, who kept me from spending endlessly frustrating hours on some R problem.
- **Miriam Steinmann** and my brother **Zelim**, for taking their time to proof-read my thesis despite having enough work to do themselves.
- **PhD Nicholas Ofiti**, for helping me with the PTF development as well as for his literature recommendations.
- **Tatjana Kraut** who (already before my thesis) introduced me to lab work and especially for assisting me during various lab tasks.
- **Michael Hilf** for his help in the lab and for always having a witty remark ready.
- **My friends**, especially the ones with whom I have spent countless hours in the Y23-G-10 office. Thanks for the serious and the light hearted discussions.
- My parents **Sabine** and **Urs** for their love and support during my studies.

Lastly, I would like to thank the **P4GES Project** for providing me with the samples and the data.

Abstract

Land-use change, and especially deforestation is of great global importance, and particularly so in the tropics. This thesis focuses on the effects of land-use change in the Eastern escarpment of Madagascar on chemical and physical soil properties. Moreover, I try to predict the saturated hydraulic conductivity (K_{sat}) with the measured soil chemical and physical characteristics. The study area is divided into three Zones of Interest (ZOI) all of which include samples of the following land-use types: Forest (F), Tree Fallow (TF), Shrub Fallow (SF) and Degraded Land (DL). Besides comparing the land-uses, the three soil depths: 0 - 10 cm (Depth 0), 10 - 20 cm (Depth 1) and 20 - 30 cm (Depth 2) were contrasted. Linear regressions (Pedotransfer Functions (PTF)) as well as Diffuse Reflectance Infrared Fourier Transform (DRIFT) spectroscopy were used to predict K_{sat}. My results show that slash-and-burn agriculture lead to a decrease of soil organic carbon (SOC) between Forest (4.15 %) and the three secondary vegetations (3.43 % - 3.75 %). A clear trend of rising $\delta\ ^{13}C$ (Delta C 13) from Forest to Degraded Land is observed, indicating the replacement of C_3 forest vegetation with C_4 pasture grasses. pH and bulk density (BD) were significantly lower in Forest soils than in Tree Fallow, Shrub Fallow and Degraded Land soils. While porosity (φ), soil organic carbon and nitrogen displayed decreasing values with increasing depth, bulk density increased.
No existing function could accurately predict K_{sat}. Five created PTFs were able to predict K_{sat} for different subsets of the data. However, they are only able to do so for individual depths of land-use. PTF VII, using nitrogen, soil organic carbon, clay and silt to predict K_{sat} of Shrub Fallow Depth 2, produced the best prediction with an R^2 of 0.814. Due to too much variance in K_{sat} and the soil spectra, no predictions could be made with the sample spectra, without having too high RMSE values.

Contents

List of Figures

List of Tables

List of Abbreviations

AfSIS	African Soil Information Services
Al	Aluminium
Al_2O_3	Aluminium oxide
ANOVA	Analysis of variance
a.s.l.	Above sea level
b	Intercept
BD	Bulk density
C	Carbon
Ca	Calcium
CAZ	Ankeniheny Zahamena Corridor
CEC	Cation exchange capacity
C/N	Carbon to Nitrogen ratio
CO_2	Carbon dioxide
Cu	Copper
CV	Coefficient of variation
DL	Degraded Land
DRIFT	Diffuse Reflectance Infrared Fourier Transform
D0, 1, 2	Depth of soil
F0, 1, 2	Depth of soil for a land-use type (F, TF, SF, DL)
EA-IRMS	Elemental analyser - isotope ratio mass spectrometry
F	Forest
f	Drainable porosity
FAO	Food and Agriculture Organisation of the United Nations
fc	Field capacity
Fe	Iron
Fe_2O_3	Iron(III) oxide
GBT	Gradient-boosted tree
H_0	Null-hypothesis
HOF	Hortonian overland flow
HYPRES	Hydraulic properties of European soils
IR	Infrared
IRMS	Isotope ratio mass spectrometry
ITCZ	Intertropical Convergence Zone
K	Potassium
K_2O	Potassium oxide
KBr	Kalium Bromide
K_{sat}	Saturated hydraulic conductivity
K_u	Unsaturated hydraulic conductivity
LC	Lack of correlation
LOOCV	Leave one out cross validation

LSD	Least significant difference
MAE	Mean absolute error
MAP	Mean annual precipitation
MAAT	Mean annual air temperature
MIR	Mid-infrared
MSD	Mean squared deviation
Mg	Magnesium
Mg_2O	Magnesium oxide
N	Nitrogen
n	Sample size
Na	Sodium
NIR	Near infrared
ns	Not significant
NU	Nonunity slope
OM	Organic matter
P	Phosphate
P_2O_5	Phosphorous pentoxide
PDB	Pee Dee Belemnite
PLSR	Partial least squares regression
PTF	Pedotransfer Function
PWP	Permanent wilting point
R^2	Coefficient of determination
RMSE	Root mean squared error
SB	Squared bias
SD	Standard deviation
SF	Shrub Fallow
Si	Silicon
SiO_2	Silicon dioxide
SOC	Soil organic carbon
SOF	Saturation excess overland flow
SOM	Soil organic matter
SO_4	Sulfate
TF	Tree Fallow
T_{clay}	Clay
T_{sand}	Sand
T_{silt}	Silt
U	Uranium
USDA	United States Department of Agriculture
UZH	University of Zurich
VIS	visible spectrum
VU	Vrije Universiteit Amsterdam
WISE	World Inventory of Soil Emission Potentials

x	Multiplicator
XRF	X-ray fluorescence
ZOI	Zone of Interest
α	Significance level
$\delta^{13}C$	Delta C 13
$\delta^{15}N$	Delta N 15
λ	Wavelength
φ	Porosity
θ_{fc}	Soil moisture content at field capacity

1 Introduction

1.1 Land-use Change

Land-use change [1] describes change from one ecosystem to another. This can occur naturally or through anthropogenic change (Guo and Gifford, 2002); 60 % of all land changes are linked to human activities (Song et al., 2018). Human induced land-use change includes, the conversion of natural landscapes (i.e. land cover) to other land-use types or the change from one land-use practice to another one (Foley et al., 2005).

Deforestation or other types of forest cover loss to obtain agricultural or pasture land is one of the most common land-use changes (FAO, 2006). While there is a net loss of tree cover in the tropics, there was a global net gain of 7.1 % ($2.24 * 10^6$ km^2) in 2016 relative to 1982, due to the increase of forest cover in the extratropics (Song et al., 2018). This shows that land-use change varies for different regions. While temperate regions are dominated by cropland intensification, reforestation/afforestation and urbanisation (Song et al., 2018), commodity-driven deforestation and slash-and-burn cultivation are prominent in the tropics (Figure 1) (Curtis et al., 2018). Slash-and-burn differs from deforestation, since deforestation implies an absence of regrowth after the removal of arboreal vegetation (Curtis et al., 2018). Between 2001 and 2015, slash-and-burn cultivation globally accounted for 24 ± 3 % (753'600 km^2) of total forest disturbance, being the third largest after commodity-driven deforestation (27 ± 5 %) and forestry (26 ±4 %) (Curtis et al., 2018).

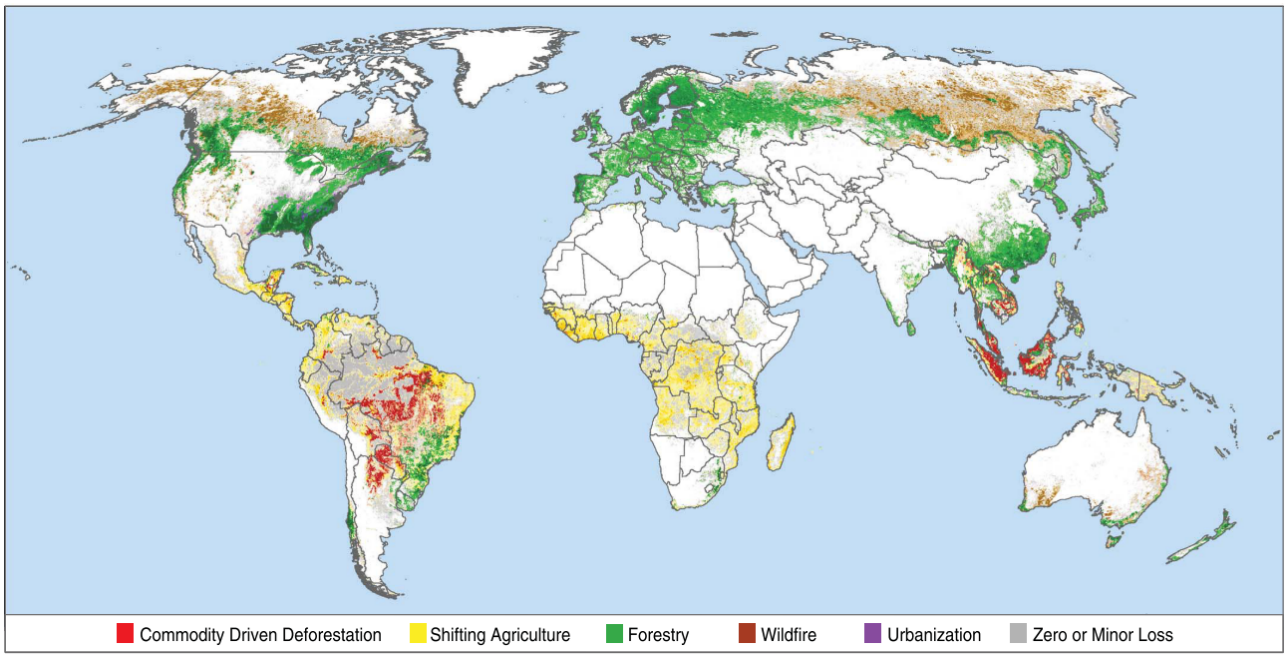

Figure 1: Primary drivers of forest cover loss for the period 2001 to 2015. Greater forest cover loss is indicated by darker colours. Source: Curtis et al. (2018)

Land-use/land cover change has been shown to affect many processes. By changing the global carbon cycle, land-use change alters the atmospheric composition - mainly through CO_2 uptake - which in turn

[1] Land-use implies the function that the land has to the people, while land cover describes the biophysical properties of a land surface (Zvoleff et al., 2002).

affects the global climate (Baudron and Giller, 2014). By altering the surface energy and the water balance, it changes the regional climate (Kalnay and Cai, 2003). Worldwide, biodiversity has decreased as a result of land-use change, principally through the loss, alteration and fragmentation of habitats (Foley et al., 2005). This thesis focuses on the land-use change/forest cover loss in Madagascar and its effects on soils and soil hydrology. Hydrology is impacted by land-use change in terms of changes in the water balance but also through changes in the soil characteristics, which affect infiltration and percolation and thus ultimatley the streamflow and water quantity. As shown by Zwartendijk et al. (2017), the saturated hydraulic conductivity (K_{sat}), particularly in the first 10 cm is different for different land-use types. Tree cover loss leads to a decline of the K_{sat} (Zimmermann et al., 2006). Knowledge of such effects are crucial, as the K_{sat} is one of the most essential soil hydrological parameters, regulating the partitioning of precipitation into surface runoff and soil and groundwater recharge, as well as biochemical cycling in soils (Jarvis et al., 2013). K_{sat} is thus an important input parameter of models that simulate solute transport and water flow, physically based catchment models, and climate and land surface models (Baroni et al., 2010; Davis et al., 1999; Agyare et al., 2007; Gutmann and Small, 2007)

1.2 Saturated Hydraulic Conductivity

The saturated hydraulic conductivity (K_{sat}) describes how easily water can be transmitted through a saturated pedologic or geologic medium. Most commonly the unit is mm h^{-1} or m s^{-1} (Fitts, 2013). In this thesis the unit $mm\ h^{-1}$ is used. Zwartendijk et al. (2017) define K_{sat} as the steady-state infiltration or percolation rate. In the laboratory K_{sat} can be measured using either a constant head approach or a falling head approach (Braudeau and Mohtar, 2014). In situ, surface K_{sat} can be measured with an double-ring infiltrometer and sub soil steady state percolation can be measured with an Amoozemeter (Zimmermann et al., 2006; Amoozegar, 1989). Knowledge of K_{sat} is needed for understanding hydrological and soil-related processes, and to inform agricultural practices, such as optimizing irrigation practices, simulating of leaching nutrients and pesticides, process and to determine groundwater recharge (Jabro, 1992).
Runoff generation depends, amongst other things, on how much water can infiltrate into and percolate within a soil in a certain amount of time. The hydraulic conductivity thus determines the likelihood of overland flow, such as the Hortonian (infiltration excess) overland flow (HOF) and saturation excess overland flow (SOF). HOF occurs when the precipitation intensity exceeds the infiltration capacity (Beven, 2004). SOF describes surface runoff, that occurs, after the soil becomes saturated (Beven, 2001). Overland flow can lead to soil erosion, thus causing sediment re-distribution and water quality issues (Bonell, 2005). The hydraulic conductivity affects a number of soils processes. The amount of water that infiltrates into a soil also affects the leaching of chemicals and nutrients (e.g. nitrogen and phosphorus) added to agricultural soils, as well as the depletion of naturally occurring nutrients in the soil.

1.3 Factors Affecting the Hydraulic Conductivity

Based on a review of Jarvis et al. (2013) K_{sat} depends strongly on the bulk density (BD), the soil organic carbon content (SOC) and land-use. Other studies do not directly mention land-use but rather soil properties, such as texture (Sand (T_{sand}), Silt (T_{silt}), Clay (T_{clay})), effective porosity (φ) and soil structure (Wagner et al., 2001; Wösten et al., 2001; Oshunsanya, 2013), which partially (e.g. the soil structure) can be affected by the land-use.
K_{sat} is generally higher for coarser material (e.g. sand) than fine-grained material, such as clay (Hiscock

and Bense, 2014). While K_{sat} is inversely related to clay and silt content, K_{sat} is positively correlated to sand content (Oshunsanya, 2013; Bonell, 2005) because the water conducting pores are generally significantly larger in coarser grained soils and pores scale flow rates increase with the radius squared (total flow with r^4, Hagen-Poiseuille equation). Despite having a high porosity, fine-grained materials have smaller pore radii (Jarvis et al., 2002). The effective porosity itself is only positively correlated with K_{sat}, if it is proportional to the pore throat radius. K_{sat} and porosity are therefore only indirectly proportional. However, since data on the pore throat size are not widely available, one often resorts to the porosity, but this does not take the effect of macropores created by roots or soil fauna into account. Bulk density and K_{sat} are negatively correlated, because the pores are smaller in a compacted soil and there are particularly fewer large pores through which water can flow quickly (Bonell, 2005). A higher bulk density due to compaction by gravity is the reason for the frequently observed decrease of K_{sat} with depth (Zwartendijk et al., 2017; Bonell, 2005). Soil organic carbon is generally positively correlated with K_{sat} because soil organic carbon affects the bulk density, as well as soil aggregation. Also soils with high numbers of roots and preferential flow along those roots tend to have high soil organic carbon. A greater soil organic carbon content leads to a lower bulk density, because soil organic carbon has an inherent low density (Davidson and Ackerman, 1993; Lal and Kimble, 2001). Therefore, soil organic carbon affects K_{sat} indirectly by decreasing the bulk density. Furthermore, soil organic carbon positively affects the K_{sat} through its influence on aggregates. soil organic carbon works like a cementation agent for soil aggregates, causing them to become more stable (Nadler et al., 1996; Beare et al., 1994). A greater aggregate stability improves the soil structure and thus affects K_{sat} positively (Pachepsky et al., 2006; Oshunsanya, 2013).

Aboveground factors that affect K_{sat} include: precipitation, the vegetation type, occurrence of freeze and thaw cycles and the climate (Jarvis et al., 2013; Hu et al., 2012). The Climate plays a key role regarding K_{sat}. Through precipitation the climate has a direct effect on K_{sat}. Indirect effects on K_{sat} are the impacts that vegetation and the soil properties have on K_{sat} because both are affected by the climate. The effect of land use on K_{sat} is a compilation of several different factors that affect K_{sat}. Land-use type defines the ground cover, as well as the intensity and frequency of soil disturbance (Lal and Kimble, 2001). Soil compaction by machinery increases and loosening by tillage decrease the bulk density (Don et al., 2011). However, the effects of compaction or loosening are only relevant in the uppermost soil horizon (Don et al., 2011). Celik (2005) observed a bulk density increase of 4.8 % and a 17.6 % decrease in K_{sat} in the uppermost 10 cm after cultivating a forested area. Vegetation, or more precisely the root system, creates macropores at the soil surface and within the soil. These macropores are important, when the soil reaches, or is close to reaching, saturation because then the water is conducted through the macropores (Davis et al., 1999). Macropores are prevalent in the first 50 cm. However, there might be a difference in the rooting density within those 50 cm (Davis et al., 1999). Zwartendijk et al. (2017) showed that if large macropores were present, infiltration was mainly via these large pores. This is the case for the Forest land-use. In the Degraded Land fewer macropores were present, leading to a more homogeneous infiltration/percolation (Zwartendijk et al., 2017). Thus, the number and size of macropores, and hence the number and size of roots is crucial for the infiltration of precipitation into the soil. Macropores can also be created by fauna that interact with the soil system. Macropores, created by flora and fauna, enhance the K_{sat} (Bonell, 2005). Even though, Jarvis et al. (2013) separate soil organic carbon and land-use, the land-use type defines the amount of biomass, which again determines the soil organic carbon.

1.4 Pedotransfer Function

As mentioned earlier, K_{sat} is a crucial parameter for many models such as physically based catchment, water flow or solute transport models (Davis et al., 1999; Baroni et al., 2010). However, the large scale data that are needed for such models and in situ measurements are frequently not possible due to monetary expenses and time required to obtain them (Schaap et al., 2001). K_{sat} is generally highly variable due to the heterogenous and anisotropic nature of soils so that many measurements are needed to characterise a site (Davis et al., 1999). To obtain such large scale K_{sat} data, widely available and accessible soil properties, such as soil organic carbon, porosity, bulk density or the soil texture can be used to estimate K_{sat} with pedotransfer functions (PTFs) (Bouma, 1989). PTFs, or as they were called originally - transfer functions (Bouma and Van Lanen, 1987) - are mathematical equations that estimate soil properties. Most often soil hydrological properties, such as K_{sat}, the unsaturated hydraulic conductivity K_u, soil moisture content at field capacity (θ_{fc}) and permanent wilting point (PWP) are estimated with PTFs. These properties are estimated from 'basic soil data' like soil texture, bulk density and/or soil organic matter, which are either readily available from soil surveys and databases, or are comparably easy to measure in the field (Wösten et al., 2001). Pedotransfer functions are widely used because obtaining the difficult to measure parameters is expensive and time consuming (Tietje and Hennings, 1996; Schaap et al., 2001). Most PTFs use multiple linear regression and empirical relations (Hodnett and Tomasella, 2002). Other approaches besides linear regression modelling are neural networks or non linear regressions (Hodnett and Tomasella, 2002; Minasny et al., 1999). Without direct measurements, all indirect methods, including PTFs, are useless, since the direct measurements provide the input for the databases. Examples of databases that are used to develope PTFs are the FAO Harmonized World Soil database (FAO/IIASA, 2009), the Africa Soil Information Service (AfSIS)(Hengl et al., 2015), Hydraulic Properties of European Soils (HYPRES) (Wösten et al., 1999) and World Inventory of Soil Emission Potentials (WISE) (Batjes, 1996). Besides being cheaper and faster, PTFs are can be used to estimate parameters on a much larger scale, which is of interest for model studies. Direct measurements on the other hand, only provide very local values for a parameter.

The two main types of PTFs are: Class and continuous PTFs. Class PTFs predict hydrological properties based on a textural class, such as silt loam or loamy sand. Class PTFs are easy to use because they only make use of textural data (Wösten et al., 1995). However, the drawback is that only the average value of a hydrological characteristic within one textural class is given, even though there can be a substantial range within a textural class (Hodnett and Tomasella, 2002). According to Gutmann and Small (2007) hydrological properties can vary even more within one class than between classes. Continuous PTFs in contrast use a soils exact textural composition. Obtaining this composition makes the approach more expensive but also more precise (Wösten et al., 1995). A third but uncommon PTF type is the soil class PTFs, which takes the soils mineralogy into account (Hodnett and Tomasella, 2002). The problem here is that soil mineralogy data is not as widely available as the texture, bulk density or organic matter and that obtaining a soil's elemental compositions is time consuming and more expensive. This might be the reason why soil class PTFs are not found in many papers. PTFs that use too specific input parameters inhibit, or at least complicate the practical application of these PTFs (Schaap et al., 2001).

While PTFs might work well in the region where the data set comes from, applying them to other regions is difficult, because the soil forming factors differ and therefore the accuracy might decrease (Pachepsky et al., 1999). Most PTFs have been created for temperate regions or were based on temperate region databases such as HYPRES (Wösten et al., 1999; Hollis et al., 2012; Tóth et al., 2015). Moreover, most of the data in

the databases to derive the PTFs come from agricultural soils. Thus, these PTFs may not be applicable to tropical soils (van den Berg et al., 1997; Young et al., 1999) due to the different chemical and physical aspects of tropical and temperate soils (Agyare et al., 2007; Tomasella and Hodnett, 2004). While the soil forming factors are the same for the tropics and the temperate regions (Prescott and Pendleton, 1952 in Minasny and Hartemink, 2011), soils in the tropics formed on material that has been altered since the Precambrian by erosion, as well as deposition processes (Sanchez and Buol, 1975). The alternating humid and dry climate it the tropics leads to the tropical soils being heavily weathered, which is one of the reasons why they differ from temperate region soils. This might be an explanation for why temperate region PTFs can be inadequate in predicting tropical soil properties. A further issue with PTFs for tropical soils is that there is a lack of tropical soil data.

1.5 Study Aim and Research Questions

The aim of this study is to broaden our knowledge of the effects of tropical land use change on soil chemical, physical and hydrological characteristics. The specific research questions and hypotheses are

1) How do physical and chemical characteristics of soils in Eastern Madagascar differ for different land use types and depths

I hypothesise that the soil mineralogy will not be significantly different for the different land use types, but soil properties such as soil organic carbon, δ^{13}C and bulk density are significantly different. Furthermore, I hypothesise the biggest differences between the land-use types will be seen at the surface.

2) Can we predict K_{sat} from soil physical and chemical properties?

Hydrological properties can be extrapolated from soil properties measured by infrared spectroscopy (DRIFT) Existing PTFs do not predict the observed K_{sat} values well, but we can create a function that is able to predict K_{sat} for soils in Eastern Madagascar.

1.6 Thesis Structure

In the next chapter, the study area, the provided data and the methods used in this thesis will be elaborated on. The results presented in chapter 3 are split into *Soil Properties* and *K_{sat} prediction*, i.e. research question 1 and 2. In the discussion chapter (4) the results will be placed into the scientific context and the research questions and hypotheses will be revisited. In the last chapter (5) the main points are summarized and an outlook for future research is given.

2 Materials and Methods

In this section, the location of study area, as well as the provided data will be described. Furthermore, the methods applied in this thesis will be explained. This includes laboratory analysis, statistical analysis and the modelling approaches. The samples used in this thesis were provided by the P4GES Project (Can Paying 4 Global Ecosystem Services values reduce poverty?) (www.p4ges.org). The P4GES project is funded by the research program espa (ecosystem services for poverty alleviation). Eleven Institution from five nations (Madagascar, Netherlands, Switzerland, UK and USA) work together with the aim to alleviate poverty through influencing the development and implementing international ecosystem service payment schemes (P4GES, 2015).
Most of the samples were gathered between October and April 2014/15 during the rainy season. Some samples were collected a year earlier, in February and March of 2014. The K_{sat} measurements and thus the sample collection took place during the rainy season, because the soil cracks in the dry season which leads to a higher K_{sat}. All laboratory analysis were carried out at the Physical Geography Laboratories at the Department of Geography at the University of Zürich. The P4GES project gathered K_{sat} data for 48 sites. Only 37 sites, with a total of 89 samples, were used in this thesis due to the lack of samples or too little samples. Furthermore, some sites were neglected because they had land-use types that were not considered in this thesis.

2.1 Study Area

2.1.1 Location

Madagascar is located just off the south-eastern part of Africa in the Indian Ocean, across from Mozambique. The study was conducted in the Ankeniheny Zahamena Corridor (CAZ) on the eastern escarpment of Madagascar (Figure 2a, e). The CAZ is a newly established protected area with an extent of 381'000 ha (Portela et al., 2012). A mosaic of land-use types including national parks, villages, comumunity-managed zones, forest plantations and agriculture surrounds the CAZ's forests, wetlands and rivers, that are known for their exceptional biodiversity (Portela et al., 2012; Zwartendijk et al., 2017). The primary forests in the study area are classified as low and medium altitude evergreen humid forests. The CAZ is home to the majority of these forests in Madagascar (Andriamananjara et al., 2016). In Madagascar, slash-and-burn land-use continues to increases due to the increase in rural population and integration of rural regions into market oriented economy (Kull et al., 2007). Styger et al. (2007) further mention the lack of land title as a reason for the increasing slash-and-burn agriculture in Madagascar, as it impedes agricultural intensification. Land-use change in Madagascar is predominantly towards slash-and-burn cultivation, mixed fruit production and degraded land (Vliet et al., 2012).
Within three broad regions or Zones of Interest (*ZOIs*) camp ground or *sites* (as they will be called hereforth) were selected. The three ZOIs are Andasibe, Anjahamana and Didy. The ZOIs will be referred to as *ZOI 2*, *ZOI 3* and *ZOI 4*, respectively. The study area is characterised by steep slopes (>20°) (Zwartendijk et al., 2017). ZOI 2 (18°56'S 48°25'E) is located in the south east of the CAZ and is the southernmost of the three ZOIs, being roughly at the same latitude as Madagascar's capital city Antananarivo (Figure 2a). The sample sites in ZOI 2 range from 971 to 1029 m.a.s.l. With sites between 100 and 512 m a.s.l. ZOI 3 (18°37'S 48°97'E) has the lowest elevation of the three ZOIs. It is located between the other two sites in terms of N-S

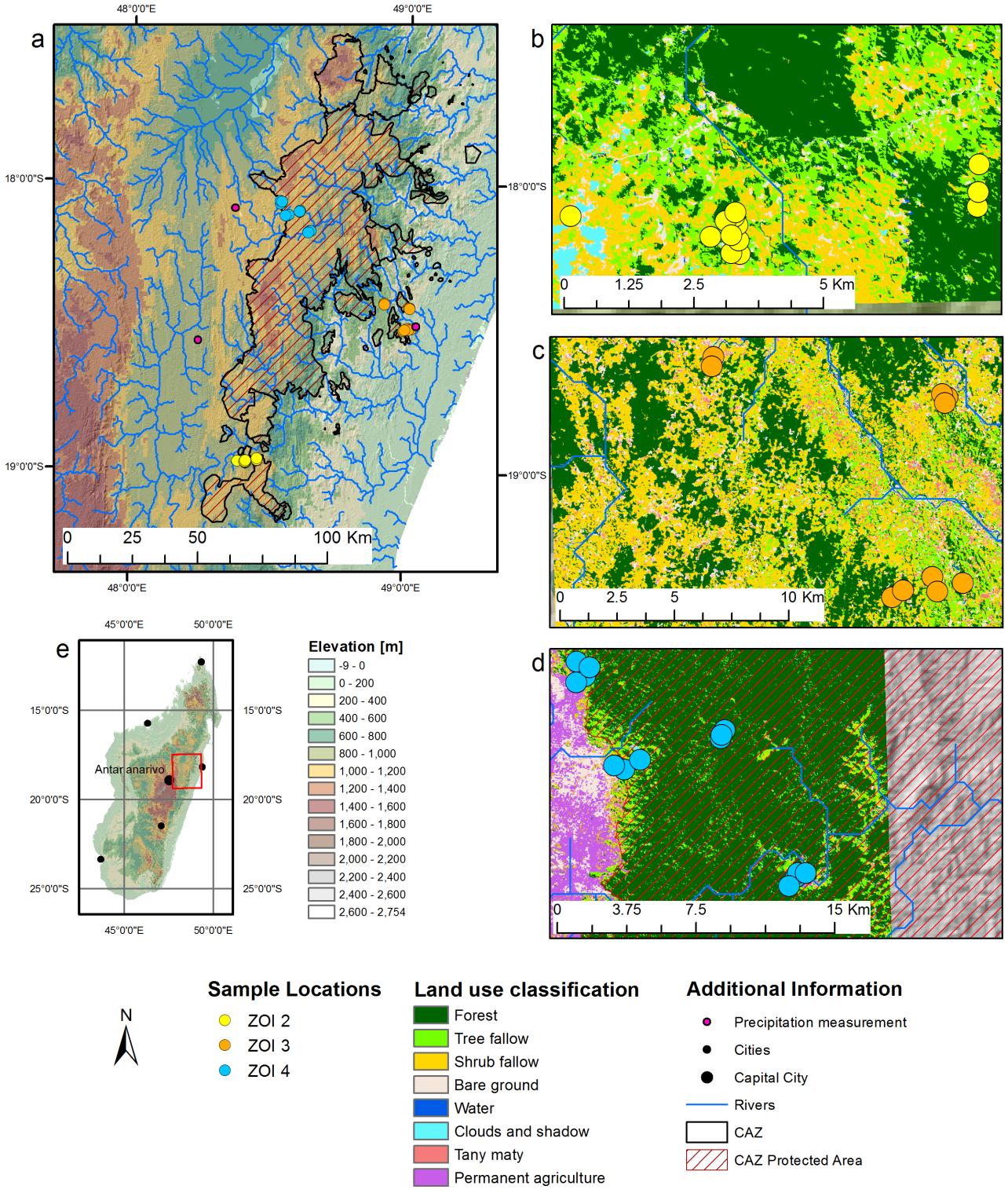

Figure 2: Overview of the Study Area. Map a shows the three ZOIs within the CAZ region. b, c, d are maps of ZOI 2, 3 and 4, respectively. Map e illustrates the location of map a within Madagascar. Sources: Land-use data: Horning and Hewson (2017) as part of P4GES project; CAZ data: P4GES project; Elevation data: Global 30 Arc-Second Elevation (GTOPO30) (USGS)

positioning and is the easternmost and wettest ZOI. ZOI 4 (18°07'S 48°32'E) is the northernmost ZOI and has a similar elevation range (942 to 1114 m a.s.l.) as ZOI 2. The sites in ZOI 3 and ZOI 4 have a similar extent of about roughly 60 km^2 and 50 km^2 with a maximum distance between the sample sites of approximately

16 km and 14 km, respectively (Figures 2c and d). ZOI 2's sample sites cover an area of approximately 4.5 km^2. The largest distance between two sites is 7 km (Figure 2b).

2.1.2 Climate

The wide range in elevation, the relative position to the dominant trade wind and the movement of the ITCZ (Intertropical Convergence Zone) leads to a great climatic variation within Madagascar (GFDRR, 2011; Tadross et al., 2008). Precipitation is higher on the east coast (up to 3700 mm per year) than on the west coast (Tadross et al., 2008; GFDRR, 2011). ZOI 3 is located in the wetter, 'prehumid bioclimate' zone whereas the other two ZOIs are located within the drier, 'humid bioclimate' zone (Andriamananjara et al., 2016). The mean annual precipitation (MAP) in CAZ is approximately 2500 mm and the mean annual air temperature (MAAT) varies between ca. 18 and 24°C (Andriamananjara et al., 2016) but within the CAZ annual rainfall varies from 1000 to 3500 mm (Soesbergen and Mulligan, 2018), making it difficult to generalise. Mean temperatures for the rainy and dry season are 22 °C and 15 °C, respectively, at 950 m a.s.l. (ZOI 2) (Zwartendijk et al., 2017). The mean annual precipitation measured in Andasibe (ZOI 2; 18°09'15"S 48°36'58"E, 929 m a.s.l.), Brickaville (ZOI 3; 18°49'11"S 49°03'53"E, 65 m a.s.l.) and Didy (ZOI 4; 19°02'12"S 46°43'57"E, 1131 m a.s.l.) are 1623 mm, 2438 mm and 1519 mm, respectively for the period 1983 to 2013 (Météo Madagascar, 2013). The rainy season takes place from November/December to March/April (Soesbergen and Mulligan, 2018; Gay-des Combes et al., 2017; Tadross et al., 2008) and accounts for approximately 75% of the annual precipitation (Soesbergen and Mulligan, 2018). The dry season lasts from April to October in the CAZ. The dry season is shortest for ZOI 3 (Figure 3). Cyclones are common during the rainy season (Gay-des Combes et al., 2017; GFDRR, 2011) and cause high inter annual variability in precipitation (Tadross et al., 2008). Gay-des Combes et al. (2017) showed the great impact of cyclones on soil degradation and thus agricultural yield.

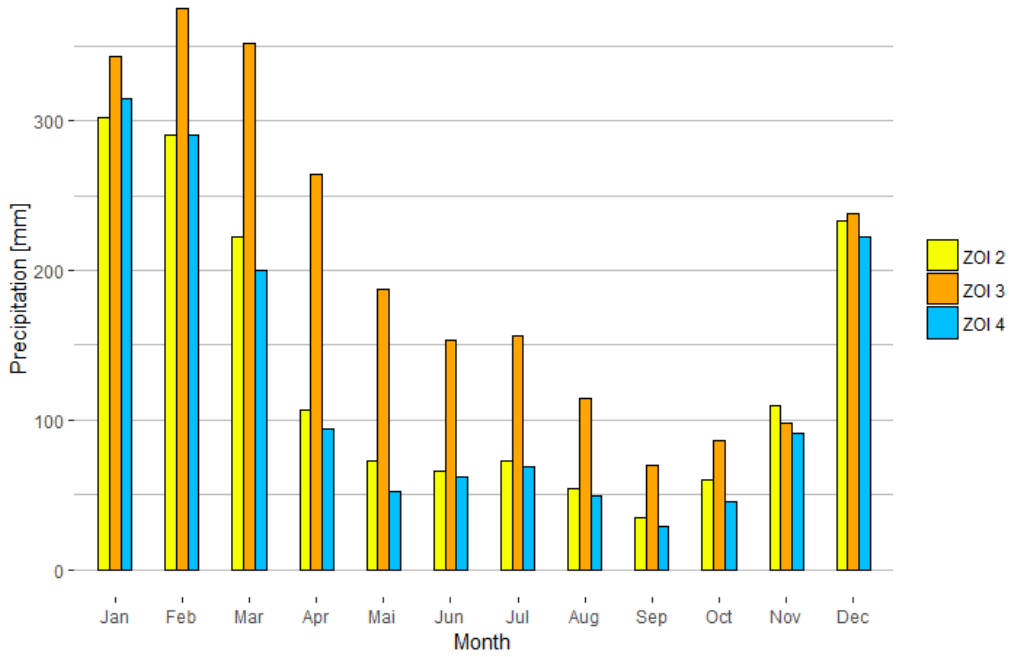

Figure 3: Comparison of the monthly precipitation averages over the period of 1983 - 2013 for the three ZOIs (Météo Madagascar, 2013). Precipitation was measured in Andasibe (ZOI 2), Brickaville (ZOI 3) and Didy (ZOI 4).

2.1.3 Geology and Soils

The geology of the study area is dominated by precambrian metamorphic and igneous basement rocks (Figure 4). The mainly metamorphic rocks include granites, migmatites and schists. Furthermore, lavas such as basalt and gabbro are present in the CAZ. Sporadically scattered ultrabasic rocks occur throughout the basement rock. Noticeable is an outcrop of nickel-rich ultrabasic rock close to ZOI 2 (not illustrated in Figure 4). Alluvial and lake deposited sedimentary rocks are also present in the CAZ (Figure 4) (Du Puy and Moat, 1996).

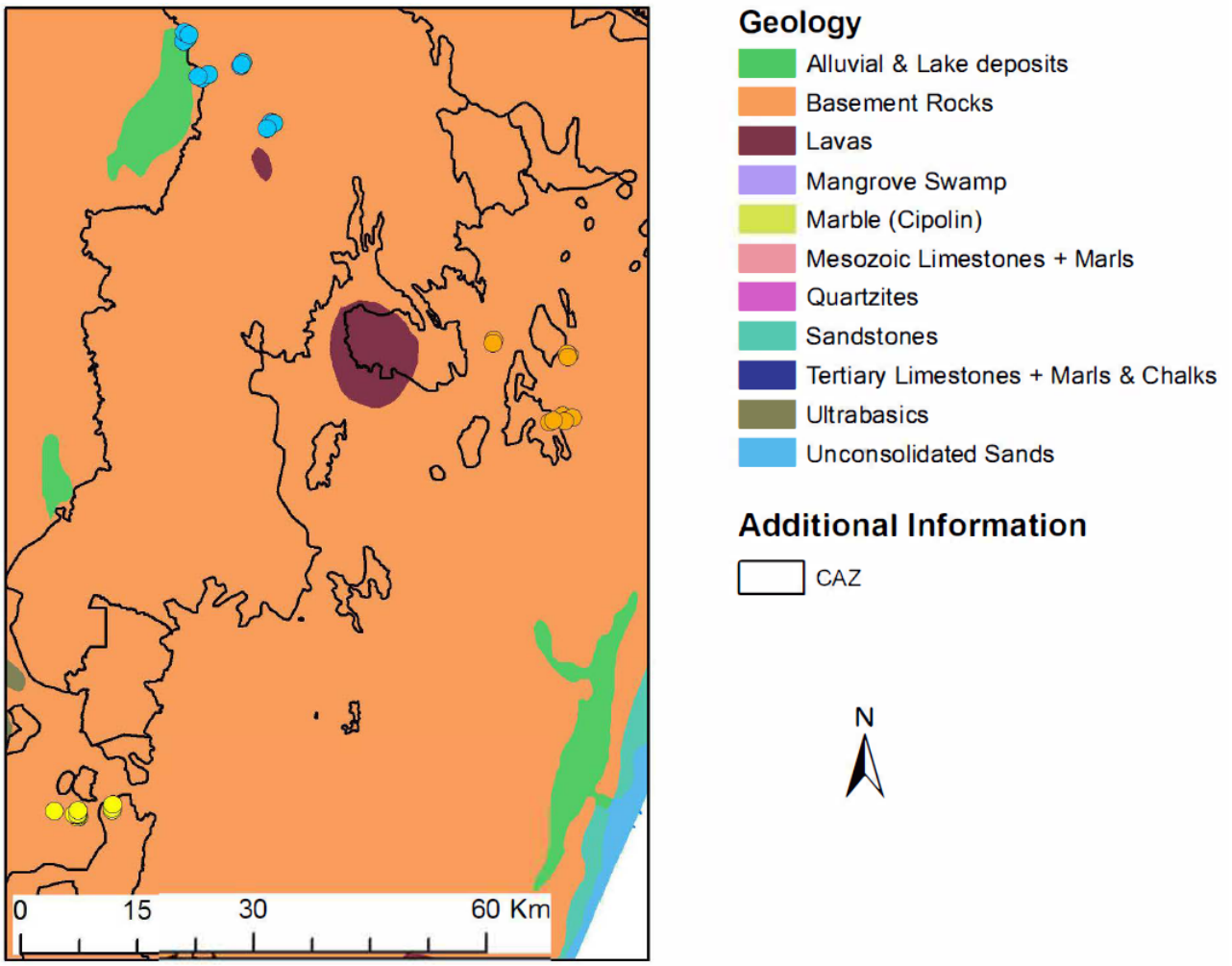

Figure 4: Geological map of the Study Area. Source: Du Puy and Moat (1996). The maps should be considered with caution, as they are rather coarse.

The soils are classified as Ferralsols (IUSS Working Group WRB, 2015). Many Ferralsols are called Oxisols (Soil Survey Staff, 2014) in the USDA classification (IUSS Working Group WRB, 2015). Ferralsols are found in hot, humid tropical regions. The heavily weathered soils have a distinctive yellow or red colour (Andriamananjara et al., 2016). They are characterised by a strongly weathered horizon, called the ferralic horizon which is dominated by low activity clays (kaolinites), quartz (sand) and oxides, predominantly Iron (Fe) and Aluminium (Al) (IUSS Working Group WRB, 2015). Due to the high decomposition rates in the tropics soil organic carbon is low (Andriamananjara et al., 2016). Ferralsols typically have a great soil depth, a good permeability and a stable microstructure making them less prone to erosion. Furthermore,

Ferralsols are well drained but also have a low available water storage capacity (IUSS Working Group WRB, 2015). In contrast to the good physical properties, the chemical properties are poor in terms of fertility. The cation exchange capacity (CEC) of Ferralsols is low. Furthermore, there is a deficit in bases (Ca, Mg, K). Given a low pH, aluminium is present, which fixates phosphate (P) and is toxic to many plant species (Deckers, 1993).

2.1.4 Land-use and Vegetation

Slash-and burn-agriculture (also swidden agriculture or *tavy* in Madagascar) is the main local agricultural system and the leading cause of deforestation. A plot of forest is cleared and the cut vegetation is burnt. The bare soil is then cultivated. As soon as the soil fertility is too low to grow crops any longer (usually after 2 years), a new plot of land is cleared, and the process starts anew. While the new plot is being cultivated, the first one lays fallow (Styger et al., 2007). After some years the fallow plot is incorporated into the slash-and-burn cycle again. Like many other practices, slash-and-burn agriculture does not have any large-scale environmental impacts as long as it is practised on a small scale (Kotto-Same et al., 1997; Styger et al., 2007) and the fallows are left to regenerate long enough. However, today, mainly due to population growth, slash-and-burn practices in Madagascar have become the leading cause of deforestation and land degradation (Styger et al., 2007). Increased population demands cultivation extension and reduction of fallow periods (Gay-des Combes et al., 2017).
Slash-and-burn impacts soil chemical and physical properties. The strongly alkaline ash of the burnt vegetation increases the soil's pH which positively affects microbial activity and thus nutrient availability (Kukla et al., 2019; Demeyer et al., 2001). However, large ash inputs can lead to nitrogen limitation in the soil because the ash contains little nitrogen (Demeyer et al., 2001). Regarding the soil physical characteristics slash-and-burn agriculture has a degrading effect. The ash can be easily eroded by wind or rain (Comte et al., 2012). The function of the fallow period in slash-and-burn agriculture is to restore the soils fertility to its initial values. However, the process of taking up nutrients from the atmosphere, as well as from the sub- and surface soil to regenerate forests takes up to 10 years (Thomaz et al., 2014; Styger et al., 2007). Over the last three decades, the fallow periods in Madagascar were reduced from 8-15 years to 3-5 years (Styger et al., 2007). The shortened fallow periods inhibit tree species to regenerate and lead to the tree species being replaced by shrubs and grassland (Styger et al., 2009). With fallow periods of 3 to 5 years the transition or degradation from forest to grassland only takes between 20 to 40 years (Styger et al., 2007).

Portela et al. (2012) mention the following land-use types in the CAZ: Cultivation, degraded humid forest, humid forest (no distinction made between low and mid altitude), littoral forest, grassland-woodland mosaic, wetland and wooded grassland-bushland. In this thesis I will only looked at four land-use types that were defined by the P4GES Project based on indicator vegetation (Figure 5): Forest, Tree Fallow, Shrub Fallow and Degraded Land. These land-use types represent the transition from Forest to (Degraded) Grassland caused by repeated slash and burn practices. Of the four categories only Forest represents primary vegetation, the other three land-use types are secondary vegetation. The Fallows are locally known as Savoka (Brand and Pfund, 1998).
More than 2'000 plant species can be found in the CAZ area (Portela et al., 2012). This plethora of plant species is the reason why only some of the most common ones will be mentioned for the Forest land-use. Typical plant or tree species for the Forest land-use are *Dalbergia*, *Diospyros*, *Ocotea*, *Symphonia* and

Tambourissa. At higher elevations Tapica (*Uapaca bojeri*) can be found (Burgess et al., 2004). The different fallows are mainly dominated by one single species or by a mixture of some major species (Styger et al., 2007). For the Tree Fallow these species are *Trema orientalis* and *Harungana madagascariensis* (both tree species). Furthermore, shrub species of the genus *Solanum* are present. In the Shrub Fallow the trees are replaced either by the endemic *Psiadia altissima* or by neophytes like the *Rubus moluccanus* or *Lantana camara*. These three types are replaced after the fifth cycle by herb vegetation such as ferns or *Imperata cylindrica* (Styger et al., 2007). After the seventh cycle the vegetation is dominated by the grass species of the *Aristida* genus. The grasslands represent the last stage of the degradation (Styger et al., 2009). Plants from some of the aforementioned genera can also be found in other land-use types. However, in that case they are non-dominant. Examples are *Trema orientalis* or *Aristrada* species in the Shrub Fallow land-use, *Harungana madagascariensis* in Shrub Fallow or *Imperata cylindrica* in Degraded Land (Styger et al., 2007). While Styger et al. (2007) state that *Harungana madagascariensis* is dominant in the Tree Fallow land-use, Figure 5 indicates that it is non dominant.

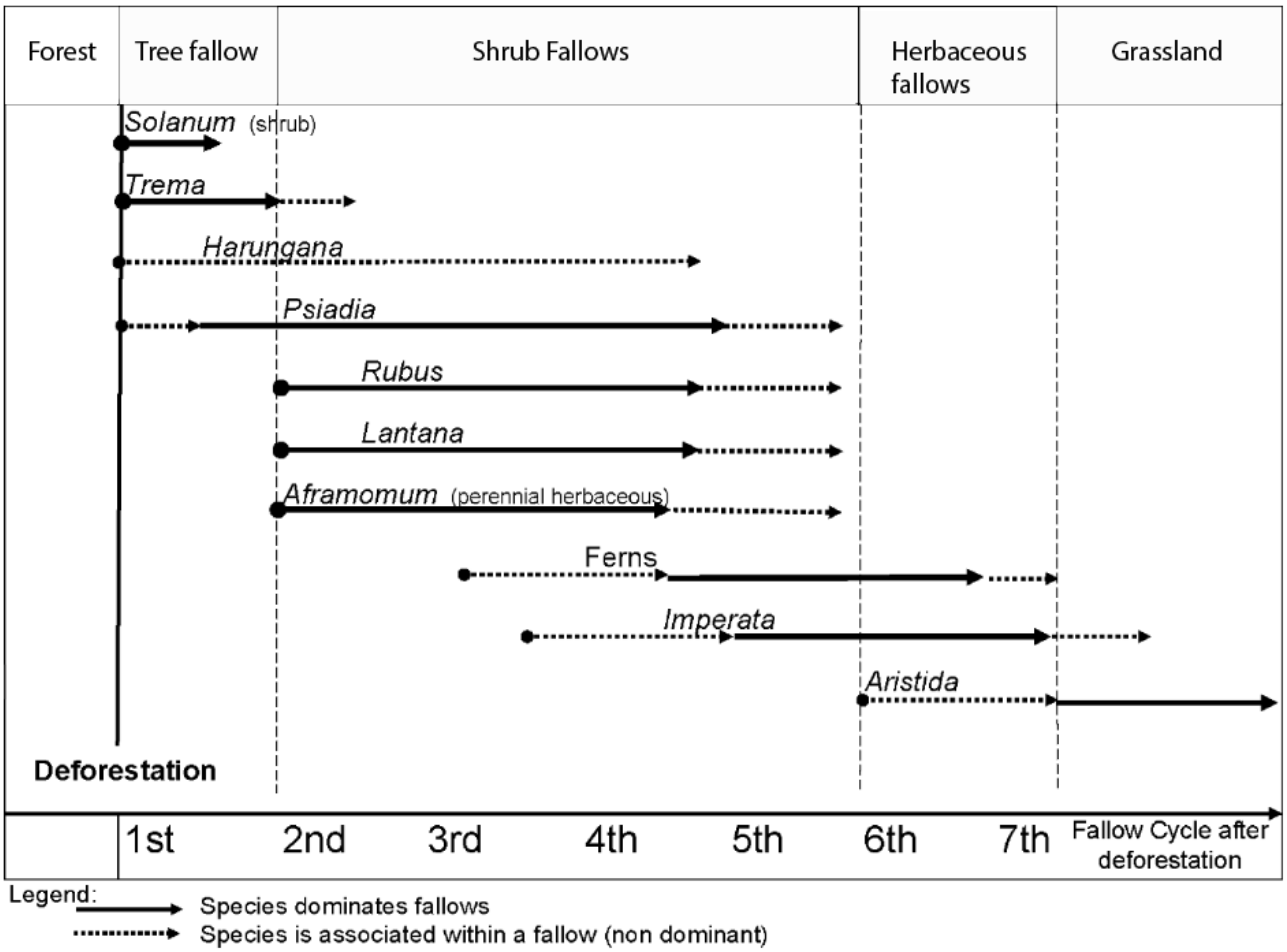

Figure 5: Dominant and non dominant plant species indicating the different land-use types and the different fallow cycles (Styger et al., 2007). In contrast to Styger et al.'s (2007) five land use types, this thesis will only consider four of them. The land use type Herbaceous Fallow was included in the Shrub Fallow land-use. In this study non-dominant plants are illustrated with a dotted line.

2.2 Data

The total number of sites used in this thesis is 37: 13 in ZOI 2, 10 in ZOI 3 and 14 in ZOI 4. The sample sites were selected based on their vicinity to all four land-use types. Forest (*F*), Tree Fallow (*TF*), Shrub Fallow (*SF*) and Degraded Land (*DL*). Out of all 89 samples, there were 19, 22, 28 and 22 samples Forest, Tree Fallow, Shrub Fallow and Degraded Land, respectively. Samples were taken at different depths below the surface: 0 - 10 cm (*Depth 0*), 10 - 20 cm (*Depth 1*) and 20 - 30 cm (*Depth 2*). These depths coincide with the main soil horizons (Zwartendijk et al., 2017). At 18 sites samples were taken from all three depths, 15 lack data for Depth 0, three were only sampled at Depth 0, and at one site only samples at Depths 0 and 1 were provided. The sample distribution between the ZOIs, land-uses and depths is illustrated in Table 1. A slope transect was selected, if it belonged to one of the four land-use types studied in this thesis (Forest, Tree Fallow, Shrub Fallow, Degraded Land). Five samples were taken along a slope transect (5 m apart) for each site and bulked to obtain one sample per depth for each sample site (Appendix: Table 13). It was ensured that the sample site were in the middle of the slope transect as samples at other sections of transect would be different due to erosion and accumulation processes. The five locations on a transect were chosen to include as much variability within a plot but not to have too much site effect. Sometimes one land-use was missing, which is why there is an unequal number of samples per land-use type. The three ZOIs were chosen to represent sites around CAZ.

The P4GES project provided porosity, bulk density, pH, K_{sat} and texture data. To measure porosity and bulk density a soil core (100 cm^3), for each of the five samples along the transect, was taken. Porosity was measured by comparing the saturated weight of the soil core with the dried (105°C for 24 hours) soil core. The bulk density was also measured with the dried soil core. The surface K_{sat} was measured with a double-ring infiltrometer. The subsurface K_{sat} was measured by the use of two Amoozemeters. For a more detailed explanation see Zwartendijk et al. (2017) or Amoozegar (1989). To measure the soil texture a scoop (little shovel/spoon) of soil at each of the five transect locations was taken, stored in zip-lock bags and oven dried (105°C for 24 hours). The soil texture was measured/analysed at the VU University in Amsterdam (The Netherlands) using a Helium-Neon Laser Optical System. The particle size distribution of the samples from site 56 and 57 was measured using X-ray absorption on a Micromeritics SediGraph® 5100 at the University of Zürich (Switzerland). The pH was measured at the VU University in Amsterdam (The Netherlands). Ten samples were analysed at the University of Zurich(see Table 13 in the Appendix): for eight samples because no data were provided and two samples were re-analysed to compare the remeasured values to the original ones. To measure the pH of the samples, they were mixed with water to create a solute. The solute's pH was then measured with a pH-meter (van Dijk, 2015). For the 10 samples 2 g of soil were used. The amount of water was adjusted to keep the same ratio as stated in van Dijk (2015).

Table 1: Overview of number of samples per ZOI specific land-use type and Depth (F = Forest, TF = Tree Fallow, SF = Shrub Fallow, DL = Degraded Land).

	ZOI 2				ZOI 3				ZOI 4			
	F	TF	SF	DL	F	TF	SF	DL	F	TF	SF	DL
Depth 0	0	4	3	1	0	0	0	0	4	3	4	3
Depth 1	0	3	4	3	3	2	3	2	4	3	4	3
Depth 2	0	3	4	3	3	2	3	2	4	3	3	3

2.3 Laboratory Analysis

From the unused remaining soil texture samples five spatulas of each of the five soil sample were bulked. If a sample had less than five spatulas of soil remaining, as much as possible was taken from it. The samples were oven dried at 60 °C for 24 hours and thereafter kept in a moisture-free environment. Organic material such as roots were extracted. All 89 samples were sieved to get rid of rocks and then milled with a Planetary Ball Mill with four Achat balls (Fritsche ®Pulverisette) in order to crush the aggregates. The samples were first milled for five and then for ten minutes. Due to the high compactness of the aggregates the samples had to be further ground with a mortar and pestle. The samples were sieved again to extract particle size < ≤ 100 μm from bigger particles. The samples were again dried at 60 °C for 24 hours. These soil samples (< ≤ 100 μm) were then used for the isotope ratio mass spectrometry (IRMS), for the X-ray flourescence (XRF) spectrometry, for the Diffuse Reflectance Infrared Fourier Transform spectroscopy (DRIFT) and for the pH remeasurements.

2.3.1 Isotope Ratio Mass Spectrometry

Isotope ration mass spectrometry (IRMS) was used to measure the relative abundance of ^{13}C and ^{15}N, the carbon and nitrogen content of the samples and the C/N ratio. Approximately 10 mg (range between 8 and 12 mg) soil per sample were weighed into tin caps with a Micro Scale Cubis MSU 6.6S-000-DM © 2009 Sartorius. After every 11 samples and after the last sample a chernozem control sample was weighed in. The global reference standard for ^{13}C is the Pee Dee Belemnite (PDB). Atmospheric nitrogen is widely used as a standard for ^{15}N (Mariotti, 1983). The isotopic signal was determined by measuring the samples with an elemental analyser IRMS (EA-IRMS) (Thermo Scientific ™EA-IRMS Delta V ™Plus) (Muccio and Jackson, 2009). The tin caps are dropped from a autosampler into a combustion chamber/tube (1800°C). The combustion produces carbon dioxide (CO_2), water vapour (H_2O), dinitrogen (N_2), nitrogen oxide (N_{O_x}), oxygen (O_2) and sulphur dioxide (SO_2). The gases are then transported by helium (He) to a reduction chamber, where the nitrogen oxides are reduced to dinitrogen and excess oxygen is extracted. In the chemical trap following the reduction chamber the water is removed. The last step is the separation of carbon dioxide and dinitrogen (Muccio and Jackson, 2009). Replicates were only made for a few samples to determine if the values were accurate. For a more detailed explanation see (Muccio and Jackson, 2009).

The percentage of carbon can be equated to soil organic carbon because the soil pH indicates that no inorganic carbon is left in the soil. The soil organic carbon was then multiplied by 1.72 (van Bemmelen factor) to approximate the (soil) organic matter (*(S)OM*) content (Soil Survey Staff, 2011). However, the van Bemmelen factor should be treated with caution as it assumes that 58% of soil organic matter is soil organic carbon. The soil organic carbon percentage can vary with soil type, depth and the type of organic matter (Pribyl, 2010). Multiplying the percentage of carbon or soil organic matter with 10 gives the amount of C or soil organic matter in g kg^{-1}. Eq. 1 was used to calculate the stocks of soil organic carbon in mg C ha^{-1}.

$$SOC = \Sigma(BD_i * C_i(1 - CF_i * t_i * 0.1) \quad (1)$$

Where SOC [mg C ha^{-1}] is the carbon stock for the three individual depths as well as for all depths combined. BD_i is the bulk density [g cm^{-3}] of the soil, C_i is the soil organic carbon in the soil [g kg^{-1}], CF_i is the the

percentage of sand (> 2 mm) in the soil and t_i is the horizon thickness [cm] (Andriamananjara et al., 2016).

2.3.2 X-ray Fluorescence Spectrometry

The elemental composition of the soil was measured with X-ray fluorescence (XRF) spectrometry. The soil sample is exposed to polychromatic short wavelength X-ray. The X-ray excites electrons to move from an inner, low energy level shell to a outer, higher energy level shell. The earlier gained energy is emitted when the electrons returns back to the inner shell. The emitted energy is called fluorescent or secondary X-rays. The characteristics of the emitted wavelength tells us which element they come from. The concentration of the element can be determined from the intensity of the emitted energy (Jenkins, 1999). For more details see (Jenkins, 1999; SPECTRO Analytical Instruments, 2005). All elements between the atomic numbers of Sodium (Na) and Uranium (U) can be analysed with XRF (SPECTRO Analytical Instruments, 2005). A big advantage of XRF is, that it is non-destructive to the elemental composition of a sample. However, for living samples the radiation is too intensive (Penner-hahn, 2013).
A sample cup was filled with approximately 5 g soil sampleand then closed with a lid. At its bottom the sample cup has a SpectroMembrane® Prolene® Thin-Film. This film had to be put onto the sample cup with producing wrinkles as this would have influence the measurement results. Seven of these cups and a SO_4 standard were placed in a Spectro XEPOS (AMETEK Materials Analysis Division) at the time. The SO_4 standard was used to ensure valid output results. The resulting percentages of the elemental concentrations (given by the Spectro XEPOS) were converted into the percentage of oxides in the soil with the help of a conversion table (Prof. Dr. Markus Egli, University of Zurich, personal communication).

2.3.3 DRIFT Spectroscopy

Diffuse Reflectance Infrared Fourier Transform spectroscopy (DRIFT) was used to measure the soil samples' MIR spectra (Griffiths and de Haseth, 2007). DRIFT is an infrared (*IR*) spectroscopy technique that is used to measure the Mid-infrared (MIR) spectra of matter. *Diffuse Reflectance* implies that the rays of the incident radiation are scattered in all directions instead of just one as in specular reflection (Arnoff, 2005). *Infrared* denotes which specific part of the electromagnetic spectrum is used: Most often MIR (4000 - 400 cm^{-1}) (Stuart, 2015). MIR is used, as it has been shown to produce better soil property identification than NIR (near infrared) or VIS-NIR (visible to NIR spectral range) (Minasny and Hartemink, 2011; Araújo et al., 2015). However, Cohen et al. (2007) successfully used VIS-NIR to predict K_{sat}. *Fourier Transform* describes a curve's decomposition into the different frequencies. For a more in-depth description of Fourier Transform and Interferometry see Griffiths and de Haseth (2007) or Stuart (2015).*Spectroscopy* describes the interaction between electromagnetic radiation and matter (Herrmann and Onkelinx, 1986).
IR spectroscopy or vibrational spectroscopy uses atomic vibrations to identify molecular structures. Most often the absorption capabilities of a material are determined by measuring the reflectance and inferring the absorption. The IR spectrum is obtained by sending IR radiation through a sample and measuring the fraction of the incidental radiation that is reflected (Stuart, 2015; Griffiths and de Haseth, 2007). This is measured with a spectrophotometer, an instrument that measures the intensity of light relative to wavelength (Griffiths and de Haseth, 2007). The measured spectrum can be plotted as a graph, with the x-axis representing the wavenumber [cm^{-1}] and the y-axis representing the absorbance/the absorbed energy (Vogt and Finlayson-Pitts, 1994). The wavenumber is the number of wavelengths (λ) per unit distance ($1/\lambda$) (Griffiths and de Haseth, 2007). Soil properties such as minerals or chemical compounds can be identified by

comparing the spectrum peaks at particular wavenumbers with the help of absorption/peak-identification tables. Cohen et al. (2007) did not produce K_{sat} prediction that were applicable for quantitative purposes. However, they were able to produce semi quantitative predictions that can be useful for mapping soil hydraulic properties for large areas and for K_{sat} estimations at field- and catchment-scale. The large data set (~ 2000 samples), the limited variation in the soil mineralogy and "only" having samples up to 15 cm depth were key points that helped to estimate K_{sat} (Cohen et al., 2007). PLSR and GBT (Gradient-boosted tree) approaches were used to predict natural log-transformed soil properties.

All samples were milled as mentioned in section 2.3. The spectra were measured with a Bruker TENSOR 27 spectrophotometer, with a resolution of 4 cm^{-1} and processed with the OPUS Spectroscopy Software (version 5.5; Bruker, 2019). Potassium Bromide (KBr) was used as reference background because it is inert to MIR. Besides being used as the reference background, KBr was measured at the beginning and end of each measurement session. To see if there were major changes. To be able to check the data for possible deviations, a Chernozem (IUSS Working Group WRB, 2015) sample was analysed at the beginning and the end of each measurement session as well as after every 15 samples.
For the analysis, first the CO_2 peak, which was caused by the respiration of the people working in the laboratory, was removed from the obtained data. Then, the baseline was corrected. Lastly, noise was removed from the spectra. The CO_2 correction was done by removing CO_2 bands with peak removal algorithms. By measuring the samples, the ideally flat baseline - lying at 0% when measuring for absorbance - can be changed due to reflection, scattering in the air, temperature, concentration or instrument anomalies (Griffiths and de Haseth, 2007). To correct this baseline offset a concave rubber band correction with 10 iterations was applied. The ruber band correction was used to divided the spectrum into sections. The lowest point in each section is determined using linear interpolation or a spline to determine the lowest point in a section. From these lowest point the baseline is estimated (Shen et al., 2018). For more details on concave rubber band correction see Pirzer and Sawatzki (2008) or Calabrò and Magazù (2010). The CO_2 band was excluded from this correction, since the spectra were already correced for CO_2 in the first data processing step. Last, the noise caused by wetness of the air has to be removed to obtain a better signal-to-noise ratio. This is done with spectral smoothing. All spectra were smoothed with 17 smoothing points. However, smoothing has a negative effect on the spectral resolution (Griffiths and de Haseth, 2007).

2.4 Data Analysis

2.4.1 Statistical analysis of soil properties

The data were analysed in RStudio (R Core Team, 2018). The tests used in this thesis all used a significance level of $\alpha = 0.05$. If p-value was lower than α the null-hypothesis (H_0) was rejected. Of all soil properties that were measured, either with IRMS or XRF Spectrometry, or for which data was provided by the P4GES Project, the most important ones were used to analyse the soil for the different ZOIs, land-use types and depths: Soil organic carbon, $\delta^{13}C$, nitrogen, $\delta^{15}N$, the carbon/nitrogen ratio, sand , silt, clay, porosity, bulk density, pH, phosphorous pentoxide (P_2O_5), potassium oxide (K_2O), magnesium oxide (Mg_2O), iron oxide (Fe_2O_3), copper (Cu), aluminium oxide (Al_2O_3) and silicon dioxide (SiO_2). Diagnostic plots (e.g. Q-Q plot) were used to test the data for normality. Using the One-Way ANOVA it was determined, whether the ZOIs, land-use types and depths were significantly different for those soil properties. Furthermore, descriptive statistics for the soil properties were compared with each other in tables as well as plots.The One-Way

Analysis of Variance (ANOVA) was used to compare the means of more than two independent groups were the same (H_0). This was done to test if the mean values for the ZOIs, land-use types and depths. A least significant difference (*LSD*) test was applied to analyse the variance between the individual groups, if the ANOVAs H_0 was rejected (Dodge, 2008).
The Coefficient of Variation (*CV*) allows for comparison between two or more different data sets in relation to their means and tells us the spread of the data. The CV [%] is obtained by dividing the standard deviation (SD) by the mean and multiply this with 100 %.

$$CV = \frac{SD}{mean} * 100\% \tag{2}$$

2.4.2 Pedotransfer Function

The first step to generate a PTF for tropical soils, is to test if existing PTF could already estimate the K_{sat} well enough. Several PTFs were found during the literature research. However, only functions that were based on the soil texture (sand, silt and clay), the bulk density, soil moisture content at field capacity , porosity, drainable porosity, soil organic carbon or the organic matter were used. PTFs with other input data had to be excluded due to the lack of those input parameters. To assess the existing Pedotransfer Functions ((multiple) linear regressions), the coefficient of determination (more commonly knowns as R^2 (Eq. 3)) the Mean Absolute Error (*MAE* (Eq. 4)), the Root Mean Square Error (*RMSE* (Eq. 5)), as well as 1-1-plots of the predicted vs. the measured values were used. The discrepancies between the predicted and the actual K_{sat} data is represented by the difference between the solid black 1-1-line and the regression curve (dashed line). This was done for the complete data set, subsets for the land-use types or depths as well as subsets for specific depths of a land-use type.

$$R^2 = \left(\frac{\Sigma_{i=1}^{n}(M_i - \overline{M})(P_i - \overline{P})}{\sqrt{\Sigma_{i=1}^{n}(M_i - \overline{M})^2}\sqrt{\Sigma_{i=1}^{n}(P_i - \overline{P})^2}} \right)^2 \tag{3}$$

$$MAE = \frac{\Sigma_{i=1}^{n} \mid M_i - P_i \mid}{n} \tag{4}$$

$$RMSE = \sqrt{\frac{\Sigma_{i=1}^{n}(M_i - P_i)^2}{n}} \tag{5}$$

$$MSD = \frac{1}{n}\Sigma_{i=1}^{n}(M_i - \overline{M})^2 \tag{6}$$

Where M is the measured value, P is the is the predicted variable and n is the number of samples (Bayabil et al., 2019). R^2 varies on a scale from 0 - 1. MAE and RMSE are each expressed in the unit of the respective soil property.If the criteria: $R^2 > 0.7$, the predicted median K_{sat} < factor 1.5 of the measured median K_{sat} (measured median $K_{sat} \pm 0.75$ of measured median K_{sat}) are met and if the 1-1-plot passes a visual inspection then the K_{sat} prediction method is considered to be accurate enough.

As a next step soil properties were correlated to K_{sat} to identify which soil parameters should be used in PTFs. Linear regression was used to create linear or multiple linear regression models. The highest correlating soil

properties were put into the linear model. Many soil characteristics had very low correlation with K_{sat} so that soil properties with correlation values as low as 0.25 had to be used. Stepwise, the least significant of the "high correlation" soil properties were removed. This process is called backwards elimination. Since these PTFs didn't work well, a trial and error approach was further used to develop the linear regressions. Like for the existing PTFs (R^2, MAE, RMSE and 1-1-plots were used to assess the accuracy of the developed PTFs. In addition to these accuracy assessment methods the mean squared deviation (*MSD*) (Eq. 6; also known as the mean squared error) was used to judge the developed PTFs. The MSD was split into 3 components to get an insight in the causes of the MSD: squared bias (*SB*), nonunity slope (*NU*) and lack of correlation (*LC*) (Gauch et al., 2003). Squared bias is caused by translation and thus occurs when the two means are not equal. The rotation of a regression causes the nonunity slope to arise. Lack of correlation is caused by data scatter. More details on the three MSD components can be found in Gauch et al. (2003). Leave One Out Cross Validation (*LOOCV*) was used to validate the performance of the new PTFs.

2.4.3 DRIFT

Peak Identification is a qualitative approach that relates spectral peaks at specific wavenumbers [cm^{-1}] with the measured sample's components (Soriano-disla et al., 2014). Peak identification was done to get an understanding of the soil spectra.

The chemometric technique: Partial Least Squares Regression (PLSR), a numeric factor analysis, was used to predict K_{sat} (McCarty et al., 2002). PLSR identifies a linear regression model by projecting the independent (here: DRIFT spectra) as well as the dependent variables (here: K_{sat}) into a new space. PLSR detects fundamental connections between the dependent and the independent variables (McCarty et al., 2002; Mevik and Wehrens, 2007). The connections are based on covariance of the independent variable with the dependent variable (Cohen et al., 2007). The number of components/ independent variables that are used to predict the dependent variable is decided by the user. The more components are used the higher the percentage of the variance is explained. However, the number of components used impacts the accuracy of the prediction, with a tendency of a higher RMSE with more components. The aim was to get at least 90 % of variance explained but at the same time still aiming to have a relatively low RMSE (threshold RMSE < 0.75 of the measured median K_{sat}). If the RMSE criterion is met, then K_{sat} will be predicted and judged after the same criteria as the PTFs. Table 9 depicts that the number of components chosen varies for the different data sets. The number of components of decided upon, depends on trade off between having a high percentage of explained variance and as little RMSE as possible. PLSR indicates to the user which peaks in the spectrum are of interest when predicting the dependent variable (K_{sat})(Cohen et al., 2007). The data set needs to be large enough that it can be separated into training and verification sets to measure the accuracy as well as the reliability of the predictions (Cohen et al., 2007). As done for the developed PTFS leave one out cross validation was used to validate the PLSR.

3 Results

3.1 Soil Characteristics

Results concerning the soil physical properties, the carbon and nitrogen related properties and the soil nutrients. Table 2 gives an overview for which soil properties the mean values are significant different per ZOI, land-use or depth. All but four (δ^{13}C, phosphorus pentoxide, silicon dioxide and bulk density) of the main soil properties are significant different for the ZOIs. Less than half of the soil properties had significant different mean values for the different depths. Approximately 2/3 of the soil properties had significant different mean values for the land-use types.

Table 2: Level of significance for the difference in the mean values of the soil properties when grouped by ZOI, the land-use type or the depths. Signficance codes: 0.0001 '***'; 0.001 '**'; 0.01 '*'; 0.05 '.'; 0.1 ' '. There is an un-equal number of samples per land-use types and ZOIs thus comparisons is need to be done.

Soil Property	Abbreviation	ZOI	Land-use	Depth
Aluminium oxide	Al_2O_3	**		*
Soil ogranic carbon	SOC	***	*	***
Carbon - nitrogen ratio	C/N	**	*	*
Copper	Cu	***		
Carbon-13	^{13}C		***	
Iron(III) oxide	Fe_2O_3	***	***	
Potassium oxide	K_2O	***	.	
Phosphorus pentoxide	P_2O_5		**	
Magnesium oxide	MgO	***		
Nitrogen	N	***		***
Nitrogen-15	^{15}N	**	**	
Silicon dioxide	SiO_2		**	*
Sand	T_{sand}	***		
Silt	T_{silt}	**	.	
Clay	T_{clay}	***		
Bulk density	BD		***	***
pH	pH	**	***	
Porosity	φ	***	*	***

Table 3 provides some descriptive statistics, such as min, median, mean and max, for the soil properties of all samples together. In Table 4 the mean and the min - max range for each land-use type per ZOI and for the all samples per ZOI are listed. No differentiation between the depths is provided in Table because there are few soil properties for which mean values were significantly different with depth.

Table 3: Description and statistics of the main soil properties (n: sample size). See Table 2 for the explanation of the soil properties.

Soil property	unit	n	Min.	1st Qu.	Median	Mean	3rd Qu.	Max.
AL_2O_3	%	89	22.9	30.5	34.3	35.7	40.3	48.1
SOC	%	89	1.9	2.8	3.4	3.7	4.4	8.7
C/N	-	89	10.4	13.5	15.0	15.5	16.6	28.2
Cu	%	89	0.0003	0.0012	0.0017	0.0024	0.0037	0.0099
$\delta_{13}C$	‰	89	-27.8	-27.0	-26.6	-26.4	-26.0	-23.2
Fe_2O_3	%	89	7.8	12.4	16.8	16.4	19.5	27.7
K_2O	%	89	0.02	0.04	0.06	0.11	0.12	1.36
P_2O_5	%	89	0.00	0.06	0.10	0.11	0.15	0.47
MgO	%	89	0.21	0.45	0.51	0.53	0.63	0.92
N	%	89	0.09	0.18	0.22	0.25	0.31	0.68
$\delta_{15}N$	‰	89	2.2	4.0	4.7	5.4	7.2	10.0
SiO_2	%	89	17.2	36.6	41.9	41.5	45.9	58.0
T_{sand}	%	89	8	37	56	49	62	88
T_{silt}	%	89	3	12	14	15	17	35
T_{clay}	%	89	8	24	30	35	43	71
BD	$g\ cm^{-3}$	89	0.83	1.11	1.19	1.22	1.29	2.19
pH	-	89	3.36	4.30	4.80	4.39	5.20	5.76
φ	%	89	34	45	53	50	56	64

Table 4: Mean and range (min-max) for the main soil properties per ZOI's and land-use types. The soil characteristics that are depth dependent are indicated with a '*'. See Table 2 for the explanation of the soil properties.

		ZOI 2					ZOI 3				
		All	F	TF	SF	DL	All	F	TF	SF	DL
Soil Properties	n	28	0	10	11	7	20	6	4	6	4
Al_2O_3 [%]*	mean	30.75	-	31.11	31.67	28.79	41.28	41.05	40.96	45.54	35.56
	range	22.93 - 38.89	-	28.73 - 33.99	28.47 - 38.89	22.93 - 32.83	27.22 - 48.07	36.22 - 48.07	36.84 - 45.70	43.98 - 47.12	27.22 - 43.34
SOC [%]*	mean	3.53	-	3.85	3.50	3.12	2.86	3.12	2.73	2.80	2.69
	range	2.02 - 8.72	-	2.02 - 8.72	2.45 - 5.10	2.13 - 4.32	1.89 - 3.64	2.11 - 3.64	2.22 - 2.97	2.15 - 3.45	1.89 - 3.24
C/N [-]*	mean	14.91	-	14.85	14.40	15.80	19.57	17.22	20.31	19.95	21.81
	range	12.82 - 18.15	-	12.82 - 17.04	12.82 - 16.71	14.42 - 18.15	15.74 - 28.16	15.74 - 19.83	17.03 - 23.33	15.76 - 24.95	15.87 - 28.16
Cu [%]	mean	0.00	-	0.00	0.00	0.00	0.00	0.00	0.00	0.00	0.00
	range	0.001 - 0.005	-	0.002 - 0.05	0.001 - 0.005	0.002 - 0.005	0.000 - 0.010	0.000 - 0.010	0.001 - 0.005	0.000 - 0.002	0.001 - 0.003
$\delta^{13}C$ [‰]	mean	-26.02	-	-26.66	-25.91	-25.29	-27.15	-27.62	-27.09	-26.73	-27.13
	range	-27.5 to -23.3	-	-27.5 to -26.1	-26.8 to -25.1	-26-3 to -23.3	-27.8 to -25.8	-27.8 to -27.2	-27.4 to -26.8	-27.3 to -25.8	-27.5 to -26.9
Fe_2O_3 [%]	mean	18.76	-	18.53	20.01	17.13	17.54	19.05	18.09	17.12	15.35
	range	10.76 - 25.91	-	12.40 - 21.73	12.72 - 25.07	10.76 - 21.94	9.04 - 25.22	13.46 - 25.22	16.81 - 19.14	13.46 - 19.28	9.04 - 20.58
K_2O [%]	mean	0.11	-	0.17	0.08	0.06	0.07	0.07	0.08	0.04	0.12
	range	0.017 - 1.356	-	0.02 - 1.36	0.02 - 0.54	0.04 - 0.09	0.02 - 0.14	0.02 - 0.11	0.04 - 0.14	0.02 - 0.07	0.11 - 0.12
P_2O_5 [%]	mean	0.09	-	0.07	0.07	0.12	0.19	0.26	0.19	0.16	0.12
	range	0 - 0.194	-	0.00 - 0.12	0.00 - 0.10	0.04 - 0.19	0.07 - 0.47	0.11 - 0.47	0.15 - 0.24	0.11 - 0.20	0.07 - 0.17
MgO [%]	mean	0.46	-	0.46	0.46	0.45	0.50	0.50	0.44	0.59	0.42
	range	0.24 - 0.72	-	0.24 - 0.72	0.33 - 0.62	0.34 - 0.50	0.21 - 0.67	0.31 - 0.59	0.24 - 0.57	0.50 - 0.67	0.21 - 0.50
N [%]*	mean	0.24	-	0.27	0.25	0.20	0.15	0.18	0.14	0.15	0.13
	range	0.137 - 0.680	-	0.14 - 0.68	0.15 - 0.40	0.14 - 0.26	0.09 - 0.22	0.11 - 0.22	0.09 - 0.17	0.09 - 0.21	0.11 - 0.18
$\delta^{15}N$ [‰]	mean	5.08	-	5.41	5.46	4.01	3.81	3.13	4.24	4.21	3.79
	range	2.28 - 9.13	-	3.95 - 8.34	2.79 - 9.13	2.28 - 5.17	2.18 - 6.19	2.18 - 4.15	3.82 - 4.82	2.84 - 6.19	3-40 - 4.34
SiO_2 [%]*	mean	43.21	-	43.29	40.69	47.08	34.83	32.33	35.35	30.88	43.97
	range	33.92 - 57.98	-	37.92 - 47.06	33.92 - 47.19	37.43 - 57.98	17.20 - 57.95	17.20 - 42.56	31.38 - 38.80	25.32 - 37.23	29.95 - 57.95
T_{sand} [%]*	mean	30.92	-	32.95	34.42	22.81	60.65	55.54	71.45	62.65	54.53
	range	8.29 - 69.73	-	8.29 - 69.73	15.70 - 64.97	12.70 - 38.00	35.32 - 88.08	38.99 - 71.75	61.99 - 78.98	42.91 - 88.08	35.32 - 67.31
T_{silt} [%]*	mean	18.08	-	16.82	15.17	24.27	11.60	12.72	8.25	10.25	15.30
	range	2.70 - 29.20	-	5.90 - 26.03	2.70 - 25.20	20.40 - 29.20	3.29 - 18.74	10.31 - 17.30	6.06 - 11.88	3.29 - 14.98	9.06 - 18.74
T_{clay} [%]*	mean	51.00	-	50.23	50.42	52.92	27.75	31.75	20.30	27.11	30.18
	range	17.53 - 70.80	-	17.53 - 65.83	22.90 - 70.80	41.60 - 66.34	8.63 - 47.59	17.94 - 44.40	14.45 - 26.13	8.63 - 42.11	23.63 - 47.59
BD [g cm^{-3}]	mean	1.25	-	1.39	1.15	1.23	1.21	1.17	1.26	1.19	1.25
	range	0.91 - 2.19	-	0.91 - 2.19	0.96 - 1.32	1.10 - 1.40	1.04 - 1.40	1.04 - 1.25	1.13 - 1.40	1.08 - 1.31	1.15 - 1.35
pH [-]*	mean	4.91	-	4.98	4.79	4.98	4.79	4.30	5.13	4.88	5.05
	range	4.40 - 5.76	-	4.49 - 5.56	4.40 - 5.76	4.70 - 5.20	3.90 - 5.50	3.90 - 4.60	4.80 - 5.50	4.60 - 5.20	4.70 - 5.30
φ [%]	mean	55.57		56.74	49.03	52.77	46.59	50.72	46.15	42.92	46.33
	range	44.60 - 63.80		52.00 - 61.80	48.80 - 63.80	44.60 - 58.00	34.42 - 56.92	41.66 - 56.92	34.42 - 56.38	37.22 - 50.06	38.32 - 53.30

* Significant difference with depth

(*Continued on next page*)

Table 4: Continued

Soil Properties	n	ZOI 4 All 41	F 12	TF 9	SF 11	DL 9
Al_2O_3 [%]*	mean	36.26	36.94	34.21	34.70	39.48
	range	28.70 - 46.56	28.70 - 46.56	30.54 - 37.88	30.21 - 40.56	33.96 - 44.25
SOC [%]*	mean	4.21	4.66	3.27	4.32	4.40
	range	2.15 - 7.11	3.12 - 6.61	2.36 - 5.18	2.15 - 6.72	2.76 - 7.11
C/N [-]*	mean	13.92	13.88	12.29	13.76	15.80
	range	10.44 - 17.34	10.44 - 15.94	11.61 - 13.52	12.34 - 17.07	14.71 - 17.34
Cu [%]	mean	0.00	0.00	0.00	0.00	0.00
	range	0.000 - 0.004	0.001 - 0.004	0.001 - 0.002	0.001 - 0.004	0.000 - 0.002
$\delta^{13}C$ [‰]	mean	-26.26	-26.92	-26.58	-26.18	-25.16
	range	-27.5 to -23.2	-27.5 to -26.4	-27.2 to -25.9	-26.9 to -25.2	-26.5 to -23.2
Fe_2O_3 [%]	mean	14.34	17.63	11.50	14.51	12.58
	range	7.80 - 27.69	11.08 - 27.69	8.84 - 14.60	11.27 - 18.03	7.80 - 21.20
K_2O [%]	mean	0.14	0.10	0.24	0.07	0.18
	range	0.03 - 0.48	0.04 - 0.18	0.17 - 0.31	0.04 - 0.21	0.03 - 0.48
P_2O_5 [%]	mean	0.09	0.11	0.05	0.10	0.06
	range	0.00 - 0.21	0.00 - 0.74	0.00 - 0.11	0.00 - 0.21	0.00 - 0.16
MgO [%]	mean	0.59	0.55	0.70	0.55	0.60
	range	0.27 - 0.92	0.40 - 0.74	0.52 - 0.92	0.27 - 0.77	0.41 - 0.76
N [%]*	mean	0.30	0.34	0.27	0.31	0.28
	range	0.17 - 0.52	0.20 - 0.52	0.19 - 0.45	0.17 - 0.50	0.18 - 0.46
$\delta^{15}N$ [‰]	mean	6.36	6.00	6.99	6.80	5.61
	range	2.75 - 9.96	2.75 - 9.22	3.83 - 9.96	4.18 - 9.55	2.99 - 9.02
SiO_2 [%]*	mean	43.63	38.99	49.09	45.01	42.52
	range	31.37 - 55.46	31.37 - 54.38	44.29 - 55.46	40.10 - 54.03	35.60 - 46.92
T_{sand} [%]*	mean	57.25	52.90	59.37	57.36	60.77
	range	28.34 - 79.93	28.34 - 71.63	51.78 - 67.72	33.34 - 79.93	54.26 - 67.04
T_{silt} [%]*	mean	14.28	16.16	13.05	14.34	12.94
	range	6.44 - 34.63	9.52 - 34.63	8.24 - 16.47	6.44 - 21.32	11.98 - 14.85
T_{clay} [%]*	mean	28.47	30.93	27.58	28.31	26.29
	range	13.63 - 45.34	16.54 - 42.60	24.04 - 32.60	13.63 - 45.34	20.86 - 31.85
BD [g cm^{-3}]	mean	1.19	1.08	1.31	1.24	1.16
	range	0.83 - 1.55	0.83 - 1.42	1.16 - 1.55	1.10 - 1.36	0.88 - 1.43
pH [-]*	mean	4.75	3.96	5.00	5.11	5.07
	range	3.36 - 5.70	3.36 - 4.60	4.50 - 5.40	4.40 - 5.68	4.30 - 5.70
φ [%]	mean	48.74	53.58	43.89	46.40	50.27
	range	34.40 - 63.40	44.60 - 63.40	34.40 - 51.20	40.20 - 54.50	36.60 - 63.40

* Significant difference with depth

3.1.1 Soil Physical Properties

All soil samples lie within 6 of the 12 USDA textural classes, mainly along the sand - clay axis (Figure 6). This coincides with De Condappa et al.'s (2008) findings of bi-modal particle-size distribution in tropical regions, where the silt content is comparatively lower than the sand and clay content. The different depths and land-use types seem to be distributed more or less evenly across the different soil texture types (Figure 6). Sand, silt and clay content are all significantly different between the three ZOIs. ZOI 2 has considerably more T_{silt} and clay and considerably less sand than the other two ZOIs (Figure 7).

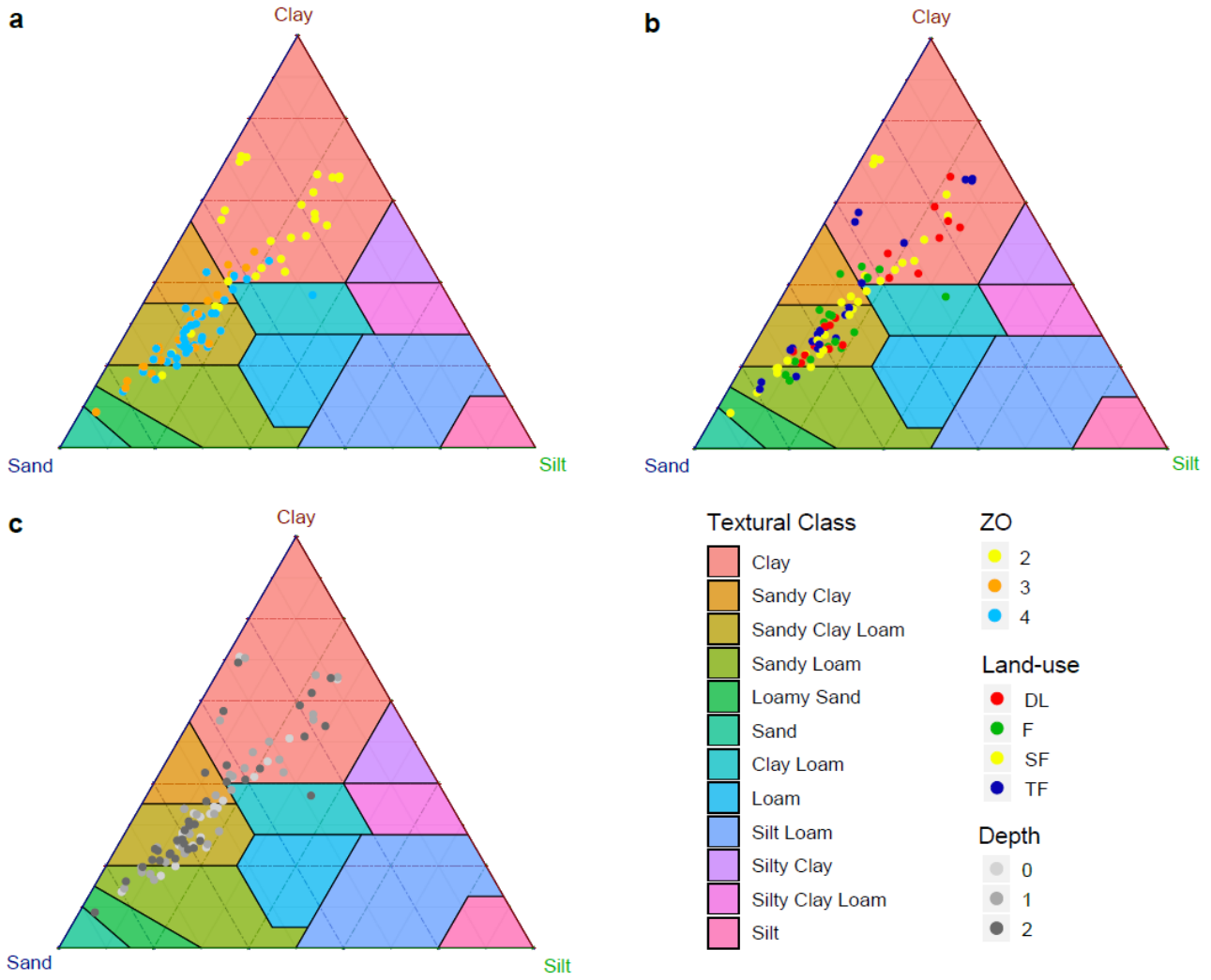

Figure 6: Soil texture of the samples, colour coded by ZOIs (a), land-use types (b) and depths (c) and the textural classes of the USDA soil classification ($T_{clay} < 0.002$ μm; $T_{silt} < 0.05$ μm; $T_{sand} > 2$ mm) (Soil Survey Staff, 2014). Data provided by the P4GES Project.

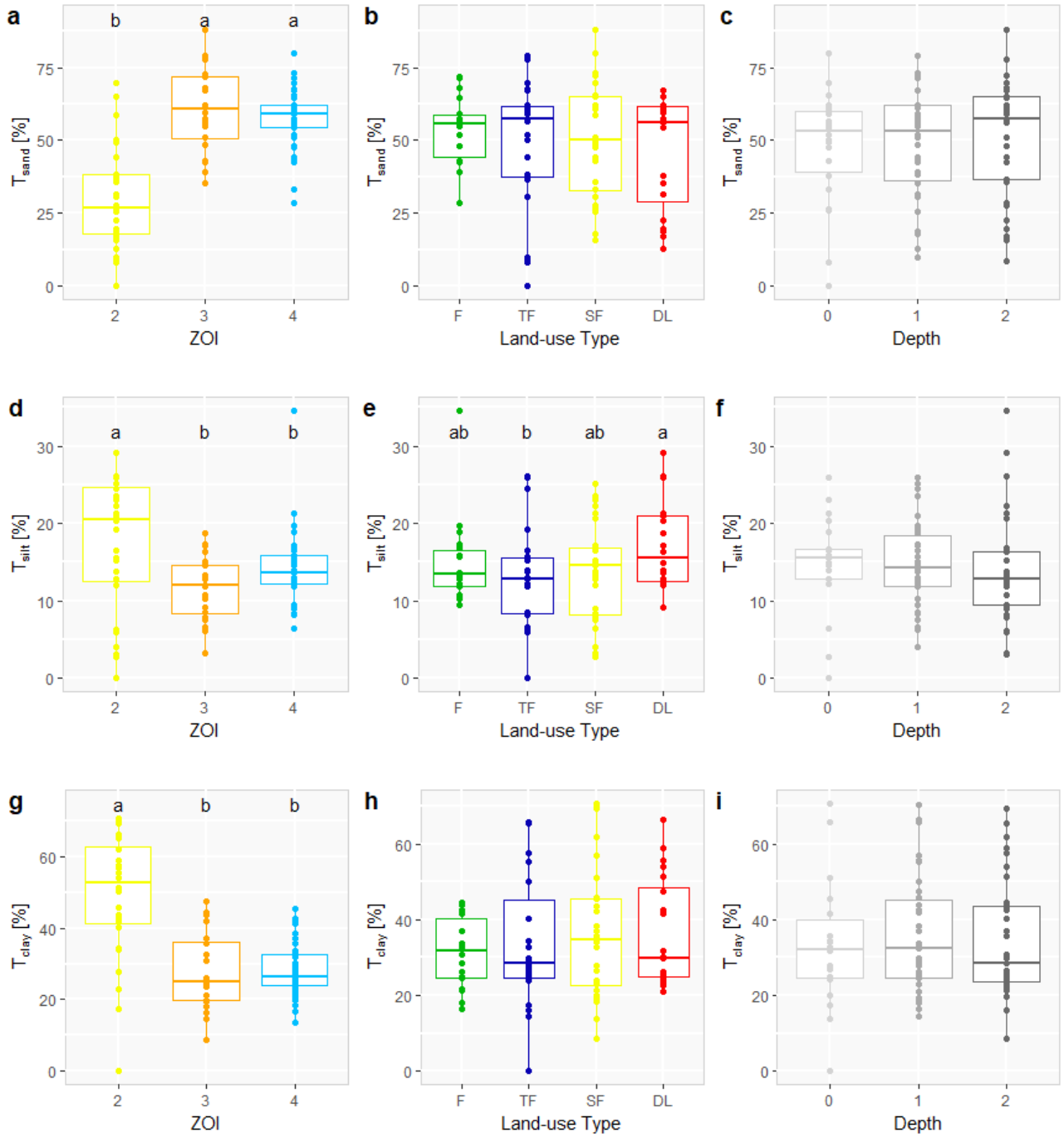

Figure 7: Percentage of sand (T_{sand}; top, a - c), silt (T_{silt}; middle, d - f) and clay (T_{clay}; bottom, g - i) grouped by ZOIs (left), the land-use (middle) and the depths (right). Different letters indicate significant differences in the mean values for the different groups. Where no letters are present the mean values did not differ for the different groups. The box of the boxplot represents the middle 50 % of the data for the group. The solid horizontal line in the box illustrates the median. The lower and upper wisker are ± 1.5 * inter-quartile range. The dots represent the actual data points. Data provided by the P4GES project.

Porosity decreased with depth below the surface and was significantly different for the ZOIs and the depths (Figure 8a - c). For both ZOI 2 and Depth 0 porosity was significantly higher than for the other two ZOIs and depths, respectively. There was no significant difference in porosity for the land-uses, although there was a weak trend of decreasing porosity with an increasing number of fallow cycles.
Bulk density (BD) differed with both land-use type and depths below the surface (Figure 8d - f). Bulk density was significantly lower in the Forest than that for the other three land-uses (Figure 8d). Moreover, bulk density increased with increasing depth (Figure 8f). A Tree Fallow sample site from ZOI 2 is an extreme outlier with bulk density > 2.0 g cm^{-3}.
The scatter in the pH was substantial, particularly for ZOI 4 and Depth 0. pH was only significantly different for the land-use types (Figure 8h), with the Forest soil being more acidic.
In Figure 9 the K_{sat} per depth and land-use type is illustrated. Especially at Depth 0 there was a clear difference in K_{sat} between Forest and Degraded Land. K_{sat} was 10 and 100 times bigger at Depth 0 than Depth 1 and Depth 2, respectively (Figure 8l; Figure 9a - c).

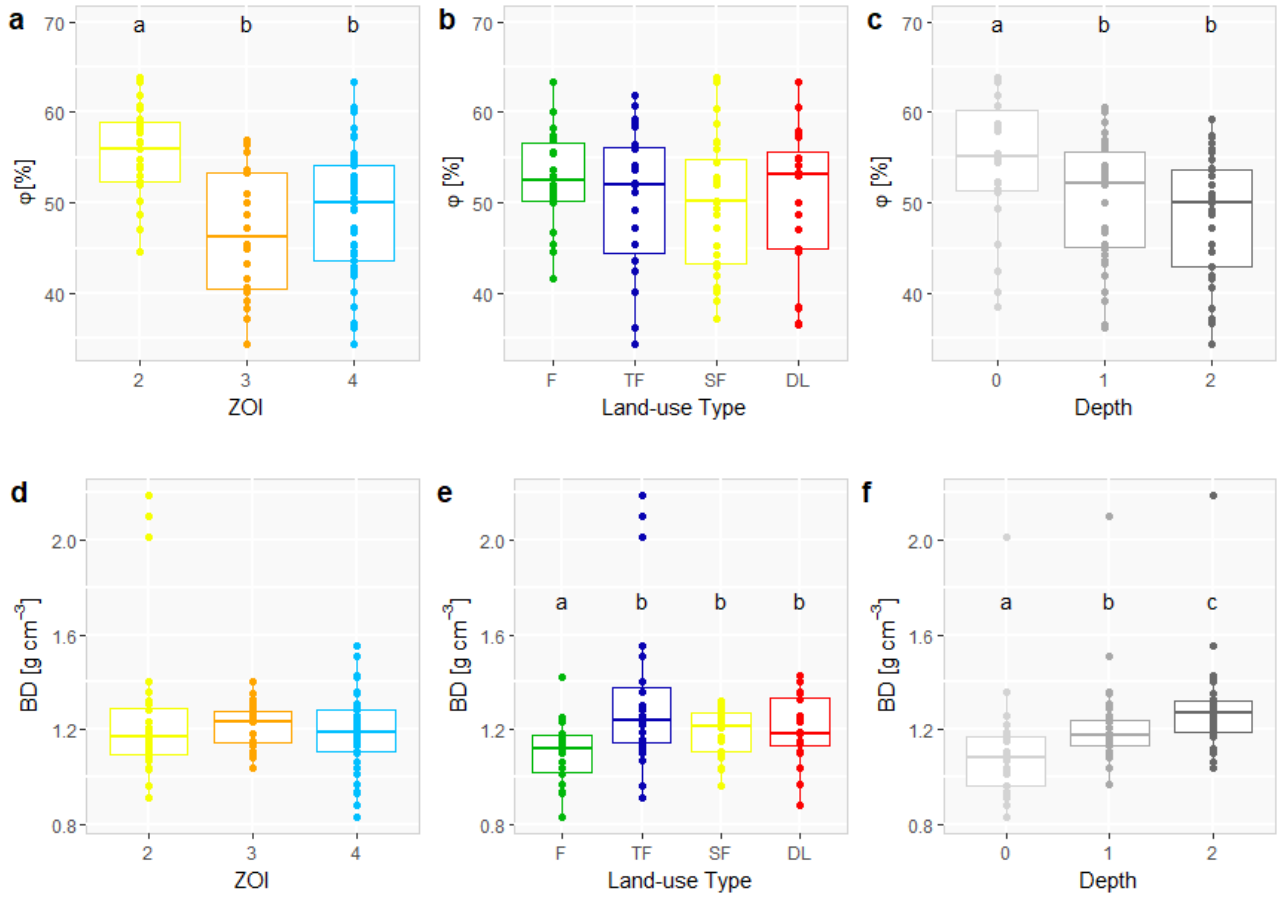

Figure 8: Boxplots of porosity (φ; top, a - c), bulk density (BD; second from top, d - f), pH (secon from bottom, g - i), K_{sat} (bottom, j - l) grouped by ZOIs (left), the land-use (middle) and the depths (right). Different letters indicate significant differences in the mean values for the different groups. Where no letters are shown the mean values did not differ for the different groups.

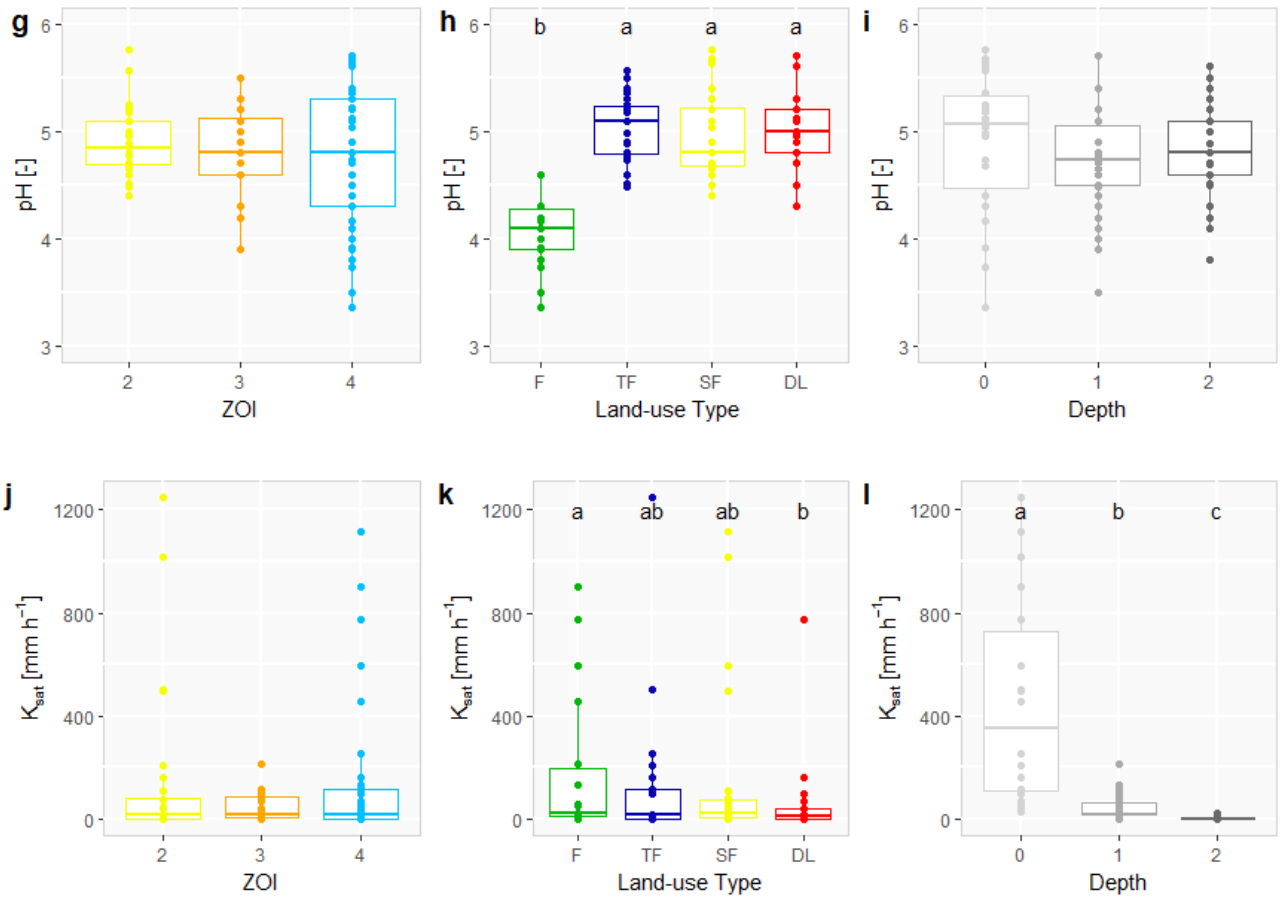

Figure 8: Continued

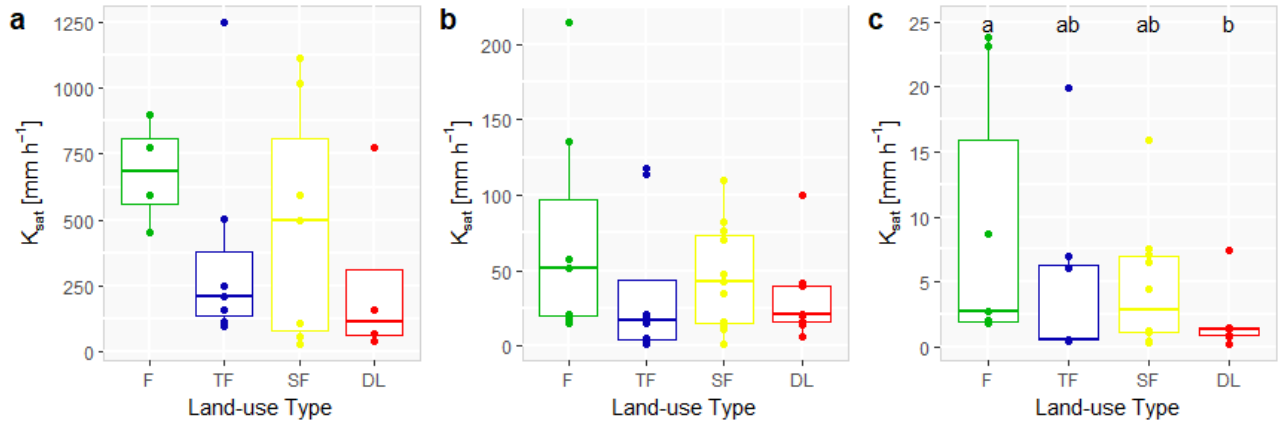

Figure 9: Boxplots of K_{sat} for the different land-use types grouped by depth. Depth 0 (a), Depth 1 (b), Depth 2 (c). Different letters indicate significant differenes in the mean values for the different groups. Where no letters are shown the mean values did not differ for the different groups.

3.1.2 Carbon and Nitrogen

Soil organic carbon clearly decreased with depth below the soil surface (Figure 10c). Concerning the land-use types, soil organic carbon was significantly higher in Forest than the other land-uses(Figure 10b). Soil organic carbon differed for the ZOIs significantly as well (Figure 10a). $\delta^{13}C$ increased from Forest to Degraded Land but did not differ for the different ZOIs nor the depths (Figure 10d - f). Like soil organic carbon, there was a clear decrease in nitrogen with increasing depth. The difference in nitrogen for the

ZOIs was similar to the pattern for soil organic carbon (Figure 10g, a).

3.1.3 Elements and Oxides

The most prominent oxides in the soil are: iron oxide, aluminium oxide and silicon oxide, ranging approximately from 10 to 50 % (Table 3). Both phosphorus pentoxide and potassium oxide make up a tiny fraction of the soil (Combined less than 0.5 % or 5 g kg^{-1}) (Figure 11).
phosphorus pentoxide did not vary significantly with depth or the ZOIs but was significantly higher in the Forest than the other land-uses (Figure 11a - c). potassium oxide was significantly higher in ZOI 4 compared to the other two ZOIs and significantly lower in the Shrub Fallow than the other three land-uses (Figure 11d - f).

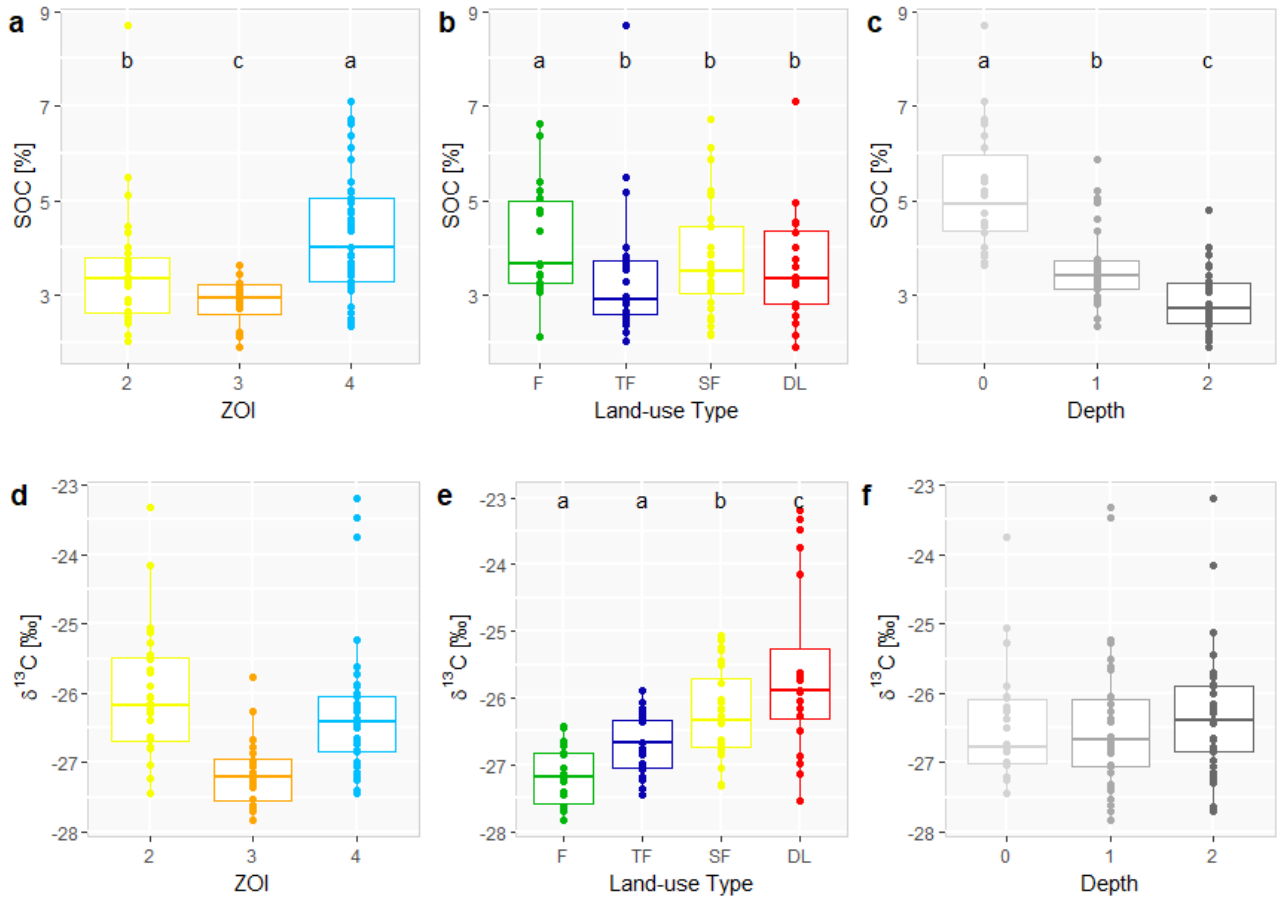

Figure 10: Boxplots of soil organic carbon (top, a - c), $\delta^{13}C$ (middle, d - f) and nitrogen (bottom, g - i) grouped by ZOIs (left), the land-use (middle) and the depths (right).Different letters indicate significant differences in the mean values for the different groups. Where no letters are shown the mean values did not differ for the different groups.

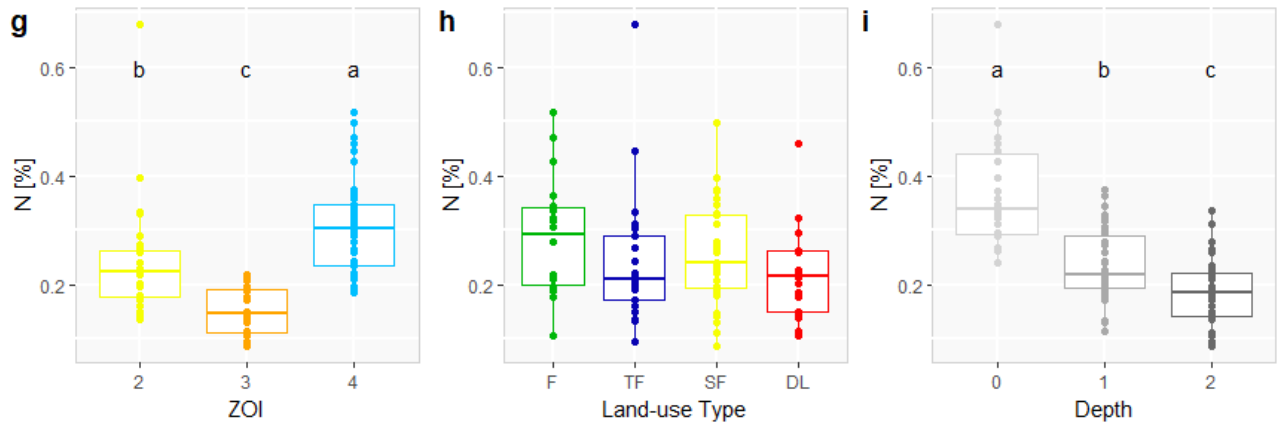

Figure 10: Continued

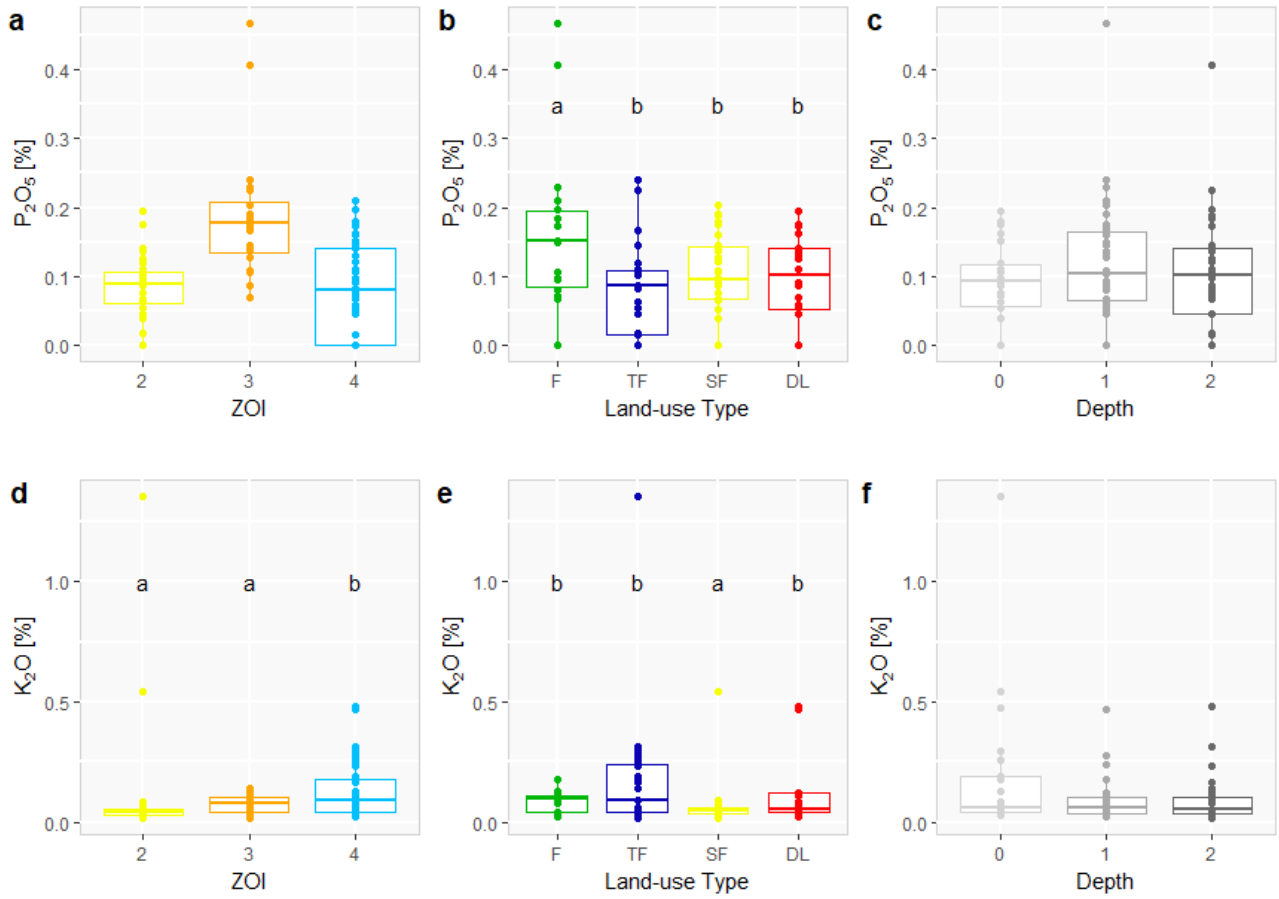

Figure 11: Boxplots of phosphorus pentoxide (P_2O_5; top, a - c) and potassium oxide (K_2O; bottom, d - f) grouped by ZOIs (left), the land-use (middle) and the depths (right). Different letters indicate significant differenes in the mean values for the different groups. Where no letters are shown the mean values did not differ for the different groups.

3.2 Pedotransfer Functions

3.2.1 Existing PTFs

To my knowledge, there is no existing PTF for the CAZ region or Madagascar. The literature review suggests that there are many PTFs to predict K_{sat}. However, many of the PTFs use less widely available input variables,

such as pore size and the air-entry pressure, for which I did not have any data. Thus, the predictive ability of these functions could not be determined. Some functions, for which the data set had all the input variables, produced far to high values (up to 10^9) or otherwise unreasonable K_{sat} values (exponents between -11 and -36, no output due to logarithm of negative numbers) and were not analysed further. Some PTFs resulted in too high $_{sat}$ values because of too big multipliers. Examples are the functions of Brakensiek et al. (1984), Campbell and Shiozawa (1994), Puckett et al. (1985), Dane and Puckett (1994), Saxton et al. (1986) (all papers found in Ghanbarian et al. (2016)). The remaining ten functions can be found in Table 5.

Table 5: The Ten existing PTFs used to predict K_{sat}.* The PTFs found in Nemes et al. (2005) were not found in the original Wösten et al. (2001) paper.

PFT no.	Function	units	Reference
1	$K_{sat} = 24^* [9.56 - 0.81 \log (T_{silt}) - 1.09 \log(T_{clay}) - 4.64 BD]$	cm day^{-1}	Jabro (1992)
2	$K_{sat} = 60.96 * 10^{(-0.6 + 0.0126 * T_{sand} - 0.0064 * T_{clay})}$	cm day^{-1}	Cosby et al. (1984)
3	$K_{sat} = 10.8731 + 3.9140 * \ln(\varphi)$	mm h^{-1}	Forrest et al. (1985) [as given in Minasny and Mcbratney (2000)]
4	$K_{sat} = 10.4778 + 3.4106 * \ln(\varphi)$	mm h^{-1}	Bristow et al. (1999) [as given in Minasny and Mcbratney (2000)]
5	$K_{sat} = 9.3413 + 4.3595 * \ln(\varphi)$	mm h^{-1}	Bridge (1968) [as given in Minasny and Mcbratney (2000)]
6	$\ln(K_s) = 20.62 - 0.96*\ln(T_{clay}) - 0.66*\ln(T_{sand}) - 0.46 * \ln(OM) - 8.43*D_b$	cm day^{-1}	Vereecken et al 1990 [as given in Nemes et al. (2005)]
7	$\ln(K_s) = 45.8 - 14.34 * D_b + 0.001481 * T_{silt}^2 - 27.5*D_b^{-1} - 0.891*\ln(T_{silt}) - 0.34 * \ln(OM)$	cm day^{-1}	Wösten et al. (2001) [as given in Nemes et al. (2005)*]
8	$\ln(K_s) = -42.6+8.71 * OM + 61.9 * D_b - 20.79 * D_b^2 - 0.2107 *OM^2 - 0.1622 * T_{clay} * OM - 5.382 * D_b * OM$	cm day^{-1}	Wösten et al. (2001) [as given in Nemes et al. (2005)*]
9	$K_{sat} = 0.023 + 0.1862 * T_{clay} - 0.0134 *\varphi$	cm h^{-1}	Oshunsanya (2013)
10	$K_{sat} = 0.0974 + 0.213*T_{clay} - 0.005 OC - 0.0157 *\varphi$	cm h^{-1}	Oshunsanya (2013)

BD/D_b = bulk density [g cm^{-3}], T_{clay} = clay [%], (S)OC = (soil) organic carbon [%], (S)OM = (soil) organic matter [%], T_{sand} = sand [%], T_{silt} = silt [%], φ = effective porosity [%]

The R^2, MAE and RMSE (Eq. 3 - 5) for these functions for the whole data set, each depth, each land use type and for each depth per land-use type are provided in Table 6. The soil properties of the existing PTFs were only a significantly correlated with K_{sat} for few data sets (Table 6). For only three functions (PTF 3, 4 and 5) was the R^2 (> 0.7) good enough to be considered further. The three PTFs produced good results for the Forest land-use type at Depth 1 (F1) (n = 7) and 2 (F2) (n = 7) but not for the other land-use types for which they over/under estimated the K_{sat}, possibly because the linear regression just used the porosity as input, despite other soil properties, such as bulk density, the texture or the soil organic carbon, having a bigger influence on K_{sat} in the other land-use types.

The three PTFs have the same structure:

$$K_{\text{sat}} = b + x * ln(\varphi),$$

Where b is the intercept, x is the multiplicator and $ln(\varphi)$ is the natural logarithm of the porosity. The three

different versions of this linear function have the same R^2 (0.83) for Depth 1 and 2 (criteria: $R^2 > 0.7$). While the R^2 is high, the plots of predicted vs. measured K_{sat} values show a bad fit (Figure 12). Figure 13 allows a comparison between PTF 3, 4 and 5 between the two depths. To do so the predicted K_{sat} values were divided by the measured K_{sat} values and then multiplied by 100 %. While the three PTFs in Depth 1 are closer to 100 % (perfect fit) than the three PTFs in Depth 2, the values are still not accurate. Also, a look at the predicted values already indicates that the prediction cannot be good. All predicted values lie within 25 and 27 mm h^{-1}. Even best of the existing PTFs provide rather bad K_{sat} predictions. The MAEs and RMSEs for PTF 3, 4 and 5 for Depth 1 are around 7.4 mm h^{-1} and 84.00 mm h^{-1}, respectively. Despite having the same R^2 as Depth 1, the three functions have lower MAE and RMSE values at Depth 2 of around 4.00 mm h^{-1} and 19 mm h^{-1}, respectively. Comparing the RMSE values of the two depth relative to the mean measured K_{sat}values (RMSE/mean measured K_{sat} * 100 %) it can be seen that Depth 1 has comparably better RMSE values (~ 115 %) than Depth 2 (~ 215 %).

The RMSE values of all three PTFs for Depth 1 and Depth 2 are ~ 84 mm h^{-1} and ~ 19 mm h^{-1} (Table 6)(median K_{sat}: Forest Depth 1 = 51.2 mm h^{-1}; Forest Depth 2 = 2.7 mm h^{-1}).

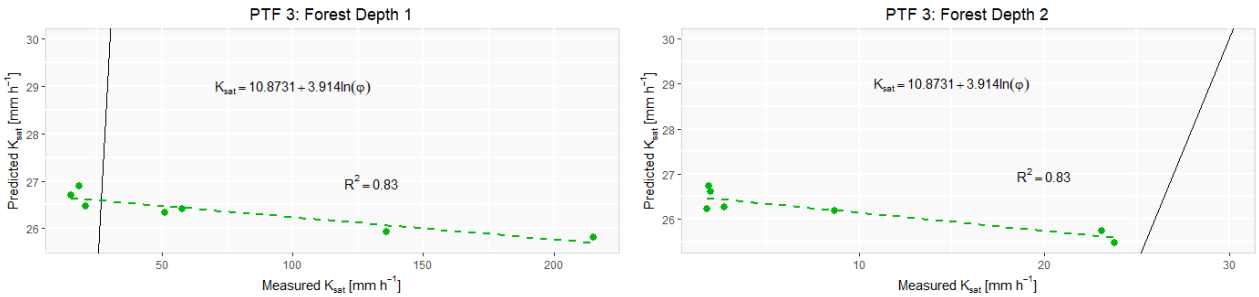

Figure 12: Plots of the predicted vs. the measured Ksat for Forest for PTF 3 for Depth 1 (left) and Depth 2 (right). The solid black line is the 1-1 line. The dashed line illustrates the linear regression curve. The function as well as R^2 is denoted in the graph.

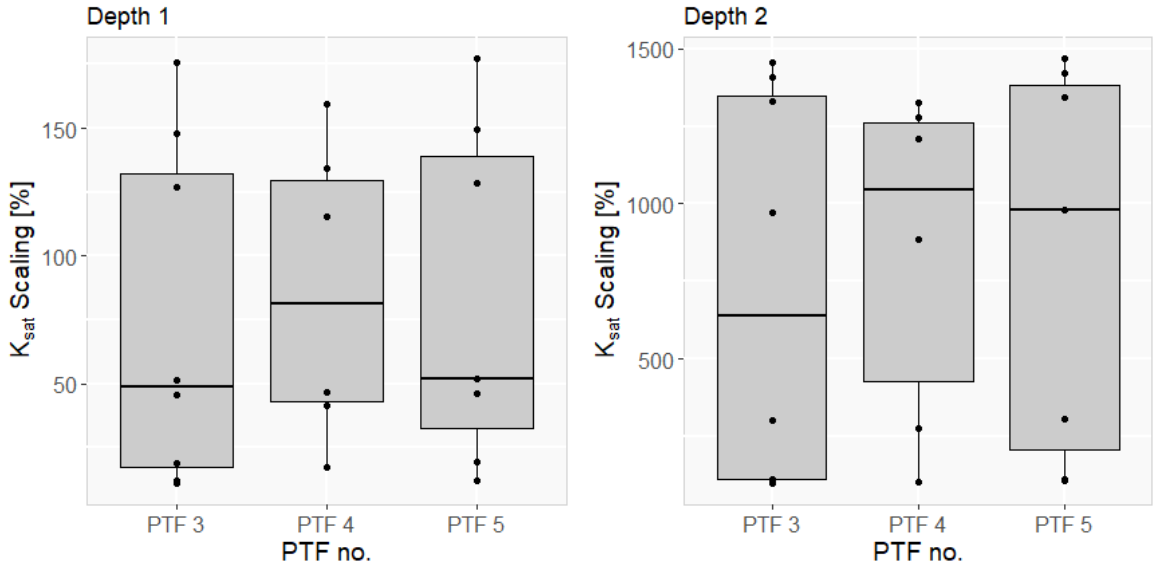

Figure 13: K_{sat} Boxplots of the ratio of the predicted and measured K_{sat} values, multiplied by 100 %, for the existing PTFs: 3, 4 and 5. Land-use Forest at Depth 1 (left) and Depth 2 (right).

Table 6: R^2, MAE and RMSE for the four land-use types Forest, Tree Fallow, Shrub Fallow, Degraded Land and the whole data set for the existing PTFs for all depths combined as well as each individual depth. 'ns' indicated that the PTF was not significant for the data set. See Table 5 for the PTFs.

R^2		all				F				TF				SF				DL			
		all	0	1	2	all	0	1	2	all	0	1	2	all	0	1	2	all	0	1	2
PTF no.	n	89	23	34	33	19	5	7	7	23	7	8	8	28	7	11	9	20	4	8	8
1		ns	ns	0.09	ns	0.47	ns	ns	ns	ns	ns	ns	ns	0.27	ns	ns	ns	ns	x	ns	ns
2		ns	ns	ns	ns	ns	ns	ns	ns	ns	ns	ns	ns	ns	ns	ns	ns	ns	x	ns	ns
3		0.11	0.19	ns	0.17	ns	ns	0.83	0.83	ns	ns	ns	ns	0.18	ns	ns	ns	ns	x	ns	ns
4		0.11	0.19	ns	0.17	ns	ns	0.83	0.83	ns	ns	ns	ns	0.18	ns	ns	ns	ns	x	ns	ns
5		0.11	0.19	ns	0.17	ns	ns	0.83	0.83	ns	ns	ns	ns	0.18	ns	ns	ns	ns	x	ns	ns
6		0.17	ns	ns	ns	0.34	ns	ns	ns	ns	ns	ns	ns	0.15	ns	0.44	ns	ns	x	ns	ns
7		ns	ns	ns	ns	ns	ns	ns	ns	ns	ns	ns	ns	ns	ns	ns	ns	ns	x	ns	ns
8		0.10	ns	ns	ns	ns	ns	ns	ns	ns	ns	ns	ns	0.28	ns	ns	ns	ns	x	ns	ns
9		ns	ns	ns	ns	ns	ns	ns	ns	ns	ns	ns	ns	ns	ns	ns	ns	ns	x	ns	ns
10		ns	ns	ns	ns	ns	ns	ns	ns	ns	ns	ns	ns	ns	ns	ns	ns	ns	x	ns	ns

MAE		all				F				TF				SF				DL			
mm h^{-1}		all	0	1	2	all	0	1	2	all	0	1	2	all	0	1	2	all	0	1	2
PTF no.	n	89	23	34	33	19	5	7	7	23	7	8	8	28	7	11	9	20	4	8	8
1		ns	ns	6.1	ns	13.6	ns	ns	ns	ns	ns	ns	ns	11.6	ns	ns	ns	ns	x	ns	ns
2		ns	ns	ns	ns	ns	ns	ns	ns	ns	ns	ns	ns	ns	ns	ns	ns	ns	x	ns	ns
3		10.7	19.6	ns	4.6	ns	ns	7.4	4.1	ns	ns	ns	ns	11.6	ns	ns	ns	ns	x	ns	ns
4		10.7	19.6	ns	4.3	ns	ns	7.4	3.9	ns	ns	ns	ns	11.6	ns	ns	ns	ns	x	ns	ns
5		10.7	19.6	ns	4.6	ns	ns	7.4	4.2	ns	ns	ns	ns	11.6	ns	ns	ns	ns	x	ns	ns
6		11.0	ns	ns	ns	14.1	ns	ns	ns	ns	ns	ns	ns	11.9	ns	6.7	ns	ns	x	ns	ns
7		ns	ns	ns	ns	ns	ns	ns	ns	ns	ns	ns	ns	ns	ns	ns	ns	ns	x	ns	ns
8		10.9	ns	ns	ns	ns	ns	ns	ns	ns	ns	ns	ns	11.9	ns	ns	ns	ns	x	ns	ns
9		ns	ns	ns	ns	ns	ns	ns	ns	ns	ns	ns	ns	ns	ns	ns	ns	ns	x	ns	ns
10		ns	ns	ns	ns	ns	ns	ns	ns	ns	ns	ns	ns	ns	ns	ns	ns	ns	x	ns	ns

RMSE		all				F				TF				SF				DL			
mm h^{-1}		all	0	1	2	all	0	1	2	all	0	1	2	all	0	1	2	all	0	1	2
PTF no.	n	89	23	34	33	19	5	7	7	23	7	8	8	28	7	11	9	20	4	8	8
1		ns	ns	56	12.1	331	ns	ns	ns	ns	ns	ns	ns	315	ns	ns	ns	ns	x	ns	ns
2		ns	ns	ns	ns	ns	ns	ns	ns	ns	ns	ns	ns	ns	ns	ns	ns	ns	x	ns	ns
3		255	508	ns	22.2	ns	ns	84	19.6	ns	ns	ns	ns	313	ns	ns	ns	ns	x	ns	ns
4		256	509	ns	20.0	ns	ns	86	17.6	ns	ns	ns	ns	313	ns	ns	ns	ns	x	ns	ns
5		255	507	ns	22.4	ns	ns	84	19.8	ns	ns	ns	ns	312	ns	ns	ns	ns	x	ns	ns
6		269	ns	ns	ns	345	ns	ns	ns	ns	ns	ns	ns	323	ns	56	ns	ns	x	ns	ns
7		ns	ns	ns	ns	ns	ns	ns	ns	ns	ns	ns	ns	ns	ns	ns	ns	ns	x	ns	ns
8		265	ns	ns	ns	ns	ns	ns	ns	ns	ns	ns	ns	323	ns	ns	ns	ns	x	ns	ns
9		ns	ns	ns	ns	ns	ns	ns	ns	ns	ns	ns	ns	ns	ns	ns	ns	ns	x	ns	ns
10		ns	ns	ns	ns	ns	ns	ns	ns	ns	ns	ns	ns	ns	ns	ns	ns	ns	x	ns	ns

x = n < 5

3.2.2 New PTFs

After learning that the existing functions only provided good R^2 for two depths of one land-use type, but do not provide otherwise good results I constructed my own PTFs. The functions that I came up with used either one or several of the following soil properties: pH, bulk density, soil organic carbon, nitrogen, porosity, sand, silt or clay. Some of the functions that I made are simple linear regressions while others are

multiple linear regressions. In the end, I developed eight functions (I, II, III (a), III (b), IV, V, VI, VII) that produced fairly decent R^2s for the relation between measured and predicted K_{sat}.

PTF I

PTF I is a PTF that predicts K_{sat} [mm h^{-1}] using a multiple linear regression with pH and the bulk density (BD)[g cm^{-3}]. This function was constructed for all Forest sites (n=19)(R^2 = 0.617) but could not predict K_{sat} for the other land-use types.

$$K_{\text{sat}} = 2643 - 291 * pH - 1143 * BD \quad \text{[I]}$$

PTF II

PTF II, is a multiple linear regression based on pH, soil organic matter (SOC)[%], nitrogen (N)[%] and bulk density (BD)[g cm^{-3}] The correlation between measured and predicted K_{sat} for this PTF were significant for the whole data set (n=89) and for the Shrub Fallow land-use (R^2s 0.528 and 0.683, respectively).

$$\begin{aligned} K_{\text{sat}} = &-10802 + 1357 * pH + 2115 * SOC \\ &+16568 * N + 3034 * BD - 372 * pH * SOC \\ &-15246 * N * BD \end{aligned} \quad \text{[II]}$$

PTF III (a) and (b)

PTF III uses only porosity as the only input variable. PTF III (a) and III (b) have different intercepts and multipliers and predict K_{sat} for the Forest for Depth 1 (a) and Depth 2 (b) for the Forest soil (both: n = 7; R^2 = 0.80). The function was also significant for the whole data set, the data set of all Depth 2's and all Shrub Fallow but the R^2 was low (< 0.2).

$$\begin{aligned} K_{\text{sat}} &= 758 - 13 * \phi \quad (a) \\ K_{\text{sat}} &= 90 - 1.6 * \phi \quad (b) \end{aligned} \quad \text{[III]}$$

ϕ is the effective porosity [%].

PTF IV

PTF IV can be used to predict K_{sat} of the Tree Fallow at Depth 1 (n = 8; R^2 = 0.760). PTF IV uses nitrogen (N)[%] as well as silt content (T_{silt} [%]; 0.05 - 0.002 mm) as input variables

$$K_{\text{sat}} = 194 - 546 * N - 3.3 * T_{silt} \quad \text{[IV]}$$

PTF V

Like equation IV, *PTF V* can also be used to predict K_{sat} for Depth 1 of the Tree Fallow (R^2 = 0.794). However, instead of silt, sand (T_{sand} [%]; 2 – 0.05 mm) - [%] is used as input variable together with nitrogen (N)[%].

$$K_{\text{sat}} = 113 - 554 * N + 0.79 * T_{sand} \quad \text{[V]}$$

PTF VI

PTF VI is the only function that was able to predict K_{sat} in the Degraded Land land-use (R^2 of 0.449 and 0.666 for the whole Degraded Land data set (n=20) and for the Depth 1 (n = 8), respectively) and is based on nitrogen (N)[%] as the only input variable. It also predicts K_{sat} for the whole data set, the whole Tree Fallow data set, as well as Tree Fallow Depth 1 and Depth 2 (R^2's = 0.313, 0.652, 0.541 and 0.498, respectively).

$$K_{\text{sat}} = 127 - 410 * N \quad \text{[VI]}$$

PTF VII

PTF VII includes nitrogen (N)[%], soil organic matter (SOC)[%], clay (T_{clay} [%]; < 0.002 mm) and silt (T_{silt} [%]; 0.05 - 0.002 mm) as the input variables and predicts the K_{sat} for Shrub Fallow Depth 2 reasonably (R^2 = 0.814).

$$K_{\text{sat}} = -19 - 156 * N + 19.7 * SOC + 0.13 * T_{clay} - 0.68 * T_{silt} \quad \text{[VII]}$$

The predictive power of PTFs III (a), III (b), IV, V, VII. is moderate to high, with R^2 values > 0.75 (up to 0.81) (Table 7). All regression curves have the same direction as the 1-1-line and follow it rather closely (Figure 14). Nevertheless, each PTF incorrectly predicts a negative K_{sat} for at least one sample. Furthermore, a trend of underestimating high K_{sat} and overestimating low K_{sat} data points can clearly be observed for PTF III (b), IV, V. Moreover, the plots illustrate a dependence on a few (high K_{sat}) data points, that influence the resulting regression curve (e.g. the two highest measured K_{sat} in III (b)).

When comparing the results of the existing PTFs: 3, 4 and 5 with PTF III (a) and (b) for the Forest for Depth 1 and 2, the three existing functions have a higher R^2 (0.83 and 0.83) (Table 6) than PTF III for both depths (Table 7). However, the MAE and especially the RMSE are much lower for PTF III (a) and (b). Furthermore, the predicted vs. measured plots for PTF III (a) and (b) (Figure 14) show much better results than the ones of PTF 3 (Figure 12), 4 and 5 (Appendix: Figure 21).

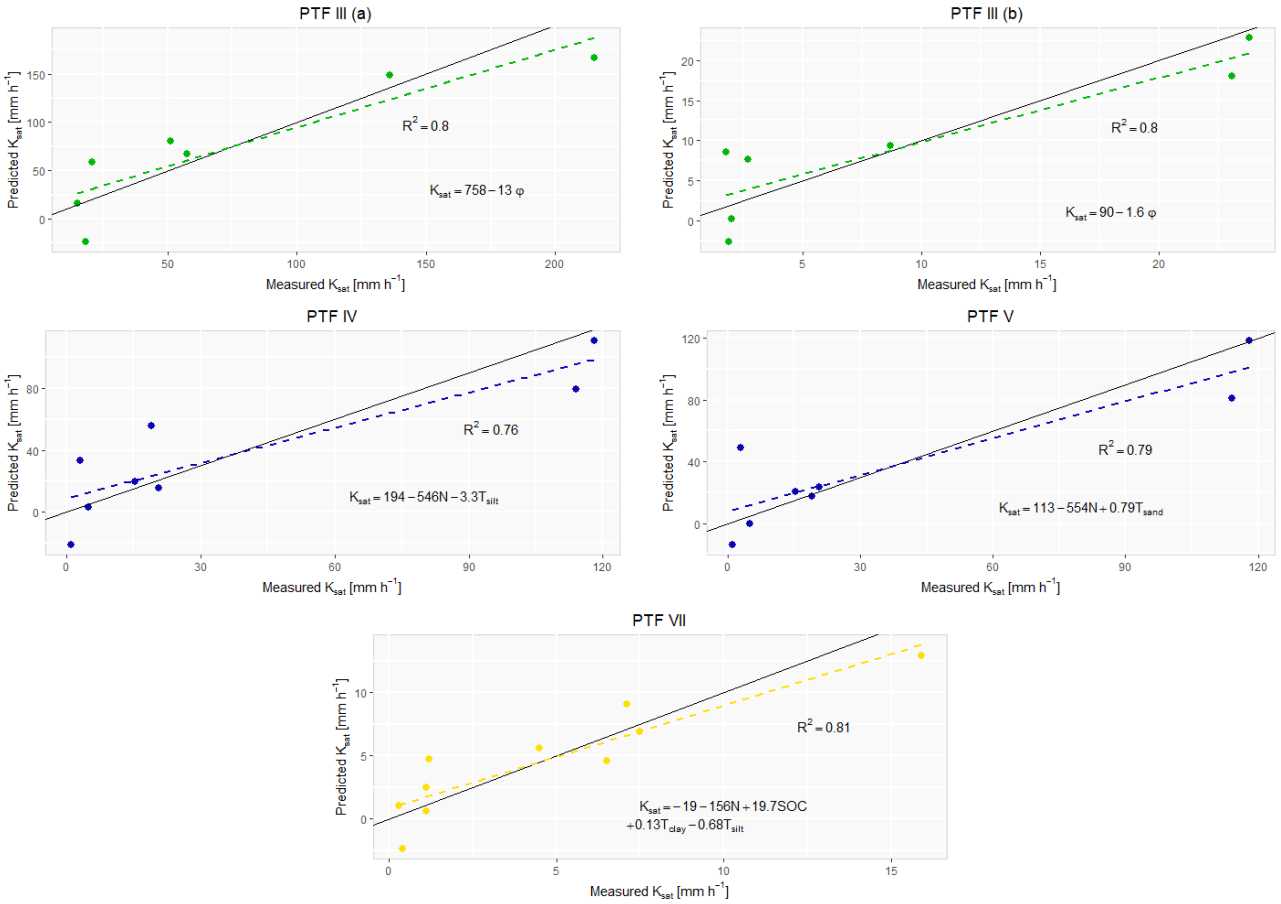

Figure 14: Plots of the predicted against the measured K_{sat} for each developed PTF with $R^2 > 0.7$. The solid black line is the 1-1 line. The respective colours represent the land-use type, but not the depth of the samples that were predicted with the PTF. The function and the R^2 of each PTF are illustrated as well. Top left: Forest, Depth 1; top right: Forest, Depth 2; middle left and right: Tree Fallow, Depth 1; bottom: Shrub Fallow, Depth 2

PTF III (a), III (b), IV, V and VII correspond to data set Forest Depth 1, Forest Depth 2, Tree Fallow Depth 1, Tree Fallow Depth 1 and Shrub Fallow Depth 2, respectively.

If two or more PTFs predict K_{sat} for the same data set, they can easily be compared. Function IV and V both, for example, predict K_{sat} for Tree Fallow Depth 1. PTF V has a larger R^2 and lower MAE and RMSE than PTF IV (Table 7). However, comparing K_{sat} between land-uses and especially between depths is much harder. To be able to compare them the predicted K_{sat} was divided by the measured values and multiplied by 100 % (as done for the existing PTFs). The resulting percentage allows for PTF comparison independent of which data set was used. The closer the values are to 100 %, the more accurate the PTFs are. Except for III (b) all median values are relatively close to 100 % (Figure 15). PTF IV, V and VII result in the most accurate mean and median predicted K_{sat} values (Figure 15).

Table 7: R^2, MAE [mm h^{-1}] and RMSE [mm h^{-1}] for Pedotransfer Functions for the four land-use types (Forest, Tree Fallow, Shrub Fallow, Degraded Land) and the whole data set of all depths combined, as well as each individual depth.

		all				**F**				**TF**				**SF**				**DL**			
		all	**0**	**1**	**2**	**all**	**0**	**1**	**2**	**all**	**0**	**1**	**2**	**all**	**0**	**1**	**2**	**all**	**0**	**1**	**2**
PTF no.	**n**	90	23	34	33	19	5	7	7	23	7	8	8	28	7	11	10	20	4	8	8
	R^2	ns	ns	ns	ns	0.62	ns	ns	ns	ns	ns	ns	ns	ns	ns	ns	ns	ns	x	ns	ns
I	MAE	ns	ns	ns	ns	11.9	ns	ns	ns	ns	ns	ns	ns	ns	ns	ns	ns	ns	x	ns	ns
	RMSE	ns	ns	ns	ns	175.2	ns	ns	ns	ns	ns	ns	ns	ns	ns	ns	ns	ns	x	ns	ns
	R^2	0.53	ns	ns	ns	ns	ns	ns	ns	ns	ns	ns	ns	0.67	ns	ns	ns	ns	x	ns	ns
II	MAE	10.0	ns	ns	ns	ns	ns	ns	ns	ns	ns	ns	ns	10.8	ns	ns	ns	ns	x	ns	ns
	RMSE	163.5	ns	ns	ns	ns	ns	ns	ns	ns	ns	ns	ns	167.7	ns	ns	ns	ns	x	ns	ns
	R^2	0.13	ns	ns	0.18	ns	ns	0.80	0.80	ns	ns	ns	ns	0.19	ns	ns	ns	ns	x	ns	ns
III	MAE	12.3	ns	ns	2.04	ns	ns	5.1	1.88	ns	ns	ns	ns	13.3	ns	ns	ns	ns	x	ns	ns
	RMSE	221.4	ns	ns	5.89	ns	ns	30.9	4.14	ns	ns	ns	ns	261.2	ns	ns	ns	ns	x	ns	ns
	R^2	ns	ns	ns	ns	ns	ns	ns	ns	ns	ns	0.76	ns	ns	ns	ns	ns	ns	x	ns	ns
IV	MAE	ns	ns	ns	ns	ns	ns	ns	ns	ns	ns	4.2	ns	ns	ns	ns	ns	ns	x	ns	ns
	RMSE	ns	ns	ns	ns	ns	ns	ns	ns	ns	ns	22.6	ns	ns	ns	ns	ns	ns	x	ns	ns
	R^2	ns	ns	ns	ns	ns	ns	ns	ns	ns	ns	0.79	ns	ns	ns	ns	ns	ns	x	ns	ns
V	MAE	ns	ns	ns	ns	ns	ns	ns	ns	ns	ns	3.7	ns	ns	ns	ns	ns	ns	x	ns	ns
	RMSE	ns	ns	ns	ns	ns	ns	ns	ns	ns	ns	20.9	ns	ns	ns	ns	ns	ns	x	ns	ns
	R^2	0.31	ns	ns	ns	ns	ns	ns	ns	0.65	ns	0.54	0.50	ns	ns	ns	ns	0.45	x	0.67	ns
VI	MAE	11.0	ns	ns	ns	ns	ns	ns	ns	7.6	ns	5.3	1.96	ns	ns	ns	ns	9.5	x	3.7	ns
	RMSE	196.3	ns	ns	ns	ns	ns	ns	ns	70.1	ns	31.2	4.52	ns	ns	ns	ns	124.2	x	16.5	ns
	R^2	ns	ns	ns	ns	ns	ns	ns	ns	ns	ns	ns	ns	ns	ns	ns	0.81	ns	x	ns	ns
VII	MAE	ns	ns	ns	ns	ns	ns	ns	ns	ns	ns	ns	ns	ns	ns	ns	1.32	ns	x	ns	ns
	RMSE	ns	ns	ns	ns	ns	ns	ns	ns	ns	ns	ns	ns	ns	ns	ns	2.01	ns	x	ns	ns

x = n <5; ns = not significant

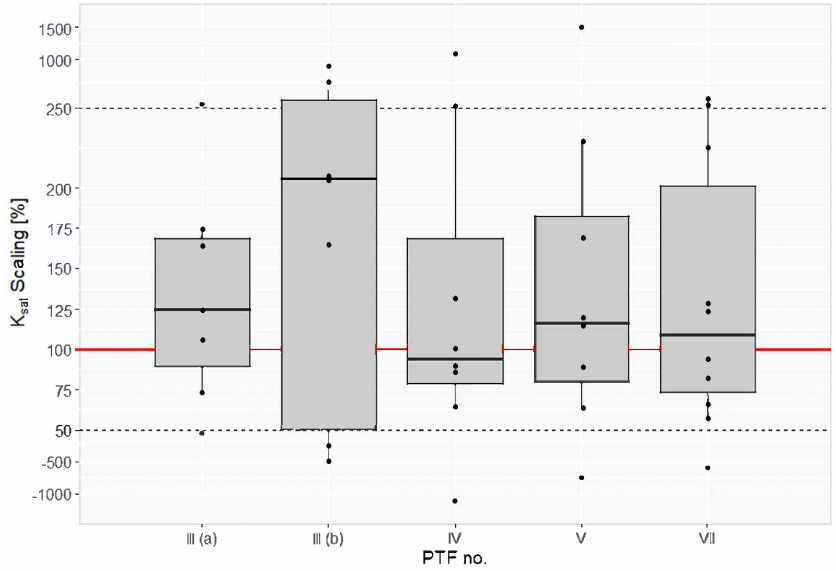

Figure 15: The ratio of the predicted and measured K_{sat} values multiplied this by 100 % for the five developed PTFs with $R^2 > 0.7$. For illustrative reasons the region between the two dashed lines is stretched. The solid red line depicts a perfect match between the predicted and measured K_{sat}. The corresponding data sets, to the PTFs, are depicted Table 8.

Table 8: Leave One Out Cross Validation (LOOCV) range for R^2, MAE [mm h^{-1}] and RMSE [mm h^{-1}] of the developed PTFs. Mean and median K_{sat} in mm h^{-1}

PTF no.	n	Forest Depth 1 6	Forest Depth 2 6	Tree Fallow Depth 1 7	Shrub Fallow Depth 2 9
III (a)	Mean K_{sat}	73.44			
	Median K_{sat}	51.20			
	R^2 range	0.78 - 0.89			
	MAE range	3.65 - 6.31			
	RMSE range	18.1 - 30.9			
III (b)	Mean K_{sat}		9.14		
	Median K_{sat}		2.70		
	R^2 range		0.67 - 0.88		
	MAE range		1.84 - 2.66		
	RMSE range		4.80 - 5.82		
IV	Mean K_{sat}			37.01	
	Median K_{sat}			17.15	
	R^2 range			0.58 - 0.87	
	MAE range			3.36 - 4.16	
	RMSE range			16.3 - 22.5	
V	Mean K_{sat}			37.01	
	Median K_{sat}			17.15	
	R^2 range			0.63 - 0.94	
	MAE range			2.94 - 3.68	
	RMSE range			10.9 - 20.9	
VII	Mean K_{sat}				4.56
	Median K_{sat}				2.85
	R^2 range				0.8 - 0.94
	MAE range				0.86 - 1.46
	RMSE range				0.95 - 2.54

Leave One Out Cross Validation (LOOCV) was applied to the PTFs with $R^2 > 0.7$. The ranges of R^2, MAE, RMSE as well as the mean and median measured K_{sat} are listed in Table 8. Comparing the MAE and RMSE ranges with the data set mean and median, it can be seen that the ranges are rather high, indicating that the predictions are not very good. After applying Leave One Out Cross Validation (n = 7) PTF V still shows better results than PTF IV That PTF V (Table 8).

Figure 16a depicts what percentage of the mean squared deviation (MSD) is caused by which of the three components. The majority of the MSD of PTF III (a) and VII are caused by lack of correlation. Furthermore, nonunity slope plays another significant role. The MSD of PTF IV and V are both roughly equally affected by lack of correlation and nonunity slope. The effects of squared bias on the overall MSD are close or equal to zero, except for III (b) where squared bias makes up more than 25% of the MSD. MSD values vary between 4 mm h^{-1} and 1000 mm h^{-1} (Figure 16b). Even considering that K_{sat} is 10-times higher in Depth 1 than Depth 2, the MSD range is tremendous. Both PTFs that predict K_{sat} at Depth 2 (III (b), VII)) have the lowest values. However, even between those two the difference is extreme: PTF III (a), IV and V have MSD values between 500 mm h^{-1} and 1000 mm h^{-1}. PTF IV have a slightly lower absolute MSD value than PTF V.

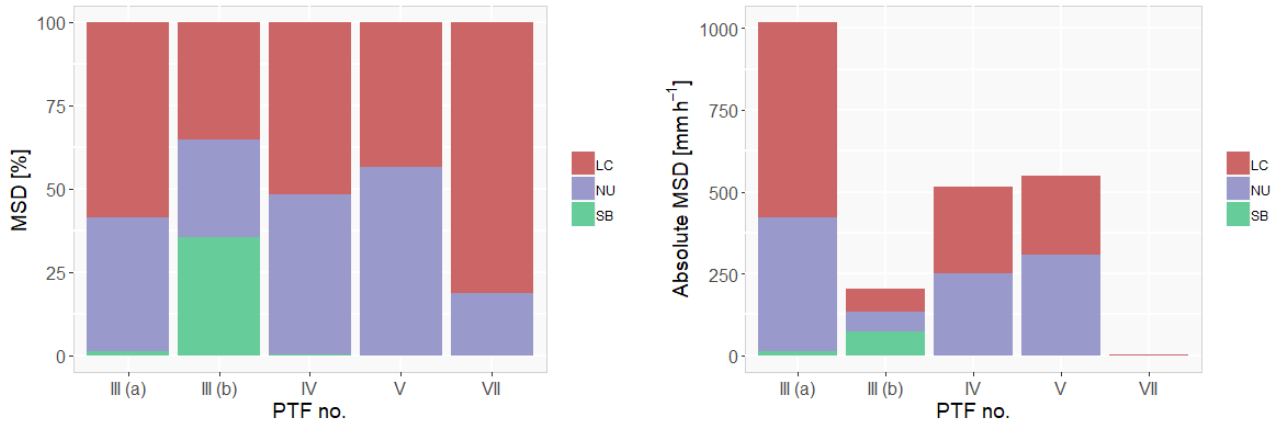

(a) MSD in percent

(b) Absolute MSD

Figure 16: The three MSD (mean square deviation) components (lack of correlation (LC), nonunity slope (NU) and the squared bias (SB), after Gauch et al. (2003), for the five created PTFs with $R^2 > 0.7$. MSD in percent (a) on the left and absolute MSD (b) on the right.

3.3 DRIFT

Figure 17 shows the average DRIFT spectra in the MIR region of the electromagnetic spectrum, of the whole data set, the individual depths and of the land-use types. All spectra are similar. Nonetheless, differences are observable. Especially the peaks and the valleys vary between the different data set means. Peaks indicate a certain soil property, such as kaolinite or lignin (Figure 17). A soil property can be indicated by one or several peaks in different areas of a MIR spectrum. The most protruding areas in the plotted MIR spectra are between ~ 3700 – 3400 cm^{-1}, with absorbance levels of 0.5 up to 0.9, as well as the region between ~ 1700 and 600 cm^{-1}. In the latter the highest peaks reach absorbance values of ~ 0.4. The spectral difference between the three ZOIs is prominent in the 3700 – 3400 cm^{-1} region (Figure 19).
How much the individual sample spectra of a data set differ from the data set's mean is illustrated in Figure 18 for the three depths. Depth 1 and Depth 2's max deviation is 0.4, Depth 0's largest deviation is ~ 0.2. The huge variation in the K_{sat} data led to unsatisfactory PLSR results. Thus, the data was partitioned into new classes. The classes comprise samples with similar measured K_{sat} value to reduce the big spread in the

data. The classes are: K_{sat} < 30 [mm h^{-1}], K_{sat} < 100 [mm h^{-1}], K_{sat} > 100 [mm h^{-1}], $log_{10}K_{sat}$* [mm h^{-1}] and $log_{10}K_{sat}$ [mm h^{-1}]. However, even the artificially created data sets are so variable that the PLSR could not generate adequate results. For all data categories the RMSEs were much too large in comparison to the mean and the median (Table 9). The high CVs are the cause of the unsatisfactory results (All = 197.3 %, Depth 0 = 83.4 %, Depth 1 = 104.1 %, Depth 2 = 135.7 %, K_{sat} < 30 = 99.1 %, K_{sat} < 100 = 127.9 %, K_{sat} ≥ 100 = 80.3 %, $log_{10}K_{sat}$* = 77.9 % and $log_{10}K_{sat}$ = 58.4 %).

Table 9: PLSR of the DRIFT spectra. RMSE [mm h^{-1}] of different sample sets in comparison with the respective K_{sat} means and medians [mm h^{-1}]. Explaind variance in %, n: sample size.

	All	Depth 0	Depth 1	Depth 2	< 30	< 100	> 100	log10*	log10
n	89	22	34	33	51	66	23	89	80
Components	6	5	5	6	5	6	5	7	6
Explained Variance	94.2	93.2	94.1	95.2	92.6	94.5	93.2	96.1	93.0
Mean K_{sat}	138.7	458.1	48.7	8.8	7.8	18.8	447.9	1.27	1.47
Median K_{sat}	28.3	465.2	33.6	2.8	5.0	8.1	353.5	1.30	1.37
RMSE	213	380	48	16	9.1	13.8	352	0.71	0.90

* includes negative numbers

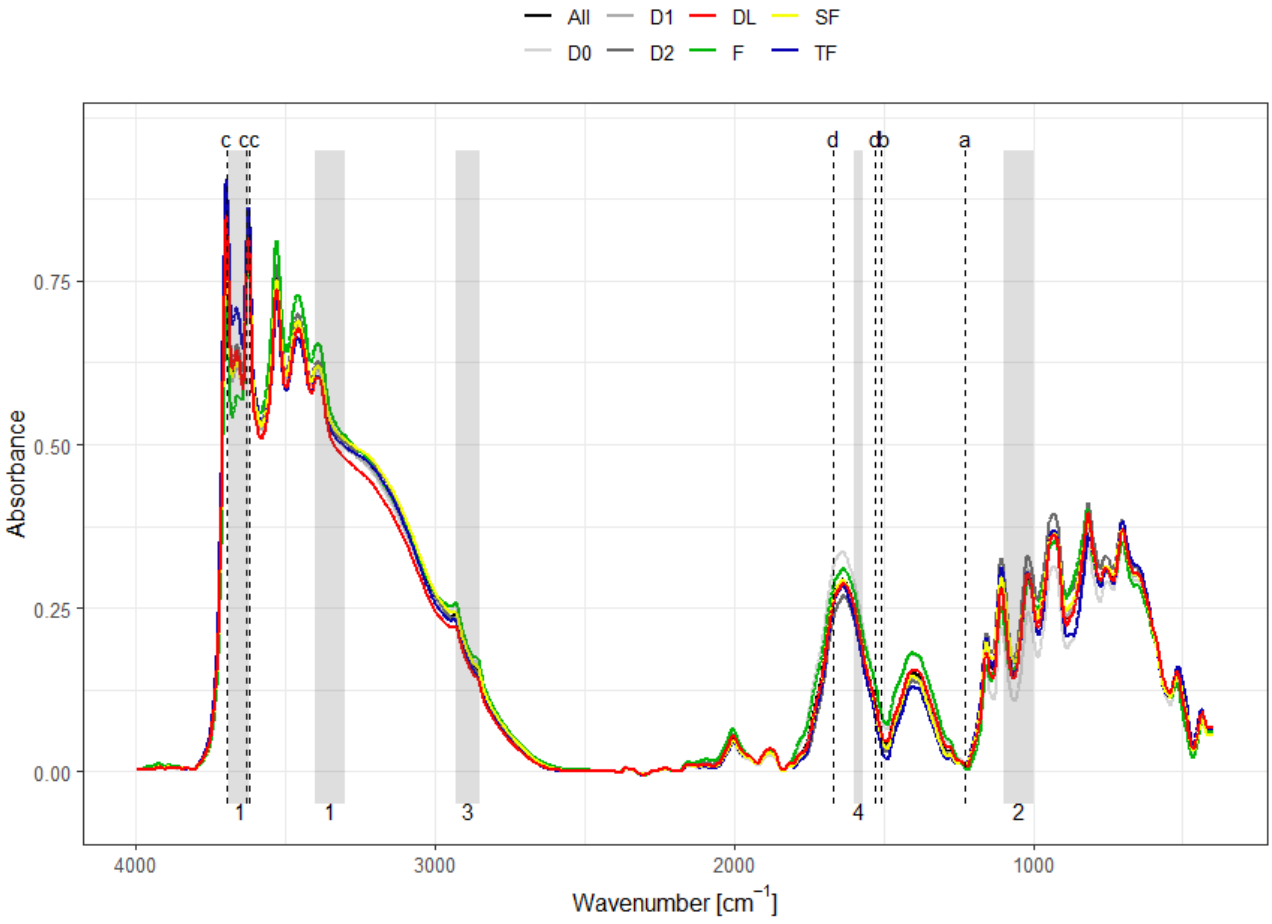

Figure 17: Mean DRIFT spectra of all depths, all land-use types and the whole data set. MIR Absorbance of the different sample sets. The vertical dashed black lines indicate the presence of lignin (a), cellulose (b), kaolinite (c) and protein amide (d), if a peak is present. The grey boxes depict a range in MIR, where a particular soil property can be found. 1, 2, 3 and 4 represent clay minerals, quartz (sand), alkyl (soil organic matter), and aromatic groups (soil organic matter), respectively.

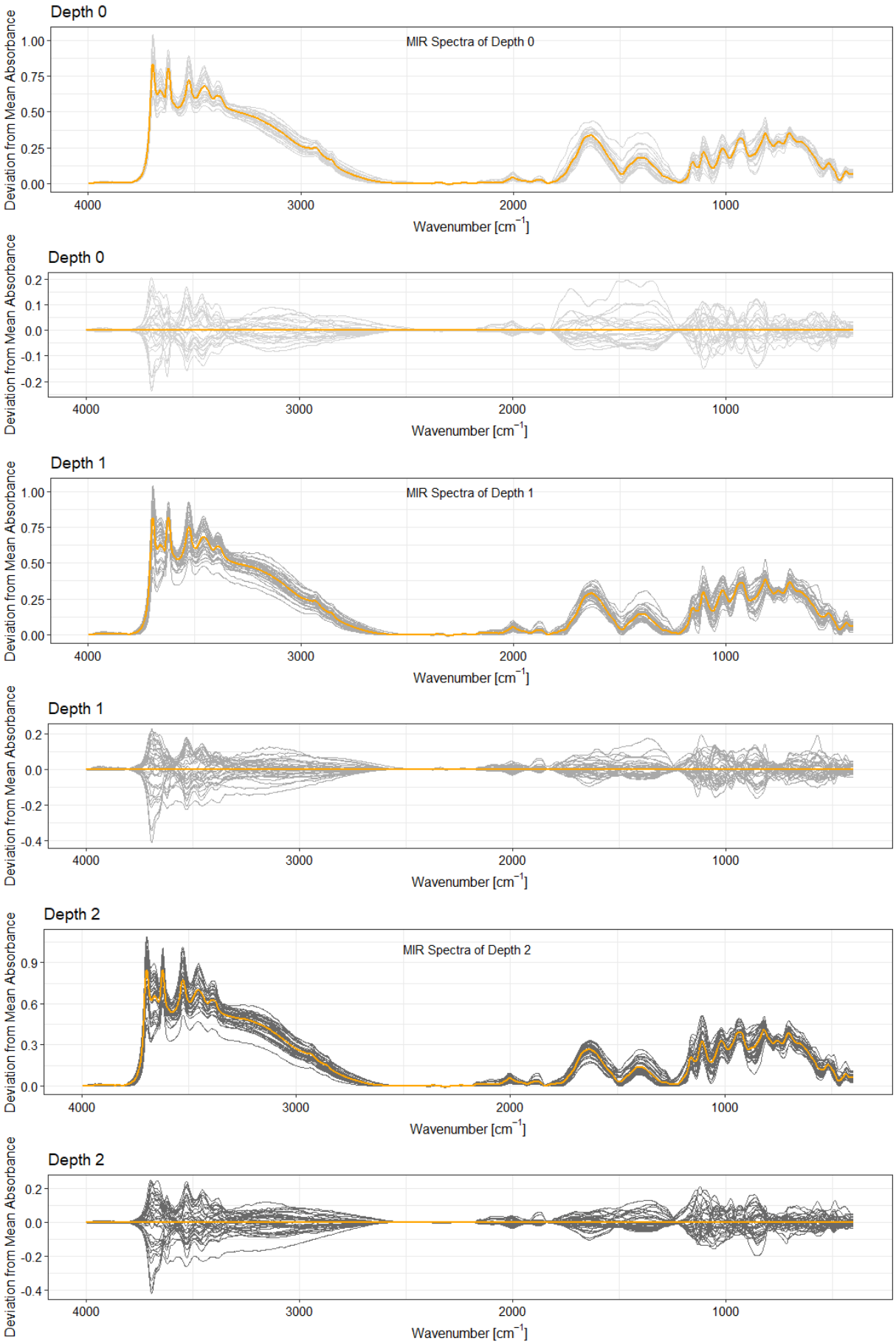

Figure 18: DRIFT plots for Depth 0: row 1 -2, Depth 1: row 3 - 4, Depth 2: row 5 - 6. Top: Deviation of each sample spectrum from the mean Absorbance of the respective data set. Bottom: Deviation from the mean Absorbance, where the mean Absorbance is equal to 0. The orange spectrum/line indicates the data sets mean.

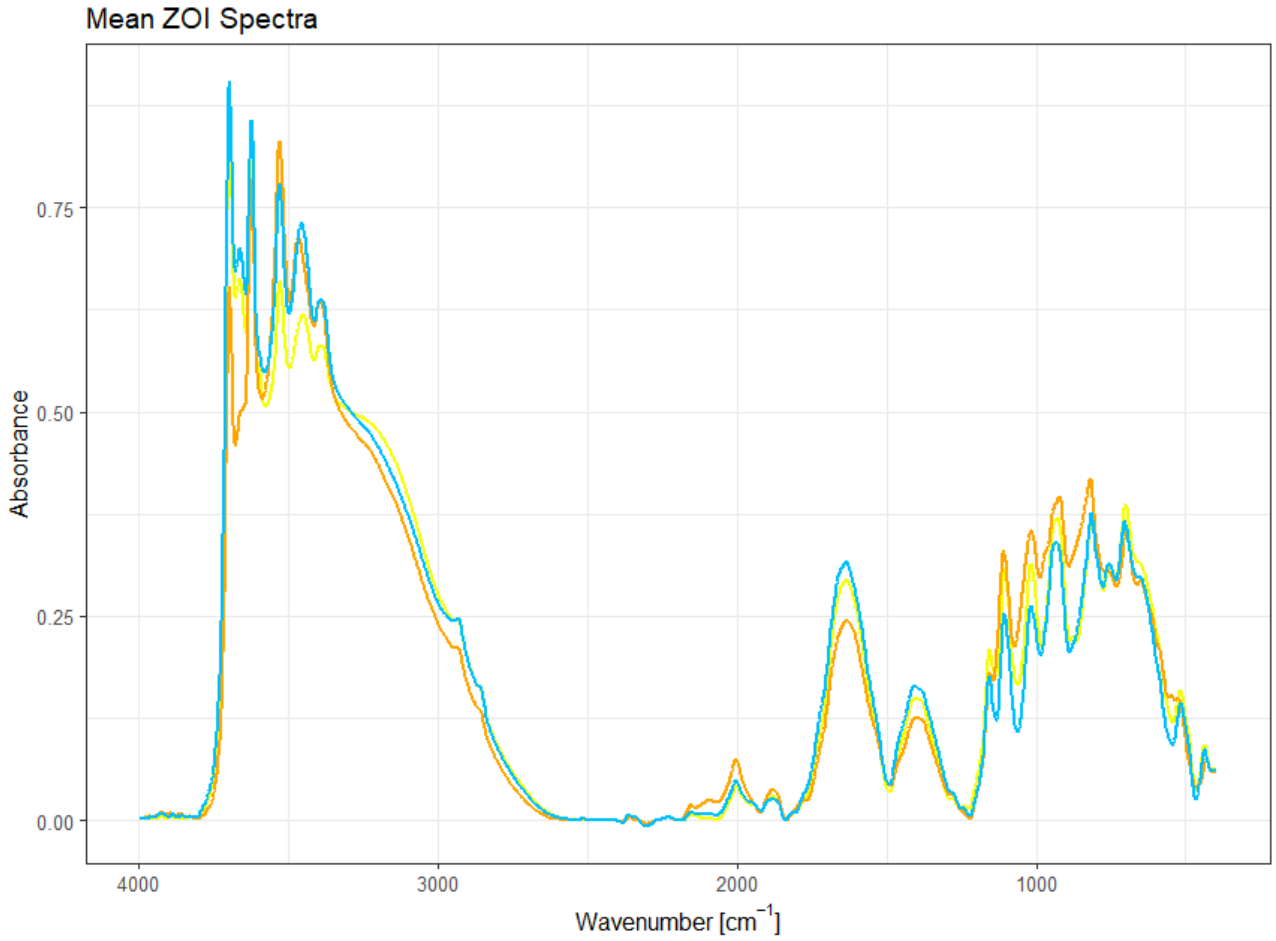

Figure 19: Mean DRIFT spectra of the three ZOIs (ZOI 2: yellow; ZOI3: orange; ZOI 4: blue) MIR Absorbance of the different sample sets.

4 Discussion

4.1 Soil Properties

4.1.1 Soil Organic Carbon

Soil organic carbon was significantly different for all three categories (ZOI, land-use, depth); (Figure 10a - c). Concerning the depths, Figure 10c illustrates that soil organic carbon decreased from Depth 0 (median: 51 g kg^{-1}) over Depth 1 (median: 36 g kg^{-1}) to Depth 2 (median: 29 g kg^{-1}), implying less soil organic carbon in the subsoil in comparison to the topsoil (Stahr et al., 2008; Schiedung et al., 2019). Johnson et al. (1995) also found a decrease in soil organic matter, and thus soil organic carbon, under forest vegetation from the uppermost soil towards deeper regions. This because the topsoil experiences a constant input of organic matter in contrast to the subsoil.
ZOI 4 contains the highest and ZOI 3 the lowest amount of soil organic carbon. Andriamananjara et al. (2016) measured a mean 110 mg C ha^{-1}, 77 mg C ha^{-1} and 99 mg C ha^{-1} for ZOI 2, 3 and 4, respectively. My findings of 91 mg C ha^{-1} for ZOI 2 are comparable to their results. However, the high variability of the sand fraction in ZOI 3 (35 – 88%) and 4 (28 - 80%) influences the amounts of soil organic carbon in mg C ha^{-1} (1) to such a degree, through the sand contents influence on the bulk density, that they are not comparable to Andriamananjara et al.'s (2016) values. Comparing the soil organic carbon of the ZOIs in g kg^{-1}, the mean values are much closer to each other (ZOI2: 35; ZOI 3: 29; ZOI 4: 42 g kg^{-1}). However, the mean soil organic carbon of the three ZOIs is significantly different (Figure 10a). The differences between the ZOIs can be explained by the uneven number of samples from the different depths per ZOI. Especially, the number of Depth 0 samples per ZOI may play an important role, because of the higher amounts of soil organic carbon. Depth 0 makes up 29 %, 0 % and 34 % of all samples in ZOI 2, 3 and 4, respectively. This explains, at least partially, the differences between the soil organic carbon amount of the three ZOIs. The reason that ZOI 3 has comparatively high mean soil organic carbon values despite not having any Depth 0 samples might be caused by the combination of the land-use type and depth distribution per ZOI.
The mean soil organic carbon content in the Forest (4.1 % or 41 g kg^{-1}) was significantly different from the other three land-use types (Appendix: Table 11). These results represent the dominant view, that the burning of vegetation and subsequent cultivation has an adverse effect on soil organic carbon (Garcıa-Oliva et al., 1999; Murty et al., 2002; Weil and Brady, 2017). Ash increases the solubility of organic carbon and can thus lead to reduced carbon contents (Kahl et al., 1996). The soil organic carbon content decreased at all depths when natural forest is converted into cultivated land (Pereira Machado Dias et al., 2019). Higher amounts of soil organic carbon are found in Forest because of the constant organic matter input from the forest vegetation. Furthermore, Pereira Machado Dias et al. (2019) state that the reduction of soil organic carbon after forest conversion are due to the agriculturally induced soil disturbances that accelerate soil organic carbon decomposition. The pH-raising ash increases the decomposition rate by accelerating microbial activity and mineralization (Demeyer et al., 2001; Weil and Brady, 2017). The mean soil organic carbon content in Tree Fallow, Shrub Fallow and Degraded Land were relatively similar and ranged between 34 – 38 g kg^{-1}. Over all land-uses, the soil organic carbon content ranking is Forest > Shrub Fallow > Degraded Land > Tree Fallow. The same order was found by Andriamananjara et al. (2016), who conducted their study in the same region, but this trend is unexpected.This may be due to the varying land-use histories (e.g. fallow period length, site specific-vegetation, time gap between the last use and the

measurements) of the sample sites. Other parameters such as the clay type or the microbial activity, that were not included in this thesis, could also have an effect on soil organic carbon.

4.1.2 Carbon 13

There was a clear trend of increasing mean δ ^{13}C from Forest (-27.15 ‰) to Degraded Land (-25.60 ‰) but only the mean values of Degraded Land and Shrub Fallow were significantly different. Additionally, to the enrichment in δ ^{13}C from Forest to Degraded Land there was an increasing variability in δ ^{13}C values for the samples. Typical δ^{13}C values for tropical C_3 plants (forests) are between -27 ‰ and -28 ‰(García-Oliva et al., 1994). C_4 pasture grasses or crops, depending on the source, have δ ^{13}C values around -13 ‰ (Townsend et al., 2002) or -15 ‰ δ^{13}C (García-Oliva et al., 1994). The 1.55 ‰ δ^{13}C enrichment, from Forest to Degraded Land, can thus depict a trend of the replacement of C_3 forests by C_4 pasture grasses in the recent past (Houghton et al., 1987). Soil organic carbon stemming from C_3 plant (forest vegetation) decomposes and is replaced over time by soil organic carbon that originates from C_4 plants, such as corn or grasses. While the soil organic carbon of all land-use types predominantly stems from the C_3 plants, the C_4-originating soil organic carbon fraction increases over the repeating slash-and-burn cycles. Assuming that the measured δ^{13}C values in the forest are 100 % from C_3 plants and that 14 ‰ δ^{13}C represent total C_4 soil organic carbon (Garcıa-Oliva et al., 1999; Houghton et al., 1987), then the calculated, faction of soil organic carbon from C_4 plants is 3 % (Tree Fallow), 7 % (Shrub Fallow) and 12 % (Degraded Land). The slight trend of increasing mean δ^{13}C with depth is because the soil organic matter is more decomposed in the subsoil and thus the δ^{13}C values are higher (Natelhoffer and Fry, 1988). The uneven distribution of depths per land-use type is also likely a reason for higher δ^{13}C in the subsoil.

4.1.3 Nitrogen

Nitrogen ranged from 1 to 10 g kg^{-1} in the soils and was significantly different for the ZOIs and depths. The land-use types were not significantly different for nitrogen. All three depths are significantly different from one another. Depth 0 (3.8 g kg^{-1}) had the highest and Depth 2 (1.9 g kg^{-1}) the lowest amount of nitrogen. This decrease of nitrogen with increasing depth was already shown by Batjes and Dijkshoorn (1999). Most soil nitrogen is part of organic molecules (soil organic matter) (Weil and Brady, 2017; Don et al., 2011). Soil nitrogen thus follows the soil organic carbon distribution (Grip et al., 2005). The relationship between depth and nitrogen is thus more likely to be caused because of the relationship between depth and soil organic carbon. Hence, soil nitrogen decrease with increasing depth is caused by longer exposure to decomposition.

Despite the similar pattern to the soil organic carbon, nitrogen usually does not differ with the land-use. However, mean nitrogen content was higher for the forest (but not significantly). During the combustion, most of the nitrogen in biomass is volatilised (Demeyer et al., 2001; Malmer et al., 2005), causing the resulting ash to be nitrogen-poor (Gay-des Combes et al., 2017). The nitrogen-poor ash can hence also not supply the soil with nitrogen. Furthermore, slash-and-burn agriculture causes the decrease of nitrogen through postburn leaching (Malmer and Grip 1994 in Malmer et al. 2005), and wind and water erosion (Ewel et al., 1981). This agricultural practice thus has a two-folded negative impact on the soils nitrogen concentration. Several studies have shown the depleting effect of slash-and-burn agriculture on nitrogen (Gay-des Combes et al., 2017; Demeyer et al., 2001; Malmer, 2004; Sanchez et al., 1983). However, as mentioned afore, my results do not show a significant difference in mean nitrogen content between the

Forest and the slash-and-burn affected land-uses (Tree Fallow, Shrub Fallow and Degraded Land); (Figure 10h). A possible explanation might be that there was enough time to replenish the nitrogen contents of the soil during the fallow periods.

4.1.4 pH

Mean pH differed with land-use (Figure 8b). For the Forest the mean pH was 4.07 and for the other land-uses the pH varied between 4.94 and 5.06. The pH of the Forest is representative of pH values of undisturbed ferralsols (Eswaran and Reich, 2005). Acidification occurs during soil formation. The old, heavily weathered tropical soils have been thoroughly leached by the high rainfall intensities. Furthermore, the high amount of Al in ferralsols (mean: 8 % aluminium$_2O_3$ in the Forest soils) amplifies the soil acidity (Weil and Brady, 2017). The reason for the higher pH values for Tree Fallow, Shrub Fallow and Degraded Land is that burning and the subsequent addition of ash to the soil increases the pH (Thomaz et al., 2014; Nye and Greenland, 1960; Ewel et al., 1981). Ash is highly alkaline, causing the pH to increase for the three land-use types which have undergone slash-and-burn agriculture. This reduces aluminium and Manganese toxicity (Demeyer et al., 2001). However, why pH was the highest for Tree Fallow, and Shrub Fallow had the lowest pH of the three-remaining land-use types can not be explained by the addition of ash. The difference in pH between Tree Fallow and Shrub Fallow was 0.16. This slight variation could be attributed to measurement inaccuracies or to the slightly different percentages of certain soil properties that affect the soil pH, such as aluminium (Weil and Brady, 2017). The mean percentage of Al_2O_3 was highest for Shrub Fallow (36 %), after the Forest (38 %), followed by Degraded Land (35 %) and Tree Fallow (34 %). This order coincides with the corresponding pH values.

4.1.5 Bulk Density

The observed increase in bulk density with depth for the samples is common (Weil and Brady, 2017) and can be ascribed to the compaction caused by the overlying soil mass. Furthermore, fewer biopores, less aggregation and lower amounts of soil organic matter lead to higher bulk density values with greater depth (Weil and Brady, 2017). The mean and median increases in bulk density from Depth 0 to Depth 1 were 11 % and 9 %, respectively. Between Depth 1 and Depth 2 the mean and median bulk density increased by 6 % and 9 %. The bulk density of one of the sample sites in ZOI 2 (Tree Fallow; between 2.0 g cm^{-3} and 2.2 g cm^{-3}) seems to be unrealistic in comparison to the rest of the samples. However, the bulk density increase from Depth 0 to Depth 2 for that sample site seems to be normal. Such high bulk density values are normally found in soils that were compacted (Weil and Brady, 2017), which does not apply to these samples. It could be that the bulk density was affected by traffic (Lal and Kimble, 2001), i.e. through compaction during the cutting, burning and use as agricultural land.

The boxplots in the land-use graph (Figure 8b) illustrate that the bulk density is significantly lower in the Forest than the three other land-use types. The literature on bulk density agrees that land-use change through deforestation increases the bulk density (Don et al., 2011; Murty et al., 2002). Weil and Brady (2017) state that surface horizons of forested areas generally have rather low bulk density. Inter alia, the higher amounts of soil organic carbon in the Forest (Andriamananjara et al., 2016), as well as biotic factors which are higher in Forest compared to the other land-use types (Weil and Brady, 2017) contribute to the low bulk density. The 9% mean bulk density increase from Forest to Degraded Land that I measured is similar to Don et al.'s (2011) 10% increase between the same land-use types, measured across the tropics.

4.1.6 Porosity

Mean porosity differed significant with depth and ZOI but not with land-use. The porosity in ZOI 2 is significantly different compared to the other ZOIs, because of its comparatively higher clay content (50 %) (Jarvis et al., 2002). The mean porosity decreased with depth from ~ 54 % at Depth 0 to ~ 48 % at Depth 2. However, only the mean porosity of the surface horizon was significantly different. The decrease in porosity with depth was related to the increased compaction in deeper parts of the soil (Weil and Brady, 2017), as well as low amounts of soil organic carbon in deeper soil horizons, which leads to decreased granulation (Weil and Brady, 2017; Ayoubi et al., 2012; Dörner et al., 2010). Porosity was similar for all land-uses with means ranging between 53 % and 50 %. Because porosity is correlated with bulk density and bulk density is affected by the land-use, lower porosities could be expected in Tree Fallow, Shrub Fallow and Degraded Land. A possible reason for the insignificant difference is that ash can contain big porous particles (Etiegni and Campbell, 1991 in Demeyer et al., 2001) and that fallow vegetation and fauna also created enough macropores (Bonell, 2005; Zwartendijk et al., 2017). It is unexpected that porosity was high for Degraded Land but this might be due to the high clay content, which tends to increase porosity (Weil and Brady, 2017). The reason for having the second highest porosity in the Forest but the lowest clay content, might be due to the many more macropores, caused by flora and fauna.

4.2 Ksat Prediction

4.2.1 Pedotransfer Functions

It was not possible to develop a PTF that could predict K_{sat} for the whole region with a sufficient accuracy, due to the inherent variability of K_{sat} caused by spatial variability (Baroni et al., 2010; Tietje and Hennings, 1996). To reduce the variability, subsets of the data based on land-use types, the depths and depths per land-use were created. Despite having smaller K_{sat} variability, the variability in the data was still considerable.

The PTFs were evaluated by comparing the predicted with the measured values. If the measured values are being used to develop the function, then we talk about evaluating the accuracy. The reliability is evaluated, when the measured values were not used to develop the PTF (Wösten et al., 2001; Patil et al., 2010).

PTFs are location specific due to their empirical nature and often perform inadequate if the soil genesis is too different (Patil and Singh, 2016). PTFs created for data sets with different soil and climatic conditions should thus be treated with caution (Wösten et al., 2001). There is thus a consensus that local PTFs should be used/developed instead of relying on PTFs developed in different regions (Patil and Singh, 2016). Three existing functions (PTF 3, 4 and 5), which all used the porosity to predict K_{sat}, provided a good R^2 for the Forest land-use at Depth 1 and Depth 2. While the criteria ($R^2 > 0.7$, predicted median K_{sat} < factor 1.5 of the measured median K_{sat}) were met, the visual inspection was not passed. The existing PTFs (PTF 3, 4, 5) did thus not predict K_{sat} accurate enough. Figure 12 (and Figure 21 in the Appendix) depict the 1-1-plots of PTF 3 (4 and 5). For Depth 1 K_{sat} is underestimated and for Depth 2 the K_{sat} is overestimated. While the measured values vary greatly, the predicted ones are all close to each other, between 24 and 28 mm h^{-1} for Depth 1 and 2. As expected the three existing PTFs performed inadequate due to different climatic and soil-originating conditions.

The PTFs developed in this thesis had lower R^2 values than the existing PTF 3, 4 and 5. However, they had better (i.e. lower) MAE and RMSE values than the existing PTFs (Figure 8) as well as more accurate

1-1-plots (Figure 14 and 21). The Leave One Out Cross Validation (Figure 8) was able to validate that the developed PTFs could predict K_{sat} within the same land-use type and depth (moderately) accurately. All developed PTFS with the exception of III (b) met the R^2 as well as the factor 1.5 criteria and passed the visual inspection. Figure 15 illustrates why PTF III (b) did not predict K_{sat} accurately. PTF III (a), IV, V and VII are capable of predicting K_{sat} for their respective depths per land-use. Despite having met the criteria, they are still faulty, as they falsely predicted negative K_{sat} values (Figure 14). Furthermore, looking at the absolute mean squared deviations (Figure 16b) it can be seen that all developed PTFs, except for VII, had very high values. Especially PTF III (a) has a particularly high mean squared deviation. The most trustworthy function is PTF VII, which had good statistical results regarding R^2, factor 1.5, mean squared deviation and the visual inspection. But it can only be used for Shrub Fallow Depth 2. If it is used for all land-uses, the factor is within 1.5 of the measured median K_{sat} and the R^2 is above the threshold. However, the variable used are already not significant for predicting K_{sat} for the data set (which renders it unusable), the RMSE values are extremely high and the 1-1-plot is not acceptable.

The three existing PTFs, as well as PTF III (a) and III (b) use porosity as the only predictor. Despite having the same structure, the existing PTFs produce unsatisfactory results because the intercept and the multiplier were determined for Australian soils (Minasny and Mcbratney, 2000). Although, the average texture was similar to the Forest in this study, the bulk density was 31 % and 21 % higher than the Forest at Depth 1 and 2, respectively. Neglecting the inclusion of soil properties such as bulk density or the root mass in the existing PTFs as well as using the natural logarithm of the porosity created large disparities between the predicted and measured K_{sat} values clearly visible in Figure 12 and 21 (Appendix). Minasny and Mcbratney (2000) state that local calibration is needed if the functions are applied to other sites. This was done for PTF III (a) and III (b) and turned out to work well (up to a factor of 1.5 for III (a) and 4.5 for III (b)). Applying adjusting PTF III to all land-uses the factor between predicted and measured K_{sat} was 12. This is because one soil property is not sufficient to predict K_{sat} of such diverse soils.

PTF IV and V have the same structure, except that PTF IV uses T_{silt} besides nitrogen as predictor, whereas PTF V used T_{sand} and nitrogen. The slightly higher accuracy (Table 7) of PTF V than IV are is due to the higher correlation between K_{sat} and sand (0.61) than T_{silt} (-0.57).

Four of the developed PTFs produced accurate K_{sat} values in regards to the defined thresholds. However, also PTF III (b) that had a too high factor for the threshold it still might be of use. Less accurate K_{sat} predictions (within a factor of 3 - 5 times the median measured K_{sat}) are still usable, as they indicate the order of magnitude of K_{sat} of a certain soil depth and land-use type. All five developed PTFs produce K_{sat} values lower than 5 factor of the median measured K_{sat} and can thus at least provide a coarse estimation of a soils K_{sat} range and give general overview.

Producing a map of spatial K_{sat} across the CAZ would not be possible with the developed functions. Firstly, because no PTF was developed to predict K_{sat} for Depth 0, mostly due to the few Depth 0 samples (n = 22) with as few as 4 samples for the Forest land-use. Secondly, no PTF could be produced for the Degraded Land, either due to the lack of significance of the soil properties towards K_{sat} or because R^2 was to low (R^2 0.67; 0.45). If one nevertheless would want to produce a spatial K_{sat} map of the CAZ the detail of the spatial would have to be considered. The coarser the resolution can be the easier it would be to produce such a map because the K_{sat} predictions would be more general (Ghanbarian et al., 2016). Independent of the spatial resolution of the map, the most fitting approach would be to predict K_{sat} for land-use and depth. Land-use on its own would not work, as K_{sat} of surface horizon is 10 and 100 times larger than in Depth

1 and 2 (Zwartendijk et al., 2017), respectively. But also just using the depth would produce inaccurate K_{sat} values because a difference, at least, between Forest and Degraded land is observable (Figure 8k). The most promising approach would be to not use one function but rather several. With this approach K_{sat} for at least one depth for three land-use types could be predicted. For this task first one would have to differentiate by depth. If developing further PTFs, it would be important to make sure that soil properties which are being use are either land-use or depth dependent, or ideally both.

4.2.2 DRIFT

The MIR spectral region displays absorption features that are of interest in K_{sat} prediction (Araújo et al., 2015) such as clay minerals, or quartz (sand)(Soriano-disla et al., 2014), as well as organic components, such as lignin (Nuopponen et al., 2006) and cellulose (Rossel et al., 2006). Soil lignin of Forest and Tree Fallow are distinctively different from non-forested land-uses (Shrub Fallow, Degraded Land) and can thus help to predict K_{sat} (Bélanger et al., 2015). In the region of ~ 3700 - 3400 cm^{-1} the presence of clay minerals such as Kaolinite, Smectite and Illite are indicated (Janik et al. (1998), Janik and Skjemstad (1995) both in Rossel et al. (2006)). The identified high absorbance peaks that correspond to clay minerals like Kaolinite coincide with the high kaolinite clay contents (60 – 90 %) in tropical soils (Hodnett and Tomasella, 2002). Differences between the clay minerals in the three ZOIs are clearly detectable (Figure 19). Despite all three ZOIs having ingenous basement rocks as parent material, the clay minerals of the three pronouncedly different. Subtle differences in the parent material lithology can lead to different arrangements of clay minerals in the soil (Mirabella et al., 2002). The presence of sand in the soil, is verified if peaks between 1000 cm^{-1} and 1100 cm^{-1} exist. Lignin and cellulose are found at ~ 1510 ± 10 (Nuopponen et al., 2006) and ~ 1230 ± 10, respectively (Dr. Samuel Abiven, University of Zurich, personal communication), respectively. Generally the deviations from the mean absorbance (Figure 18) were not big. However, the spectral regions that play the biggest part in the PLS prediction of K_{sat} had deviations from the mean of -0.2 to 0.4 and -0.2 to 0.2. Taking into account, that the absorbance ranges from 0 - 1 the deviations in those locations are considerably large.

PLSR was not able to predict K_{sat} from the DRIFT measurements in the MIR spectral range due to unacceptably high RMSE values (Table 9). The source of the extremely high RMSE values, compared to the means and medians of the individual data sets, is the relatively large deviation from the individual sample spectra to their mean spectrum, as well as the large K_{sat} variation itself. Thus, instead of working with the land-use type spectra, the individual depth spectra were used. However, the combination of all land-uses of one depth again lead to high variations, since the land-use types have different K_{sat} values (Zwartendijk et al., 2017) as well as varying soil physical and chemical characteristics. Also, the last approaches (artificially dividing the K_{sat} data as well as applying a logarithmic scale) did not drastically improve the RMSE. The inherent K_{sat} variability is just too big and leads to the inaccurate prediction (Tietje and Hennings, 1996). Soil properties such as aggregate stability, macroaggregation or particle shape which are known to influence K_{sat}, for which presently no spectral predictions are known (Cohen et al., 2007), affect the K_{sat} and thus lead to prediction inaccuracies if these are based on DRIFT.

5 Conclusion

1) How do soil physical and chemical characteristics of soils in Eastern Madagascar differ for different land use types and depths?

Soil organic carbon, bulk density, and pH were significantly different between the Forest and the other land-uses (Tree Fallow, Shrub Fallow, Degraded Land). The soil organic carbon was significantly higher in Forest than in the other three land-uses because burning leads to a smaller organic matter input in the Fallows and the (Degraded) Grassland compared to the Forest. The deforestation and hence the difference in the soil organic carbon impacted the bulk density. Having more soil organic carbon, resulted in the Forest having a significantly lower bulk density. pH was also significantly lower in the Forest than for the other land-uses. The ash that is added to the soil during the slash-and-burn practice, increases the pH (Demeyer et al., 2001). While $\delta\ ^{13}C$ was only significantly different for two land-use types, there was a clear trend of increasing $\delta\ ^{13}C$ from Forest to Degraded Land, implying that the soil organic carbon from C_3 forest vegetation is over time/over increased agricultural usage replaced by C_4 grasses. There was no significant difference in porosity and nitrogen. A significant difference between Forest and Tree Fallow, Shrub Fallow, Degraded Land was expected due to porosity correlation with bulk density. The varying clay contents are most likely the source of the lack of significant difference. Despite, the similar pattern to the soil organic carbon concentration, nitrogen was not significantly different for the different land-uses.
Soil depth affected all soil physical and chemical characteristics, except for pH. There was no significant difference in pH because the soils are old and have already undergone acidification. soil organic carbon, nitrogen (which follows soil organic carbon) and porosity decrease with depth. The observed decrease of soil organic carbon with greater depth is a widely known phenomena (Stahr et al., 2008). Nitrogen most likely decreased with depth because of the decline in soil organic carbon (Weil and Brady, 2017). Even though the decrease in porosity with depth was not significantly different between Depth 1 and Depth 2, a trend of decline is still observable. The decline in porosity with depth is caused by the increasing compaction with depth, as well as the decreasing number of biopores, aggregation and soil organic matter (Weil and Brady, 2017). These factors also account for the significant increase in bulk density from Depth 0 over Depth 1 to Depth 2.

2) Can we predict K_{sat} from soil physical and chemical properties in tropical soils?

None of the ten existing PTFs was able to predict K_{sat} accurately. Three PTFs (PTF 3, 4 and 5), all using porosity as the only predictor, had a high R^2 but did not predict the K_{sat} values well as indicated by the high RMSE values and the large deviation of the regression curve from the 1-1 line. The reason for the overall unsatisfactory results of existing PTFs is that they are location-specific (Patil and Singh, 2016) and are thus, in many cases, not applicable to different soils in different climates (Wösten et al., 2001). Calibrating an existing function to a new location can provide accurate or moderately accurate predictions, as PTF III (a) and III (b) show, respectively.
It was not possible to create an accurate enough PTF ($R^2 > 0.7$, predicted median K_{sat} < factor 1.5 of the measured median K_{sat},1-1-plot) for the whole data set, depth-specific data sets nor for land-use-specific data sets. PTFs only proved to be accurate for data sets that were depth- and land-use-specific. However, it was not possible to come up with a PTF for each depth per land-use. PTF III (a) and III (b) were able to

provide a rather accurate K_{sat} prediction for the Forest for Depth 1 and Depth 2, respectively. PTF IV and V were both able to accurately predict K_{sat} for Depth 1 of the Tree Fallow sites. PTF VII produced arguably best results for all created PTFs but only for Depth 2 of the Shrub Fallow. The inherent K_{sat} variability is highlighted by the overall high percentage of the mean squared deviation component: lack of correlation. The PTFs can be used to, at least, roughly estimate K_{sat} within a factor of 4.5 for 40 % of all samples. However, they should not be trusted too much, as each of them falsely predicts negative K_{sat} values and they could be off by more than a factor 12, if the land-use and depth specific PTF is applied to other land-uses and/or depths.

Despite adjusting the K_{sat} threshold to create data sets with smaller variability in K_{sat}, the variability was too high to obtain accurate enough predictions based on too high RMSE values. However, Cohen et al. (2007) showed that K_{sat} can be predicted with spectroscopy and PLSR. Future studies should use bigger and possibly less diverse data sets to predict K_{sat} with DRIFT.

6 References

Agyare, W. A., Park, S. J., and Vlek, P. L. G. (2007). Artificial Neural Network Estimation of Saturated Hydraulic Conductivity. *Vadose Zone Journal*, 6:423–431.

Amoozegar, A. (1989). A compact constant-head permeameter for measuring saturaed hydraulic conducitivy of the vadose zone. *Soil Science Society of America Journal*, 53(5):1356–1361.

Andriamananjara, A., Hewson, J., Razakamanarivo, H., Andrisoa, R. H., Ranaivoson, N., Ramboatiana, N., Razafindrakoto, M., Ramifehiarivo, N., Razafimanantsoa, M.-P., Rabeharisoa, L., Ramananantoandro, T., Rasolohery, A., Rabetokotany, N., and Razafimbelo, T. (2016). Land cover impacts on aboveground and soil carbon stocks in Malagasy rainforest. *Agriculture, Ecosystems and Environment*, 233:1–15.

Araújo, S. R., Söderström, M., Eriksson, J., Isendahl, C., Stenborg, P., and Demattê, J. A. (2015). Determining soil properties in Amazonian Dark Earths by reflectance spectroscopy. *Geoderma*, 237:308–317.

Arnoff, S. (2005). *Remote sensing for GIS managers*. ESRI Press, Redelands CA.

Ayoubi, S., Mokhtari Karchegani, P., Reza Mosaddeghi, M., and Honarjoo, N. (2012). Soil aggregation and organic carbon as affected by topography and land use change in western Iran. *Soil & Tillage Research*, 121:18–26.

Baroni, G., Facchi, A., Gandolfi, C., Ortuani, B., Horeschi, D., and Van Dam, J. C. (2010). Uncertainty in the determination of soil hydraulic parameters and its influence on the performance of two hydrological models of different complexity. *Hydrology and Earth System Sciences*, 14:251–270.

Batjes, N. H. (1996). Development of a world data set of soil water retention properties using pedotransfer rules. *Geoderma*, 71:31–52.

Batjes, N. H. and Dijkshoorn, J. A. (1999). Carbon and nitrogen stocks in the soils of the Amazon Region. *Geoderma*, 89:273–286.

Baudron, F. and Giller, K. E. (2014). Agriculture and nature: Trouble and strife ? *Biological Conservation*, 170:232–245.

Bayabil, H. K., Dile, Y. T., Tebebu, T. Y., Engda, T. A., and Steenhuis, T. S. (2019). Geoderma Evaluating infiltration models and pedotransfer functions: Implications for hydrologic modeling. *Geoderma*, 338:159–169.

Beare, M. H., Hendrix, P. F., and Coleman, D. C. (1994). Water-Stable Aggregates and Organic Matter Fractions in Conventional- and No-Tillage Soils. *Soil Science Society of America Journal*, 58:777–786.

Bélanger, É., Lucotte, M., Grégoire, B., Moingt, M., Paquet, S., Davidson, R., Mertens, F., Passos, C. J. S., and Romana, C. (2015). Lignin signatures of vegetation and soils in tropical environments. *Advances in Environmental Research*, 4(4):247–262.

Beven, K. (2001). *Rainfall-Runoff Modelling. The Primer*. Wiley-Blackwell, Chichester, 2 edition.

Beven, K. (2004). Robert E. Horton's perceptual model of infiltration processes. *Hydrological Processes*, 18:3447–3460.

Bonell, M. (2005). Runoff generation in tropical forests. In Bonell, M. and Bruijnzell, L. A., editors, *Forests, Water and People in the Humid Tropics. Past, Present and future Hydrological Research for Integrated Land and Water Management Book II*, chapter 14, pages 314–406. Cambridge University Press, Cambridge.

Bouma, J. (1989). Using soil survy data for quantitative land evaluation. *Advances in soil science*, pages 1777–213.

Bouma, J. and Van Lanen, H. A. J. (1987). *Tranfer fuctions and treshold values: from soil characteristics to land Qualities. Workshop on Quantified Land Evaluation Process, Vol 6*. ITC Publ.

Brand, J. and Pfund, J. L. (1998). Site-and watershed-level assessment of nutrient dynamics under shifting cultivation in eastern Madagascar. *Agriculture, Ecosystems and Environment*, 71:169–183.

Braudeau, E. F. and Mohtar, R. H. (2014). A framework for soil-water modeling using the pedostructure and Structural Representative Elementary Volume (SREV) concepts. *Frontiers in Environmental Science*, 2:1–13.

Burgess, N., Hales, J. D., Underwood, E., Dinerstein, E., Olson, D., Ituoa, I., Shipper, J., Ricketts, T., and Newman, K. (2004). *Terrestrial ecoregions of Africa and Madagascar: a conservation assessment*. Island Press, Washington.

Calabrò, E. and Magazù, S. (2010). Inspections of Mobile Phone Microwaves Effects on Proteins Secondary Structure by Means of Fourier Transform Infrared Spectroscopy. *J. Electromagnetic Analysis & Applications*, 2:607–617.

Celik, I. (2005). Land-use effects on organic matter and physical properties of soil in a southern Mediterranean highland of Turkey. *Soil and Tillage Research*, 83(2):270–277.

Cohen, M., Mylavarapu, R. S., Bogrekci, I., Lee, W. S., and Clark, M. W. (2007). Reflectance Spectroscopy for Routine Agronomic Soil Analyses. *Soil Science*, 172(6):469 – 485.

Comte, I., Davidson, R., Lucotte, M., Reis de Carvalho, C. J., De Assis Oliveira, F., Pantoja da Silva, B., and Rousseau, G. X. (2012). Agriculture , Ecosystems and Environment Physicochemical properties of soils in the Brazilian Amazon following fire-free land preparation and slash-and-burn practices. *"Agriculture, Ecosystems and Environment"*, 156:108–115.

Cosby, B., Hornberger, G., Clapp, R., and Ginn, T. (1984). A statistical exploration of soil moisture characteristics to the physical properties of soils. *Water Resources Research*, 20:682–690.

Curtis, P. G., Slay, C. M., Harris, N. L., Tyukavina, A., and Hansen, M. C. (2018). Classifying drivers of global forest loss. *Science*, 261:1108–1111.

Davidson, E. A. and Ackerman, I. L. (1993). Changes in soil carbon inventories following cultivation of previously untilled soils. *Biogeochemistry*, 20:161–193.

Davis, S. H., Vertessy, R. A., and Silberstein, R. P. (1999). The sensitivity of a catchment model to soil hydraulic properties obtained by using different measurement techniques. *Hydrological Processes*, 13:677–688.

De Condappa, D., Galle, S., Dewandel, B., and Haverkamp, R. (2008). Bimodal Zone of the Soil Textural Triangle :. *Soil Science Society of America Journal*, 72:33–40.

Deckers, J. (1993). Soil fertility and environmental problems in different ecological zones of the developing countries in Sub-Saharan Africa. In van Reuler, H. and Prins, W., editors, *The role of plant nutrients for sustainable food crop production in Sub-Saharan Africa*, chapter 1.4, pages 37–52. Ponsen & Looijen, Wageningen.

Demeyer, A., Nkana, J. C. V., and Verloo, M. G. (2001). Characteristics of wood ash and in uence on soil properties and nutrient uptake : an overview. *Bioresource Technology*, 77:287 – 295.

Dodge, Y. (2008). Least Significant Difference Test.

Don, A., Schumacher, J., and Freibauer, A. (2011). Impact of tropical land-use change on soil organic carbon stocks - a meta-analysis. *Global Change Biology*, 17:1658–1670.

Dörner, J., Dec, D., Peng, X., and Horn, R. (2010). Geoderma Effect of land use change on the dynamic behaviour of structural properties of an Andisol in southern Chile under saturated and unsaturated hydraulic conditions. *Geoderma*, 159:189–197.

Du Puy, D. and Moat, J. (1996). A redefined classification of the primary vegetation of Madagascar based on the underlying geology: using GIS to map itsdistribution and to assess its conservatoin status. *Biogeograhic de Madagascar*, pages 205–218.

Eswaran, H. and Reich, P. F. (2005). World Soil Map: Oxisols.

Ewel, J., Berish, C., Brown, B., Price, N., and Raich, J. (1981). Slash and Burn Impacts on a Costa Rican Wet Forest Site. *Ecology*, 62(3):816–829.

FAO (2006). Global forest resouces assessment 2005. Progress towards sustain management. *FAO Forestry Paper*, 147.

FAO/IIASA (2009). Harmonized World Soil Database (Version 1.1). Technical report, FAO, IIASA,ISRIC,ISS-CAS,JCR, Rome, Laxenburg.

Fitts, C. R. (2013). *Groundwater Science*. Academic Press, Oxford, 2nd edition.

Foley, J. A., DeFries, R., Asner, G. P., Barford, C., Bonan, G., Carpenter, S. R., Chapin, F. S., Coe, M. T., Daily, G. C., Gibbs, H. K., Helkowski, J. H., Holloway, T., Howard, E. A., Kucharik, C. J., Monfreda, C., Patz, J. A., Prentice, I. C., Ramankutty, N., and Snyder, P. K. (2005). Global Consequences of Land Use. *Science*, 309(July):570–574.

Garcıa-Oliva, F., Sanford, R. L., and Kelly, E. (1999). Effects of slash-and-burn management on soil aggregate organic C and N in a tropical deciduous forest. *Geoderma*, 88:1–12.

García-Oliva, F., Casar, I., Morales, P., and Maass, J. M. (1994). Forest-to-pasture conversion influences on soil organic carbon dynamics in a tropical deciduous forest. *Oecologia*, 99:392–396.

Gauch, H. G., Hwang, J. T. G., and Fick, G. W. (2003). Model Evaluation by Comparison of Model-Based Predictions and Measured Values. *Computing Handbook, Third Edition: Computer Science and Software Engineering*, 95(6):1442–1446.

Gay-des Combes, J. M., Robroek, B. J. M., Hervé, D., Guillaume, T., Pistocchi, C., Mills, R. T. E., and Buttler, A. (2017). Agriculture , Ecosystems and Environment Slash-and-burn agriculture and tropical cyclone activity in Madagascar : Implication for soil fertility dynamics and corn performance. *Agriculture, Ecosystems and Environment*, 239:207–218.

GFDRR (2011). Vulnerability, Risk REduction, and Adaptation to Climate Change. Technical report, World Bank Group, Washington DC.

Ghanbarian, B., Taslimitehrani, V., and Pachepsky, Y. A. (2016). Scale-Dependent Pedotransfer Functions Reliability for Estimating Saturated Hydraulic Conductivity. *arXiv preprint arXiv:1610.06958*, pages 1–31.

Griffiths, P. R. and de Haseth, J. A. (2007). *Fourier Transform Infrared Spectrometry*. John Wiley & Sons, Inc., Hoboken, New Jersey, 2nd edition.

Grip, H., Fritsch, J., and Bruijnzeel, L. A. (2005). Soil and water impacts during forest conversion and stabilisation to new land use. In Bonell, M. and Bruijnzeel, L. A., editors, *Forests, Water and People in the Humid Tropics. Past, Present and future Hydrological Research for Integrated Land and Water Management Book II*, chapter 22, pages 561 – 589. Cabridge University Press, Cambridge.

Guo, L. B. and Gifford, R. M. (2002). Soil carbon stocks and land use change : a meta analysis. *Global Change Biology*, 8:345–360.

Gutmann, E. D. and Small, E. E. (2007). A comparison of land surface model soil hydraulic properties estimated by inverse modeling and pedotransfer functions. *Water Resource Research*, 43:1–13.

Hengl, T., Heuvelink, G. B. M., Kempen, B., Leenaars, J. G. B., Walsh, M. G., Shepherd, K. D., Sila, A., MacMillan, R. A., Mendes de Jesus, J., Tamene, L., and Tondoh, J. E. (2015). Mapping Soil Properties of Africa at 250 m Resolution : Random Forests Significantly Improve Current Predictions. *PLoS ONE*, 10(6):1–26.

Herrmann, R. and Onkelinx, C. (1986). Quantities and Units in Clinical Chemistry: Nebulizer and Flame Properties in Flame Emission and Absorption Spectrometry. *Pure & Appl. Chem.*, 58(12):1737–1742.

Hiscock, K. M. and Bense, V. F. (2014). *Hydrogeology Principles and practice*. Wiley Blackwell, Chichester, 2 edition.

Hodnett, M. G. and Tomasella, J. (2002). Marked differences between van Genuchten soil water-retention parameters for temperate and tropical soils : a new water-retention pedo-transfer functions developed for tropical soils. *Geoderma*, 108:155–180.

Hollis, J. M., Hannam, J., and Bellamy, P. H. (2012). Empirically-derived pedotransfer functions for predicting bulk density in European soils. *European Journal of Soil Science*, 63:96–109.

Horning, N. and Hewson, J. (2017). Very high resolution derived land cover/use classifications for the Corridor ANkeniheny-Zahamena (CAZ), Madagascar.

Houghton, B. R. A., Boone, R. D., Fruci, J. R., Hobbie, J. E., Melillo, J. M., Palm, C. A., Peterson, B. J., Shaver, G. R., and Woodwell, G. M. (1987). The flux of carbon from terrestrial ecosystems to the atmosphere in 1980 due to changes in land use : geographic distribution of the global flux. *Tellus*, 39B:122–139.

Hu, W., Shao, M. A., and Si, B. C. (2012). Seasonal changes in surface bulk density and saturated hydraulic conductivity of natural landscapes. *European Journal of Soil Science*, 63:820–830.

IUSS Working Group WRB (2015). *World reference base for soil resources 2014, updated 2015 International soil classification system for naming soils and creating legends for soil maps*. FAO, Rome.

Jabro, J. (1992). Estimation of Saturated Hydraulic Conductivity of Soils From Particle Size Distribution and Bulk Density Data. *American Society of Agricultural Engineers*, 35:557 – 560.

Jarvis, N., Koestel, J., Messing, I., Moeys, J., and Lindahl, A. (2013). Influence of soil , land use and climatic factors on the hydraulic conductivity of soil. *Hydrology and Earth System Sciences*, 17:5185–5195.

Jarvis, N. J., Zavattaro, L., Rajkai, K., Reynolds, W. D., Olsen, P.-A., McGechan, M., MEcke, M., Mohanty, B., Leeds-Harrison, P. B., and Jacques, D. (2002). Indirect estimation of near-saturated hydraulic conductivity from readily available soil information. *Geoderma*, 108:1–17.

Jenkins, R. (1999). *X-Ray Fluorescence Spectrometry*. Wiley and Sons.

Johnson, M. G., Levine, E. R., and Kern, J. S. (1995). Soil organic matter: distribution, genesis, and management to reduce greenhouse gas emissions *. *Water, Air and soil Pollution*, 82:593–615.

Kahl, S., Fernandez, I. J., Rustad, L. E., and Peckenham, J. (1996). Threshold Application Rates of Wood Ash to an Acidic Forest Soil. *Journal of Environmental Quality*, 25:220–227.

Kalnay, E. and Cai, M. (2003). Impact of urbanization and land-use change on climate. *Nature*, 423:528–531.

Kotto-Same, J., Woomer, P. L., Appolinaire, M., and Louis, Z. (1997). Carbon dynamics in slash-and-burn agriculture and land use alternatives of the humid forest zone in Cameroon. *Agriculture, Ecosystems and Environment*, 65:245–256.

Kukla, J., Whitfeld, T., Cajthaml, T., Baldrian, P., Veselá-Šimáčková, H., Novotný, V., and Frouz, J. (2019). The effect of traditional slash - and - burn agriculture on soil organic matter , nutrient content , and microbiota in tropical ecosystems of Papua New Guinea. *Land Degradation & Development*, 30:166–177.

Kull, C. A., Ibrahim, C. K., and Meredith, T. C. (2007). Tropical Forest Transitions and Globalization : Neo- Liberalism , Migration , Tourism , and International Conservation Agendas. *Society and Natural Resources*, 20:723 – 737.

Lal, R. and Kimble, J. M. (2001). Importance of soil bulk density and methods of its importance. In Lal, R., Kimble, J. M., Follell, R. F., and Stewart, B. A., editors, *Assessment Methods for Soil Carbon*, chapter 3, pages 31–44. Lewis Publishers, London.

Malmer, A. (2004). Streamwater quality as affected by wild fires in natural and manmade vegetation in Malaysian Borneo. *Hydrological Processes*, 18:853–864.

Malmer, A., Van Noordwijk, M., and A, B. L. (2005). Effects of shifting cultivatio and forest fire. In Bonell, M. and Bruijnzeel, L. A., editors, *Forests, Water and People in the Humid Tropics. Past, Present and future Hydrological Research for Integrated Land and Water Management Book II*, chapter 21, pages 533 – 560. Cambridge University Press, Cambridge.

Mariotti, A. (1983). Atmospheric nitrogen is a reliable standard for natural 15N abundance measurements. *Nature*, 303:685 – 687.

McCarty, G. W., Reeves, V. B., Follett, R. F., and Kimble, J. M. (2002). Mid-Infrared and Near-Infrared Diffuse Reflectance Spectroscopy for Soil Carbon Measurement. *Soil Science Society of America Journal*, 66:640–646.

Météo Madagascar (2013). Precipitation Data CAZ 1983-2013. Technical report. Technical report, Ministère des Transports et de la Météorologie, Antananarive.

Mevik, B.-H. and Wehrens, R. (2007). The pls Package: Principal Component and Partial Least Squares Regression in R. *Journal of Statistical Software*, 18(2):1–23.

Minasny, B. and Hartemink, A. E. (2011). Earth-Science Reviews Predicting soil properties in the tropics. *Earth-Science Reviews*, 106:52–62.

Minasny, B. and Mcbratney, A. B. (2000). Evaluation and development of hydraulic conductivity pedotransfer functions for Australian soil. *Aust. J. Soil Research*, 38:905–926.

Minasny, B., Mcbratney, A. B., and Bristow, K. L. (1999). Comparison of different approaches to the development of pedotransfer functions for water-retention curves. *Geoderma*, 93:225–253.

Mirabella, A., Egli, M., Carnicelli, S., and Sartori, G. (2002). Influence of parent material on clay minerals formation i Podzols of Trentino, Italy. *Clay Minerals*, 37(4):699 – 707.

Muccio, Z. and Jackson, G. P. (2009). Isotope ratio mass spectrometry. *Analyst*, 134:213–222.

Murty, D., Kirschbaum, M. U. F., McMurtrie, R. E., and McGilvary, H. (2002). Does conversion of forest to agricultural land change soil carbon and nitrogen ? a review of the literature. *Global Change Biology*, 8:105–123.

Nadler, A., Levy, G. J., Keren, R., and Eisenberg, H. (1996). Sodic Calcareous Soil Reclamation as Affected by Water Chemical Composition and Flow Rate. *American Society of Agricultural Engineers*, 60:252–257.

Natelhoffer, K. J. and Fry, B. (1988). Controls on Natural Nitrogen-15 and Carbon-13 Abundances in Forest Soil Organic Matter. *Soil Science Society of America Journal*, 52(6):1633 – 1640.

Nemes, A., Rawls, W. J., and Pachepsky, Y. A. (2005). Influence of Organic Matter on the Estimation of Saturated Hydraulic Conductivity. *Soil Science Society of America Journal*, 69(4):1330–1337.

Nemes, A., Schaap, M. G., and Wösten, J. H. M. (2003). Functional Evaluation of Pedotransfer Functions Derived from Different Scales of Data Collection. *Soil Science Society of America Journal*, 57:1093–1102.

Nuopponen, M. H., Birch, G. M., Sykes, R. J., Lee, S. J., and Steward, D. (2006). Estimation of Wood Density and Chemical Composition by Means of Diffuse Reflectance Mid-Infrared Fourier Transform (DRIFT-MIR) Spectroscopy. *Journal of Agricultural Food Chemistry*, 54:34–40.

Nye, P. and Greenland, D. (1960). *The soil under shifting cultivation.* Commonwealth Agricultural Bureaux, Farnham Royal, Bucks, England.

Oshunsanya, S. (2013). Predicting saturated hydraulic conductivity from selected properties of Alfisol using Pedo-transfer functions - a case study of the Iwo sandy loam , Ibadan , southwest Nigeria. *Ife Journal of Science*, 15(1):135–143.

P4GES (2015). P4GES - Can Paying for Global Ecosystem Services reduce poverty.

Pachepsky, Y. A., Rawls, W. J., and Lin, H. S. (2006). Hydropedology and pedotransfer functions. *Geoderma*, 131:308–316.

Pachepsky, Y. A., Rawls, W. J., and Timlin, D. J. (1999). The Current Status of Pedotransfer Functions : Their Accuracy , Reliability , and Utility in Field and Regional Scale Modeling. In Corwin, D. L., Loague, K., and Ellsworth, T. R., editors, *Assessment of Non-Pont Source Pollutoin in the Vadose Zone*, pages 223–234. American Geophysical Union, Washington, DC.

Patil, N. G., Pajput, G. S., Nema, R. K., and Singh, R. B. (2010). Predicting hydraulic properties of seasonally impounded soils. *Journal of Agricultural Science*, 148:159–170.

Patil, N. G. and Singh, S. K. (2016). Pedotransfer Functions for Estimating Soil Hydraulic Properties : A Review. *Pedosphere: An International Journal*, 26(4):417–430.

Penner-hahn, J. E. (2013). Technologies for Detecting Metals in Single Cells. In Banci, L., editor, *Metallomics and the Cell*, chapter 2, pages 15–40. Springer, Dordrecht.

Pereira Machado Dias, F., Hübner, R., De Jesus Nunes, F., Mozena Leandro, W., and Alisson da Silva Xavier, F. (2019). Effects of land-use change on chemical attributes of a Ferralsol in Brazilian Cerrado. *Catena*, 177:180–188.

Pirzer, M. and Sawatzki, J. (2008). Method and device for correcting a spectrum.

Portela, R., Nunes, P. A. L. D., Onofri, L., Villa, F., Shepard, A., and Lange, G.-m. (2012). Assessing and Valuing Ecosystem Services in Ankeniheny-Zahamena Corridor (CAZ), Madagascar. Technical report, A Demonstration Case Study for the Wealth Accounting and the Valuation of Ecosystem Services (WAVES) Global Partnership.

Pribyl, D. W. (2010). A critical review of the conventional SOC to SOM conversion factor. *Geoderma*, 156:75–83.

R Core Team (2018). R: a Language and Environment for Statistical Computing.

Rawls, W. J., Pachepsky, Y., and Shen, M. H. (2001). Testing soil water retention estimation with the MUUF pedotransfer model using data from the southern United States. *Journal of Hydrology*, 251:177 – 185.

Rossel, R. A. V., Walvoort, D. J. J., Mcbratney, A. B., Janik, L. J., and Skjemstad, J. O. (2006). Visible , near infrared , mid infrared or combined diffuse reflectance spectroscopy for simultaneous assessment of various soil properties. *Geoderma*, 131:59–75.

Sanchez, P. A. and Buol, S. W. (1975). Soils of the Tropics and the World Food Crisis. *Science*, 188(4188):598–603.

Sanchez, P. A., Villachia, J. H., and Brandy, D. E. (1983). Soil fertility dynamics after clearing a tropical rainforest in Peru. *Soil Science Society of America Journal*, 47:1171 – 1178.

Schaap, M. G., Leij, F. J., and Genuchten, M. T. V. (2001). rosetta : a computer program for estimating soil hydraulic parameters with hierarchical pedotransfer functions. *Journal of Hydrology*, 251:163–176.

Schiedung, M., Tregurtha, C. S., Beare, M. H., Thomas, S. M., and Don, A. (2019). Deep soil flipping increases carbon stocks of New Zealand grasslands. *Global change biology*, pages 1–14.

Shen, X., Xu, L., Ye, S., Hu, R., Jin, L., Xu, H., and Liu, W. (2018). Automatic baseline correction method for the open-path Fourier transform infrared spectra by using simple iterative averaging. *Optics EXPRESS*, 26(10):609–614.

Soesbergen, A. V. and Mulligan, M. (2018). Uncertainty in data for hydrological ecosystem services modelling : Potential implications for estimating services and beneficiaries for the CAZ Madagascar. *Ecosystem Services*, 33:175–186.

Soil Survey Staff (2011). *Soil Survey Laboratory Information Manual. Soil Survey Investigation Report No. 45, Version 2*. U.S. Department of Agriculture, Natural Resources Conservation Service.

Soil Survey Staff (2014). *Keys to Soil Taxonomy*. USDA-Natural Resources Conservation Services, Washington, DC, 12th edition.

Song, X.-p., Hansen, M. C., Stehman, S. V., Potapov, P. V., Tyukavina, A., Vermote, E. F., and Townshend, J. R. (2018). Global land change from 1982 to 2016. *Nature*, 560:639 – 643.

Soriano-disla, J. M., Janik, L. J., Viscarra Rossel, R. A., Macdonald, L. M., and Mclaughlin, M. J. (2014). The Performance of Visible , Near- , and Mid- Infrared Reflectance Spectroscopy for Prediction of Soil Physical , Chemical , and Biological Properties. *Applied Spectroscopy Reviews*, 49(2):139–186.

SPECTRO Analytical Instruments (2005). XRF Fundamentals. Technical report, AMETEK SPECTRO ANALYTICAL INSTRUMENTS.

Stahr, K., Kandeler, E., Herrmann, L., and Streck, T. (2008). *Bodenkunde und Standortlehre*. Ulmer Verlag, Stuttgart, 3rd edition.

Stuart, B. (2015). Infrared spectroscopy. In *Kirk-Othmer Encyclopedia of Chemical Technology*, volume 14, pages 224–243. John Wiley & Sons, Inc., 5 edition.

Styger, E., Fernandes, E. C. M., Rakotondramasy, H. M., and Rajaobelinirina, E. (2009). Degrading uplands in the rainforest region of Madagascar : Fallow biomass , nutrient stocks , and soil nutrient availability. *Agroforest Syst*, 77:107–122.

Styger, E., Rakotondramasy, H. M., Pfeffer, M. J., Fernandes, E. C. M., and Bates, D. M. (2007). Influence of slash-and-burn farming practices on fallow succession and land degradation in the rainforest region of Madagascar. *Agriculture, Ecosystems and Environment*, 119:257–269.

Tadross, M., Randriamarolaza, L., Rabefitia, Z., and Ki Yip, Z. (2008). Climate Change in Madagascar, Past and Future. Technical Report. Technical report, Climate Systems Analysis Group. University of Cape Town, Sowth Africa, and NAtional Meteorological Office, Antananarivo.

Thomaz, E. L., Antoneli, V., and Doerr, S. H. (2014). Catena Effects of fi re on the physicochemical properties of soil in a slash-and-burn agriculture. *Catena*, 122:209–215.

Tietje, O. and Hennings, V. (1996). Accuracy of the saturated hydraulic conductivity prediction by pedo-transfer functions compared to the variability within FAO textural classes. *Geoderma*, 69(1-2):71–84.

Tomasella, J. and Hodnett, M. G. (2004). Pedotransfer functions for tropical soils. *Development in Soil Science*, 30:415–429.

Tóth, B., Weynants, M., Nemes, A., Makó, A., Bilas, G., and Tóth, G. (2015). New generation of hydraulic pedotransfer functions for Europe. *European Journal of Soil Science*, 66(1):226–238.

Townsend, A. R., Asner, G. P., White, J. W. C., and Tans, P. P. (2002). Land use effects on atmospheric sink in tropical latitudes C imply a sizable terrestrial CO 2. *Geophysical Research Letters*, 29(10):13–16.

(USGS), U. G. S. (2018). USGS EROS Archive - Digital Elevation - Global 30 Arc-Second Elevation (GTOPO30).

van den Berg, M., Klamt, E., Van Reeuwijk, L. P., and Sombroek, W. G. (1997). Pedotransfer functions for the estimation of moisture retention characteristics of Ferralsols and related soils. *Geoderma*, 78:161–180.

van Dijk, E. J. C. (2015). *BSc thesis: The soil nitrogen- , carbon content and pH of different land covers in Eastern-Madagascar*. VU University.

Vliet, N. V., Mertz, O., Heinimann, A., Langanke, T., Pascual, U., Schmook, B., Adams, C., Schmidt-Vogt, D., Messerli, P., Leisz, S., Castella, J.-C., Jørgensen, L., Birch-Thomsen, T., Hett, C., Bech-Bruun, T., Ickowitz, A., Chi, K., Yasuyuki, K., Fox, J., Padoch, C., Dressler, W., and Ziegler, A. D. (2012). Trends , drivers and impacts of changes in swidden cultivation in tropical forest-agriculture frontiers : A global assessment. *Global Environmental Change*, 22:418–429.

Vogt, R. and Finlayson-Pitts, B. J. (1994). A Diffuse Reflectance Infrared Fourier Transform Spectroscopic (DRIFTS) Study of the Surface Reaction of NaCl with Gaseous NO2 and HNO3. *Journal of Physical Chemistry*, 98:3747–3755.

Wagner, B., Tarnawski, V. R., Hennings, V., Müller, U., Wessolek, G., and Plagge, R. (2001). Evaluation of pedo-transfer functions for unsaturated soil hydraulic conductivity using an independent data set. *Geoderma*, 102:275–297.

Weil, R. R. and Brady, N. C. (2017). *The nature and properteis of soils / Nyle C. Brady, Ray R. Weil.* Pearson Educational Limited, Essex, 15 edition.

Wösten, J. H. M., Finke, P. A., and Jansen, M. J. W. (1995). Comparison of class and continuous pedotransfer functions to generate soil hydraulic characteristics. *Geoderma*, 66:227–237.

Wösten, J. H. M., Lilly, A., Nemes, A., and Le Bas, C. (1999). Development and use of a database of hydraulic properties of European soils. *Geoderma*, 90:169–185.

Wösten, J. H. M., Pachepsky, Y. A., and Rawls, W. J. (2001). Pedotransfer functions : bridging the gap between available basic soil data and missing soil hydraulic characteristics. *Journal of Hydrology*, 251:123–150.

Young, M. D. B., Gowing, J. W., Hatibu, N., Mahoo, H. M. F., and Payton, R. W. (1999). Assessment and Development of Pedotransfer Functions for Semi-Arid Sub-Sahmm Africa. *Phys. Chem. Earth*, 24(7):845–849.

Zimmermann, B., Elsenbeer, H., and De Moraes, J. M. (2006). The influence of land-use changes on soil hydraulic properties: Implications for runoff generation. *Forest Ecology and Management*, 222:29–38.

Zvoleff, A., WAndersee, S., An, L., and López-Carr, D. (2002). Land Use and Cover Change. *BioScience*, 52:143–150.

Zwartendijk, B. W., van Meerveld, I. H. J., Ghimire, C. P., Bruijnzeel, L. A., Ravelona, M., and Jones, J. P. (2017). Rebuilding soil hydrological functioning after swidden agriculture in eastern Madagascar. *Agriculture, Ecosystems and Environment*, 239:101–111.

7 Appendix

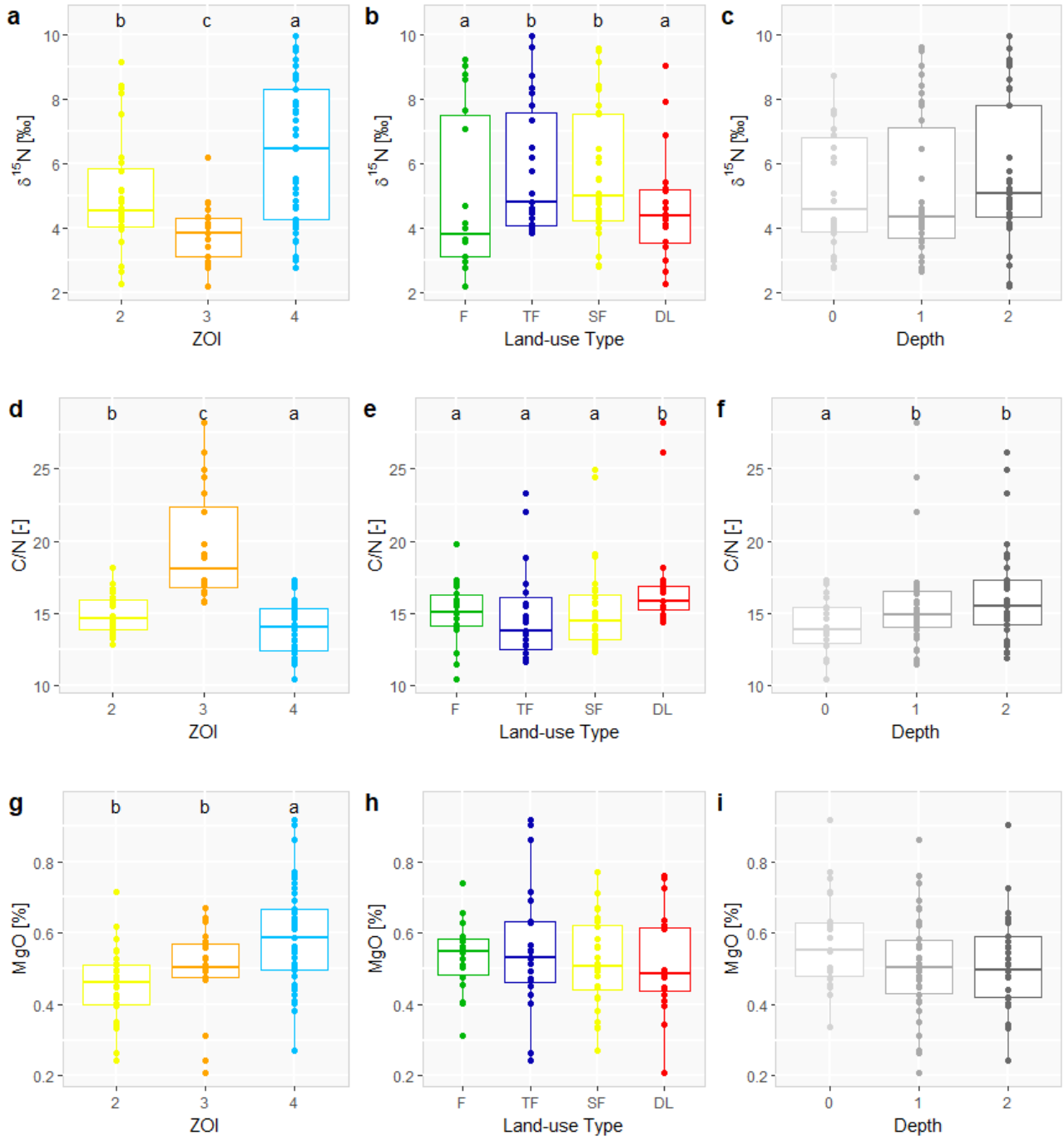

Figure 20: Boxplots of δ^{15}N (a - c), carbon nitrogen ratio (C/N; d - f), magenesium oxide (MgO; g - i), copper (Cu; j - l), silicon dioxide(SiO_2; m - o), aluminium oxide (AL_2O_3; p - r) and iron(III) oxide (Fe_2O_3; s - u) grouped by ZOIs (left), the land-use (middle) and the depths (right). Different letters indicate significant differences in the mean values for the different groups. Where no letters are shown the mean values did not differ for the different groups.

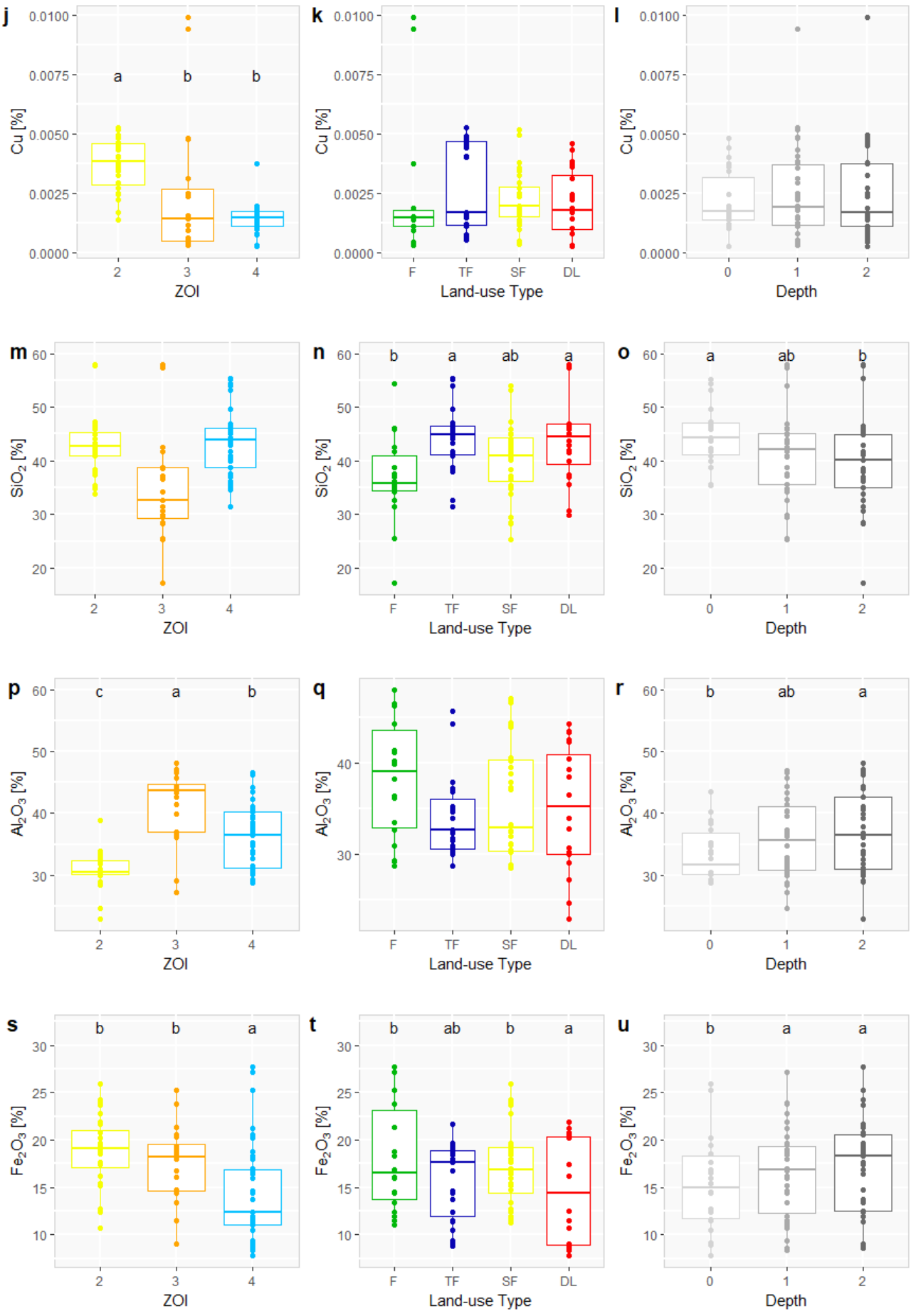

Figure 20: Continued

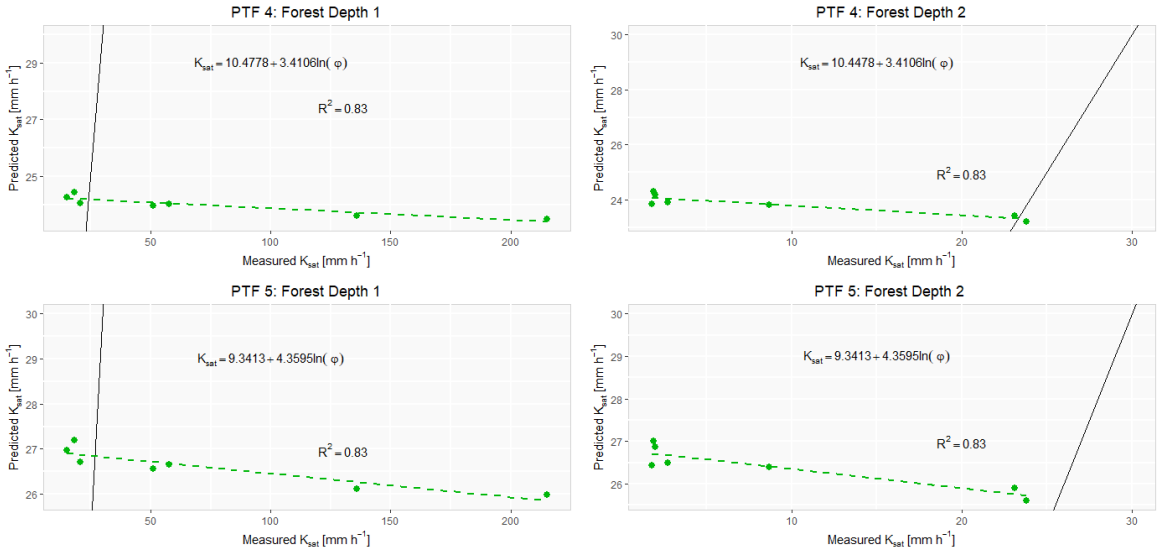

Figure 21: Plots of the predicted vs. the measured K_{sat} for Forest for PTF 4 for Depth 1 (left) and Depth 2 (right) and for PTF 5 for Depth 1 (left) and Depth 2 (right). The solid black line is the 1-1 line. The dashed line illustrates te linear regression curve. The function as well as R^2 of each PTF is denoted in the graph.

Table 10: Mean values and the min - max range of the most important soil properties for each depth per ZOI. No samples of Depth 0 in ZOI 3 were gathered.

		ZOI 2			ZOI 3			ZOI 4		
		D0	D1	D2	D0	D1	D2	D0	D1	D2
Soil Properties	n	8	10	10	0	10	10	14	14	13
Al_2O_3 [%]	mean	31.43	30.48	30.47	-	41.33	41.24	34.64	36.33	38.34
	range	28.73 - 38.89	24.70 - 32.83	22.93 - 33.99	-	27.22 - 46.95	29.10 - 48.07	29.20 - 43.52	28.70 - 46.49	30.93 - 46.56
SOC [%]	mean	4.9	3.4	2.6	-	3.2	2.6	5.3	4.1	3.3
	range	3.62 - 8.72	2.84 - 3.75	2.02 - 3.27	-	2.82 - 3.46	1.89 - 3.64	3.69 - 7.11	2.35 - 5.87	2.36 - 4.80
C/N [-]	mean	14.4	14.9	15.3	-	18.9	20.2	14.0	13.8	14.1
	range	12.82 - 16.47	13.24 - 17.04	12.82 - 18.15	-	15.74 - 28.16	16.87 - 26.16	10.44 - 17.34	11.48 - 16.82	11.93 - 16.87
Cu [%]	mean	0.0032	0.0039	0.0040	-	0.0024	0.0025	0.0016	0.0015	0.0013
	range	0.0014 - 0.0048	0.0022 - 0.0053	0.0025 - 0.0049	-	0.0003 - 0.0094	0.0005 - 0.0099	0.0003 - 0.0037	0.0003 - 0.0037	0.0003 - 0.0019
$\delta^{13}C$ [‰]	mean	-26.4	-25.9	-25.9	-	-27.3	-27.0	-26.5	-26.2	-26.1
	range	-27.45 to -25.07	-26.80 to -23.32	-26.77 to -24.15	-	-27.83 to - 26.27	-27.71 to -25.77	-27.45 to -23.75	-27.40 to -23.48	-27.05 to -23.18
Fe_2O_3 [%]	mean	17.8	18.8	19.6	-	17.1	18.0	14.0	14.6	14.4
	range	12.40 - 25.91	10.76 - 23.93	12.50 - 24.24	-	11.51 - 23.75	9.04 - 25.218	7.80 - 25.23	8.36 - 27.15	8.56 - 27.70
K_2O [%]	mean	0.3	0.0	0.0	-	0.1	0.1	0.1	0.1	0.1
	range	0.03 - 1.36	0.02 - 0.07	0.02 - 0.09	-	0.02 - 0.12	0.02 - 0.14	0.04 - 0.48	0.03 - 0.47	0.03 - 0.48
P_2O_5 [%]	mean	0.1	0.1	0.1	-	0.2	0.2	0.1	0.1	0.1
	range	0.00 - 0.19	0.00 - 0.18	0.00 - 0.14	-	0.09 - 0.47	0.07 - 0.41	0.00 - 0.18	0.00 - 0.21	0.00 - 0.20
MgO [%]	mean	0.5	0.4	0.4	-	0.5	0.5	0.6	0.6	0.6
	range	0.34 - 0.72	0.26 - 0.59	0.24 - 0.53	-	0.21 - 0.67	0.24 - 0.64	0.43 - 0.92	0.27 - 0.86	0.40 - 0.90
N [%]	mean	0.4	0.2	0.2	-	0.2	0.1	0.4	0.3	0.2
	range	0.24 - 0.68	0.18 - 0.27	0.14 - 0.23	-	0.12 - 0.22	0.09 - 0.22	0.26 - 0.52	0.19 - 0.37	0.18 - 0.34
$\delta^{15}N$ [‰]	mean	4.8	5.0	5.4	-	3.6	4.0	5.4	6.6	7.1
	range	2.79 - 7.51	2.66 - 8.43	2.28 - 9.13	-	2.76 - 4.55	2.18 - 6.19	2.75 - 8.72	3.58 - 9.61	3.98 - 9.96
SiO_2 [%]	mean	43.2	43.7	42.8	-	35.3	34.3	45.4	43.3	41.7
	range	35.45 - 47.19	34.81 - 57.98	33.92 - 57.77	-	25.32 - 57.34	17.20 - 57.95	35.55 - 55.16	34.66 - 54.04	31.37 - 55.46
Sa [%]	mean	38.3	27.4	29.3	-	56.7	64.6	56.1	58.7	56.9
	range	8.29 - 69.73	9.86 - 58.57	8.63 - 64.97	-	35.32 - 78.98	42.41 - 88.08	33.34 - 79.93	42.49 - 73.30	28.34 - 69.61
Sil [%]	mean	16.7	19.0	18.2	-	12.8	10.4	14.8	13.5	14.5
	range	2.70 - 25.88	4.00 - 26.00	3.10 - 29.20	-	6.57 - 18.74	3.29 - 16.31	6.44 - 21.32	8.30 - 19.62	8.24 - 34.63
Cl [%]	mean	45.0	53.6	52.6	-	30.5	25.1	29.0	27.8	28.6
	range	17.53 - 70.80	27.70 - 70.50	22.99 - 69.40	-	14.45 - 47.59	8.63 - 44.40	13.63 - 45.34	16.54 - 41.74	21.42 - 42.60
BD [g cm^{-3}]	mean	1.14	1.27	1.34	-	1.16	1.26	1.09	1.21	1.27
	range	0.91 - 2.01	1.08 - 2.10	1.11 - 2.19	-	1.04 - 1.29	1.10 - 1.40	0.83 - 1.36	0.97 - 1.51	1.04 - 1.55
pH [-]	mean	5.18	4.74	4.85	-	4.67	4.91	4.73	4.72	4.79
	range	4.68 - 5.76	4.40 - 5.20	4.51 - 5.20	-	3.90 - 5.20	4.20 - 5.50	3.36 - 5.68	3.50 - 5.70	3.80 - 5.60
φ [%]	mean	59.65	54.98	52.90	-	48.33	44.84	51.51	48.17	46.98
	range	52.20 - 63.80	47.00 - 60.40	44.60 - 59.20	-	39.12 - 56.92	34.42 - 55.62	38.60 - 63.40	36.20 - 60.60	34.40 - 57.40

Table 11: Mean values and the min - max range of the most important soil properties for all three depths and all four land- use types.

		D0	D1	D2	F	TF	SF	DL
Soil Properties	n	22	34	33	19	22	28	20
Al_2O_3 [%]	mean	33.47	36.08	36.83	38.31	24.04	35.97	34.96
	range	28.73 - 43.52	24.70 - 46.95	22.93 - 48.07	28.70 - 48.07	28.73 - 45.70	38.47 - 47.12	22.93 - 44.25
SOC [%]	mean	5.18	3.59	2.87	4.15	3.43	3.75	3.61
	range	3.62 - 8.72	2.35 - 5.87	1.89 - 4.80	2.11 - 6.61	2.02 - 8.72	2.15 - 6.72	1.89 - 7.11
C/N [-]	mean	14.17	15.63	16.29	14.99	14.80	15.38	17.00
	range	10.44 - 17.34	11.48 - 28.16	11.93 - 26.16	10.44 - 19.83	11.61 - 23.33	12.34 - 24.95	14.42 - 28.16
Cu [%]	mean	0.0022	0.0025	0.0025	0.0024	0.0028	0.0022	0.0021
	range	0.0003 - 0.0048	0.0003 - 0.0094	0.0003 - 0.0099	0.0003 - 0.0099	0.0005 - 0.0053	0.0004 - 0.0052	0.0003 - 0.0046
$\delta^{13}C$ [‰]	mean	-26.46	-26.43	-26.32	-27.15	-26.70	-26.22	-25.60
	range	-27.45 to -23.75	-27.83 to -23.32	-27.71 to -23.18	-27.83 to -26.42	-27.45 to -25.88	-27.32 to -25.07	-27.54 to -23-18
Fe_2O_2 [%]	mean	15.36	16.56	17.07	18.11	15.71	17.24	14.73
	range	7.80 - 25.91	8.36 - 27.15	8.56 - 27.695	11.08 - 27.69	8.84 - 21.73	11.27 - 25.91	7.80 - 21.94
K_2O [%]	mean	0.19	0.09	0.09	0.09	0.18	0.06	0.13
	range	0.03 - 1.36	0.02 - 0.47	0.02 - 0.48	0.02 - 0.18	0.02 - 1.36	0.02 - 0.54	0.03 - 0.48
P_2O_5 [%]	mean	0.09	0.12	0.10	0.16	0.08	0.10	0.09
	range	0.00 - 0.19	0.00 - 0.47	0.00 - 0.41	0.00 - 0.47	0.00 - 0.24	0.00 - 0.20	0.00 - 0.19
MgO [%]	mean	0.58	0.51	0.51	0.53	0.55	0.52	0.51
	range	0.34 - 0.92	0.21 - 0.86	0.24 - 0.90	0.31 - 0.74	0.24 - 0.92	0.27 - 0.77	0.21 - 0.76
N [%]	mean	0.37	0.24	0.19	0.29	0.24	0.26	0.22
	range	0.24 - 0.68	0.12 - 0.37	0.09 - 0.34	0.11 - 0.52	0.09 - 0.68	0.09 - 0.50	0.11 - 0.46
$\delta\ ^{15}N$ [‰]	mean	5.16	5.23	5.66	5.04	5.82	5.70	4.68
	range	2.75 - 8.72	2.66 - 9.61	2.18 - 9.96	2.18 - 9.22	3.82 - 9.96	2.79 - 9.55	2.28 - 9.02
SiO_2 [%]	mean	44.62	41.07	39.78	36.77	44.18	40.17	44.41
	range	35.45 - 55.16	25.32 - 57.98	17.20 - 57.95	17.20 - 54.38	31.38 - 55.46	25.32 - 54.03	29.95 - 57.98
Sa [%]	mean	50.19	48.92	51.36	53.78	50.76	50.09	46.24
	range	8.29 - 79.93	9.86 - 78.98	8.63 - 88.08	28.34 - 71.75	8.29 - 78.98	15.70 - 88.08	12.70 - 67.31
Sil [%]	mean	15.45	14.92	14.22	15.01	13.72	13.63	17.38
	range	2.70 - 25.88	4.00 - 26.00	3.10 - 34.63	9.52 - 34.63	5.90 - 26.03	2.70 - 25.20	9.06 - 29.20
Cl [%]	mean	34.36	36.16	34.42	31.20	35.52	34.83	36.39
	range	13.63 - 70.80	14.45 - 70.50	8.63 - 69.40	16.54 - 44.40	14.45 - 65.83	8.63 - 70.80	20.86 - 66.34
BD [g cm^{-3}]	mean	1.11	1.21	1.29	1.11	1.34	1.19	1.20
	range	0.83 - 2.01	0.97 - 2.10	1.04 - 2.19	0.83 - 1.42	0.91 -2.19	0.96 - 1.32	0.88 - 1.43
pH [-]	mean	4.90	4.71	4.84	4.07	5.02	4.94	5.03
	range	3.36 - 5.76	3.50 - 5.70	3.80 - 5.60	3.36 - 4.60	4.49 - 5.56	4.40 - 5.76	4.30 - 5.70
φ [%]	mean	54.47	50.22	48.13	52.62	49.87	49.74	50.35
	range	38.60 - 63.80	36.20 - 60.60	34.40 - 59.20	41.66 - 63.40	34.40 - 61.80	37.22 - 63.80	36.60 - 63.40

Table 12: Mean values and the min - max range of the most important soil properties for all three depths per land-use type.

		F			TF		
		D0	D1	D2	D0	D1	D2
Soil Properties	n	4	7	7	7	8	8
Al_2O_3 [%]	mean	32.57	38.59	41.31	31.78	34.91	35.14
	range	29.20 - 38.28	28.70 - 46.49	30.93 - 41.18	28.73 - 35.21	29.98 - 45.70	30.38 - 44.28
SOC [%]	mean	5.78	4.02	3.35	4.93	3.09	2.46
	range	4.73 - 6.61	3.18 - 5.20	2.11 - 4.80	3.62 - 8.72	2.50 - 3.74	2.02 - 2.82
C/N [-]	mean	13.52	14.84	15.99	13.32	15.26	15.64
	range	10.44 - 14.99	11.48 - 17.16	12.22 - 19.83	11.61 - 16.47	11.63 - 22.05	11.93 - 23.33
Cu [%]	mean	0.0020	0.0026	0.0024	0.0027	0.0029	0.0029
	range	0.0011 - 0.0037	0.0003 - 0.0094	0.0005 - 0.01	0.0012 - 0.0048	0.0005 - 0.0053	0.0006 - 0.0049
$\delta^{13}C$ [‰]	mean	-27.09	-27.26	-27.05	-26.90	.26.72	.26.51
	range	-27.45 to -26.83	-27.83 to -26.42	-27.71 to -26.44	-27.45 to -26.07	-27.37 to -26.15	-27.18 to -25.88
Fe_2O_3 [%]	mean	17.05	18.18	18.64	14.60	15.91	16.47
	range	11.48 - 25.23	11.08 - 27.15	12.00 - 27.69	9.10 - 19.48	9.42 - 19.48	8.84 - 21.73
K_2O [%]	mean	0.10	0.09	0.08	0.32	0.12	0.12
	range	0.04 - 0.18	0.02 - 0.18	0.02 - 0.11	0.03 - 1.36	0.02 - 0.28	0.02 - 0.31
P_2O_5 [%]	mean	0.10	0.19	0.17	0.06	0.10	0.08
	range	0.07 - 0.15	0.07 - 0.47	0 - 0.41	0 - 0.12	0 - 0.24	0 - 0.23
MgO [%]	mean	0.52	0.52	0.55	0.64	0.53	0.50
	range	0.45 - 0.59	0.31 - 0.74	0.40 - 0.66	0.47 - 0.92	0.26 - 0.86	0.24 - 0.90
N [%]	mean	0.43	0.28	0.22	0.37	0.21	0.16
	range	0.32 - 0.52	0.19 - 0.36	0.11 - 0.34	0.27 - 0.68	0.13 - 0.30	0.09 - 0.22
$\delta^{15}N$ [‰]	mean	5.15	4.90	5.13	5.32	5.80	6.30
	range	2.75 - 7.65	2.76 - 9.02	2.18 - 9.22	3.82 - 8,72	3.82 - 9.61	4.02 - 9.96
SiO_2 [%]	mean	43.70	36.56	33.02	46.82	43.33	42.71
	range	35.55 - 54.38	25.55 - 45.87	17.20 - 41.71	41.00 - 55.16	32.56 - 54.04	31.38 - 55.46
Sa [%]	mean	53.50	55.47	52.25	49.43	50.37	52.14
	range	42.77 - 59.33	38.99 - 71.75	28.34 - 68.11	8.29 - 69.73	9.86 - 78.98	8.63 - 77.77
Sil [%]	mean	15.65	13.88	15.78	16.40	13.03	12.41
	range	12.12 - 18.85	9.53 - 19.62	9.52 - 34.63	12.11 - 25.88	6.30 - 24.52	5.90 - 26.03
Cl [%]	mean	30.85	30.65	31.97	34.17	36.60	35.45
	range	24.45 - 41.43	16.54 - 43.71	21.22 - 44.40	17.53 - 65.83	14.45 - 65.62	16.17 - 65.34
BD [$g\,cm^{-3}$]	mean	0.93	1.11	1.20	1.24	1.35	1.41
	range	0.83 - 1.01	0.97 - 1.23	1.06 - 1.42	0.91 - 2.01	1.10 - 2.10	1.12 - 2.19
pH [-]	mean	3.80	3.99	4.31	5.18	4.91	4.98
	range	3.36 - 4.16	3.50 - 4.30	3.80 - 4.60	4.74 - 5.56	4.49 - 5.40	4.50 - 5.50
φ [%]	mean	57.15	52.55	50.12	53.17	49.09	47.76
	range	51.60 - 63.40	45.42 - 60.00	41.66 - 7.40	42.40 - 61.80	36.20 - 59.00	34.40 - 59.20

(Continues on next page)

Table 12: continued

		SF			DL		
		D0	D1	D2	D0	D1	D2
Soil Properties	n	7	11	10	4	8	8
Al_2O_3 [%]	mean	33.93	36.33	36.45	36.52	34.71	34.42
	range	30.21 - 40.26	28.47 - 46.95	28.91 - 47.12	30.09 - 43.52	24.70 - 43.34	22.93 - 44.25
SOC [%]	mean	5.13	3.62	2.87	5.13	3.70	2.77
	range	2.87 - 6.72	2.35 - 5.87	2.15 - 4.00	4.32 - 7.11	2.82 - 4.95	1.89 - 4.01
C/N [-]	mean	14.25	15.38	15.85	16.14	17.06	17.38
	range	12.80 - 17.07	12.42 - 24.45	12.34 - 24.95	15.33 - 17.34	14.42 - 28.16	14.53 - 26.16
Cu [%]	mean	0.0020	0.0023	0.0025	0.0017	0.0022	0.0022
	range	0.0012 - 0.0034	0.0004 - 0.0052	0.0005 - 0.005	0.0003 - 0.0036	0.0003 - 0.0043	0.0003 - 0.0046
$\delta^{13}C$ [‰]	mean	-26.14	-26.29	-26.13	-25.60	-25.59	-25.62
	range	-26.85 to -25.07	-27.32 to -25.23	-27.30 to -25.13	-26.49 to -23.75	-27.54 to -23.32	-27.14 to -23.18
Fe_2O_3 [%]	mean	15.78	17.24	17.90	14.29	14.87	14.80
	range	11.58 - 25.91	11.27 - 23.93	11.99 - 24.24	7.80 - 20.25	8.35 - 21.94	8.56 - 20.79
K_2O [%]	mean	0.13	0.05	0.06	0.15	0.12	0.12
	range	0.03 - 0.54	0.02 - 0.07	0.02 - 0.21	0.04 - 0.48	0.03 - 0.47	0.03 - 0.48
P_2O_5 [%]	mean	0.09	0.11	0.10	0.11	0.10	0.08
	range	0 - 0.18	0 - 0.20	0 - 0.21	0 - 0.19	0 - 0.18	0 - 0-14
MgO [%]	mean	0.55	0.50	0.52	0.57	0.49	0.50
	range	0.34 - 0.77	0.27 - 0.67	0.33 - 0.65	0.43 - 0.75	0.21 - 0.76	0.34 - 0.73
N [%]	mean	0.36	0.24	0.19	0.32	0.23	0.16
	range	0.24 - 0.50	0.13 - 0.37	0.09 - 0.31	0.26 - 0.46	0.12 - 0.32	0.11 - 0.26
$\delta^{15}N$ [‰]	mean	5.43	5.60	6.12	4.43	4.42	5.08
	range	2.79 - 7.56	3.09 - 9.50	2.82 - 9.55	2.99 - 6.89	2.66 - 7.91	2.28 - 9.02
SiO_2 [%]	mean	43.80	39.85	38.90	43.14	44.43	45.02
	range	35.45 - 53.28	25.32 - 54.03	28.22 - 48.00	39.98 - 56.92	29.95 - 57.98	30.63 - 57.95
Sa [%]	mean	46.88	47.95	53.37	53.83	43.05	45.63
	range	25.92 - 79.93	18.00 - 73.30	15.70 - 88.08	38.00 - 62.14	12.70 - 67.04	16.85 - 67.31
T_{silt} [%]	mean	14.48	14.61	12.58	15.49	18.17	17.53
	range	2.70 - 23.12	4.00 - 25.20	3.10 - 22.30	12.84 - 20.40	12.10 - 26.00	9.06 - 29.20
T_{clay} [%]	mean	38.63	37.44	34.06	30.68	38.78	36.85
	range	13.63 - 70.80	18.40 - 70.50	8.63 - 69.40	24.23 - 41.60	20.86 - 66.34	22.75 - 58.98
BD [$g\,cm^{-3}$]	mean	1.10	1.20	1.26	1.08	1.18	1.28
	range	0.96 - 1.22	1.08 - 1.31	1.11 - 1.36	0.88 - 1.26	0.97 - 1.36	1.04 - 1.43
pH [-]	mean	5.19	4.85	4.87	5.00	4.96	5.13
	range	4.40 - 5.76	4.40 - 5.40	4.60 - 5.40	4.30 - 5.60	4.50 - 5.70	4.80 - 5.60
φ [%]	mean	54.64	48.94	46.60	53.75	51.09	47.92
	range	40.20 - 63.80	39.12 - 60.40	37.22 - 56.60	38.60 - 63.40	36.60 - 60.60	36.80 - 57.20

Table 13: All soil samples and their texture and pH measurement locations.

Sample No.	Academic institution		Sample No.	Academic institution	
	Texture measurement	pH measurement		Texture measurement	pH measurement
09_1	VU	VU/UZH	32_2	VU	VU
09_2	VU	VU/UZH	33_0	VU	VU
13_1	VU	VU	33_1	VU	VU
13_2	VU	VU	34_0	VU	VU
14_1	VU	VU	34_1	VU	VU
14_2	VU	VU	34_2	VU	VU
15_1	VU	VU	35_0	VU	VU
15_2	VU	VU	35_1	VU	VU
16_0	VU	VU	35_2	VU	VU
16_1	VU	VU	36_0	VU	VU
16_2	VU	VU	36_1	VU	VU
17_0	VU	VU	36_2	VU	VU
17_1	VU	VU	37_0	VU	VU
17_2	VU	VU	37_1	VU	VU
18_0	VU	VU	37_2	VU	VU
18_1	VU	VU	38_0	VU	VU
18_2	VU	VU	38_1	VU	VU
19_0	VU	VU	38_2	VU	VU
19_1	VU	UZH	39_0	VU	VU
19_2	VU	UZH	39_1	VU	VU
21_1	VU	VU	39_2	VU	VU
21_2	VU	VU	40_0	VU	VU
22_1	VU	VU	40_1	VU	VU
22_2	VU	VU	40_2	VU	VU
23_1	VU	VU	41_0	VU	VU
23_2	VU	VU	41_1	VU	VU
24_1	VU	VU	41_2	VU	VU
24_2	VU	VU	42_0	VU	VU
25_1	VU	VU	42_1	VU	VU
25_2	VU	VU	42_2	VU	VU
26_1	VU	VU	43_0	VU	VU
26_2	VU	VU	43_1	VU	VU
27_1	VU	VU	43_2	VU	VU
27_2	VU	VU	44_0	VU	VU
28_1	VU	VU	44_1	VU	VU
28_2	VU	VU	44_2	VU	VU
29_1	VU	VU	53_0	VU	VU
29_2	VU	VU	54_0	VU	VU
30_1	VU	VU	56_0	UZH	UZH
30_2	VU	VU	56_1	UZH	UZH
31_0	VU	VU	56_2	UZH	UZH
31_1	VU	VU	57_0	UZH	UZH
31_2	VU	VU	57_1	UZH	UZH
32_0	VU	VU	57_2	UZH	UZH
32_1	VU	VU			

VU: Vrije Universiteit Amsterdam
UZH: University of Zurich

Declaration of Originality

I hereby declare that the submitted thesis is the result of my own, independent work. All external sources are explicitly acknowledged in the thesis.

Florencio Zanitti

Zurich, 27th June, 2019